

ENCLOSURE 1

ENTERGY NUCLEAR OPERATIONS, INC. PALISADES NUCLEAR PLANT

RELIEF REQUEST NUMBER RR 4-21 PROPOSED ALTERNATIVE

in Accordance with 10 CFR 50.55a(z)(2)
Hardship Without a Compensating
Increase in Level of Quality and Safety

1. ASME CODE COMPONENT(S) AFFECTED / APPLICABLE CODE EDITION

Components / Numbers: See Enclosure Table 1
Pressure Retaining Dissimilar Metal Piping Butt Welds
Containing Alloy 82/182

Code of Record: American Society of Mechanical Engineers (ASME) Section XI,
2001 Edition through 2003 Addenda as amended by
10 CFR 50.55a
ASME Code Case N-770-1, "Alternative Examination
Requirements and Acceptance Standards for Class 1 PWR
Piping and Vessel Nozzle Butt Welds Fabricated with UNS
N06082 or UNS W86182 Weld Filler Material With or Without
Application of Listed Mitigation Activities, Section XI, Division 1"

N-770-1 Inspection Item: A-2 and B

Description: Class 1 Pressurized Water Reactor (PWR) pressure retaining
Dissimilar Metal Piping and Vessel Nozzle Butt Welds containing
Alloy 82/182

Unit / Inspection Interval: Palisades Nuclear Plant (PNP) / Fourth 10-Year Interval
December 13, 2006 through December 12, 2015

2. APPLICABLE CODE REQUIREMENTS

The ASME Boiler and Pressure Vessel Code, Rules for Inservice Inspection of Nuclear Power Plant Components, Section XI, 2001 Edition through 2003 Addenda, as amended by 10 CFR 50.55a.

With the issuance of a revised 10 CFR 50.55a in June 2011, the Nuclear Regulatory Commission (NRC) staff incorporated, by reference, Code Case N-770-1. Specific implementing requirements are documented in 10 CFR 50.55a(g)(6)(ii)(F) and are listed below:

- A. Regulation 10 CFR 50.55a(g)(6)(ii)(F)(1) states "Licensees of existing, operating pressurized water reactors as of July 21, 2011 must implement the requirements of ASME Code Case N-770-1, subject to the conditions specified in paragraphs

**ENCLOSURE 1
PROPOSED ALTERNATIVE**

(g)(6)(ii)(F)(2) through (g)(6)(ii)(F)(10) of this section, by the first refueling outage after August 22, 2011.”

- B. Regulation 10 CFR 50.55a(g)(6)(ii)(F)(3) states that baseline examinations for welds in Code Case N-770-1, Table 1, Inspection Items A-1, A-2, and B, must be completed by the end of the next refueling outage after January 20, 2012.

The welds covered by this proposed alternative would be classified as Inspection Items A-2 and B (described below) for which visual and essentially 100 percent volumetric examination, as amended by 10 CFR 50.55a(g)(6)(ii)(F)(4), in part, are required, per NRC interpretation.

ASME Code Case N-770-1, Table 1, Examination Categories, as amended by 10 CFR 50.55a(g)(6)(ii)(F)		
CLASS 1 PWR Pressure Retaining Dissimilar Metal Piping and Vessel Nozzle Butt Welds Containing Alloy 82/182		
Parts Examined	Insp Item	Extent and Frequency of Examination
Unmitigated butt weld at Hot Leg operating temperature (-2410) ≤ 625°F (329°C)	A-2	Bare metal visual examination each refueling outage. Essentially 100% volumetric examination for axial and circumferential flaws in accordance with the applicable requirements of ASME Section XI, Appendix VIII, every five years. Baseline examinations shall be completed by the end of the next refueling outage after January 20, 2012.
Unmitigated butt weld at Cold Leg operating temperature (-2410) ≥ 525°F (274°C) and < 580°F (304°C)	B	Bare metal visual examination once per interval. Essentially 100% volumetric examination for axial and circumferential flaws in accordance with the applicable requirements of ASME Section XI, Appendix VIII, every second inspection period not to exceed 7 years. Baseline examinations shall be completed by the end of the next refueling outage after January 20, 2012.

ASME Section XI, Appendix VIII, Supplement 10, “Qualification Requirements for Dissimilar Metal Piping Welds,” is applicable to dissimilar metal (DM) welds without cast materials.

3. REASON FOR REQUEST

Examinations of the DM welds listed in Enclosure Table 1 of this request could not be performed as required by ASME Code Case N-770-1, as conditioned by 10 CFR 50.55a(g)(6)(ii)(F).

These DM welds are nominal pipe size (NPS) 2 inches and greater full penetration branch connection welds installed in primary coolant loop piping. See the Enclosure for typical configuration.

ENCLOSURE 1 PROPOSED ALTERNATIVE

The relevant conditions for this proposed alternative are ASME Section XI Code Case N-770-1, and 10 CFR 50.55a(g)(6)(ii)(F) items (1) and (3), which address performing the required baseline examinations.

Regulation 10 CFR 50.55a(g)(6)(ii)(F)(1) requires that licensees implement the requirements of ASME Code Case N-770-1, subject to the conditions specified in paragraphs (g)(6)(ii)(F)(2) through (g)(6)(ii)(F)(10) of this section, by the first refueling outage after August 22, 2011.

Regulation 10 CFR 50.55a(g)(6)(ii)(F)(3) requires that baseline examinations for welds in Code Case N-770-1 Table 1, Inspection Items A-1, A-2, and B be completed by the end of the next refueling outage after January 20, 2012.

Relief is requested from 10 CFR 50.55a(g)(6)(ii)(F) items (1) and (3) for performance of required baseline volumetric examinations of the eight cold leg welds and one hot leg weld listed in the Enclosure Table 1.

Hardship

The PNP welds in question are outside of the current Performance Demonstration Initiative (PDI) demonstrated joint configurations. That is, there currently are no PDI demonstrated volumetric techniques for this PNP weld joint configuration. Volumetric examination techniques for this complex weld configuration (see Attachment 1, Figures 1 and 2) require development and demonstration through the PDI qualification program. Under the PDI program, representative mock-ups would need to be fabricated in accordance with the PDI specimen fabrication program in order to develop examination techniques. Qualification of procedures and personnel would be needed in order to reliably perform qualified examinations of these welds. It is estimated that these activities would take a minimum of approximately 18 months.

Attempting "best effort" phased array ultrasonic examinations on these welds for which relief is requested without the needed technique development and demonstrations would not produce reliable results. Even though qualified procedures exist for the weld thickness and diameter, the geometry would negatively impact sound path calibration, search unit focusing, proper inside diameter impingement angles, and cause mis-orientation angles. As a result, this geometric complexity of the configuration would challenge the capability of current procedures to reliably characterize and size indications identified during the examinations and could lead to false-positive indications, as well as unnecessary increased radiation exposure to examination personnel.

Additional information concerning the hardships associated with the use of a manual phased array ultrasonic search unit, an eddy current or ultrasonic inspection from the inner diameter of the component, and a high-angle ultrasonic inspection method, and dose estimates associated with these methods, is provided in the ENO response to question RAI-2.2 in Reference 3.

A design mitigation strategy has not been approved for this weld configuration. Creating a mitigation strategy would require significant time for development of tooling, qualification of procedures and personnel, and mockup verification, in order to develop an approved method that would also minimize radiation exposure to personnel.

ENCLOSURE 1 PROPOSED ALTERNATIVE

Due to the location of the welds, performing unplanned manual phased array ultrasonic test examinations of the nine welds would involve significant radiation exposure to personnel. Total dose incurred by examination, radiation protection, and supervisory personnel during ultrasonic testing of the nine weld locations is estimated to be at least 37 rem. This total includes preparation activities, and credits dose reduction controls and measures such as shielding, decontamination of components, high efficiency particulate air filter ventilation units, cameras, and remote telemetry. Dose rates vary, on contact, from 120 mrem/hour to 15000 mrem/hour for the weld locations. General area dose rates in the vicinity of the weld locations vary from 25 mrem/hour to 200 mrem/hour.

The ENO response to question RAI-2.1 in Reference 3 provides detailed radiological dose estimates associated with performing unplanned volumetric inspections and dose estimates associated with performing the volumetric inspections with appropriate planning and foresight. The total dose for performing unplanned volumetric inspections was estimated to be approximately 37 Rem. The estimated total dose with appropriate planning and foresight was estimated to be 14.5 Rem. Reference 3 provides a breakdown of dose for each weld for erecting and removing scaffolding, conducting surveys, removing insulation, etc. The times for each activity along with the general area dose rates and dose rates at 30 cm from the nozzles are provided in the reference.

Development of a qualified procedure for the volumetric inspections would include identification of examination techniques that would minimize radiological exposure to examination personnel.

4. PROPOSED ALTERNATIVE AND BASIS FOR USE

Proposed Alternative

- 1) Perform periodic system leakage tests in accordance with ASME Section XI Examination Category B-P, Table IWB-2500-1.
- 2) Perform visual examinations (per Code Case N-722-1) and dye penetrant surface examinations (per ASME Section XI Examination Category B-J, Table IWB-2500-1) of the welds in accordance with ASME requirements.
- 3) Perform a volumetric examination, using ASME Code, Section XI, Appendix VIII, Supplement 10 qualified procedures, equipment and personnel, on each of the nine subject welds of this alternative during the next scheduled refueling outage (1R24).
- 4) Until the next scheduled refueling outage, if unidentified PCS leakage increases by 0.15 gpm above the WCAP-16465NP baseline mean, and is sustained for 72 hours, ENO will take action to be in Mode 3 within 6 hours and Mode 5 within 36 hours, and perform bare metal visual examinations of the nine subject welds of this alternative, unless it can be confirmed that the leakage is not from these welds.

Regulation 10 CFR 50.55a(g)(6)(ii)(F)(1) states "Licensees of existing, operating pressurized water reactors as of July 21, 2011 must implement the requirements of ASME Code Case N-770-1, subject to the conditions specified in paragraphs (g)(6)(ii)(F)(2) through (g)(6)(ii)(F)(10) of this section, by the first refueling outage after August 22, 2011."

ENCLOSURE 1 PROPOSED ALTERNATIVE

Regulation 10 CFR 50.55a(g)(6)(ii)(F)(3) states that baseline examinations for welds in Code Case N-770-1, Table 1, Inspection Items A-1, A-2, and B, must be completed by the end of the next refueling outage after January 20, 2012.

Pursuant to 10 CFR 50.55a(z)(2), ENO will comply with 10 CFR 50.55a(g)(6)(ii)(F) by completing the baseline volumetric examinations as required by Code Case N-770-1, for each of the nine subject welds of this alternative, prior to the end of the next scheduled refueling outage (1R24), currently scheduled to start in fall 2015.

Basis for Use

Table 1 in Attachment 1 of this enclosure describes the eight cold leg welds and one hot leg weld that have not been examined in accordance with Code Case N-770-1 examination requirements, as required by 10 CFR 50.55a(g)(6)(ii)(F) items (1) and (3).

Examination History

Table 1 in Attachment 1 also provides examination history information for the nine weld locations for which relief is requested. No evidence of through-wall cracking for these components has been identified during these inspections. Moreover, for the three weld locations that were not subject to surface or visual examinations during the 1R23 refueling outage (i.e., weld no.'s 3, 6, and 7 in Table 1), maintenance activities in the vicinity of the weld locations during the 1R23 refueling outage did not identify observations of leakage from the welds.

Structural Evaluation

Background

ENO submitted a proposed alternative (relief request number RR 4-18) concerning volumetric examinations of the subject branch connection welds on February 25, 2014 (Reference 1), and supplemental information was submitted on March 1, March 4, March 6, March 9, and March 11, 2014 (References 2 through 7).

ENO provided the following three calculations in the March 6, 2014 supplemental submittal (Reference 4):

1. Structural Integrity Associates, Inc, Calculation 1200895.306, "Hot Leg Drain Nozzle Weld Residual Stress Analysis and Circumferential Crack Stress Intensity Factor Determination," Revision 0, dated March 6, 2014.
2. Structural Integrity Associates, Inc., Calculation 1200895.307, "Hot Leg Drain Nozzle Crack Growth Analyses," Revision 0, March 6, 2014.
3. Structural Integrity Associates, Inc., Calculation 1200895.308, "Hot Leg Drain Nozzle Limit Load Analyses for Flawed Nozzle-to-Hot Leg Weld," Revision 0, March 6, 2014.

The SmartCrack software program was used to analyze crack propagation in the branch connection welds. SmartCrack uses a closed-form solution approach to calculate stress intensity factors for a crack with a two-dimensional residual stress field, and requires assumptions to be made concerning the model geometry, crack dimensions, boundary

ENCLOSURE 1 PROPOSED ALTERNATIVE

conditions, and stress field. This closed-form solution approach allowed for expeditiously analyzing crack growth under the time constraints imposed during the refueling outage in 2014.

On March 12, 2014 (Reference 8), the NRC staff verbally authorized the use of relief request number RR 4-18 at PNP until the next scheduled refueling outage, scheduled in the fall of 2015 (1R24). A NRC safety evaluation detailing the technical basis for the verbal authorization was subsequently issued on September 4, 2014 (Reference 9). The safety evaluation credited the ENO flaw and structural evaluation, in addition to the identified hardship and conditions of relief identified in the proposed alternative, in concluding that ENO had provided sufficient information to demonstrate reasonable assurance of the structural integrity of the nine subject welds for one cycle of operation without performing a volumetric examination.

On February 27, 2015, SI verbally notified ENO of a discrepancy discovered in a calculation that was submitted on March 6, 2014 (Reference 4) in support of relief request number RR 4-18. In a letter to ENO dated March 6, 2015, SI stated that the discrepancy was discovered in the residual stress calculation (File No. 1200895.306) within the load application for the normal operating conditions (NOC) evaluation. Specifically, the inside diameter surface elements adjacent to the circumferential free end and the axial free end of the hot leg pipe did not receive pressure loading (i.e., the effective pressure was 0 psig), while the remaining internal surfaces were pressurized to 2,122 psig for the NOC cycles.

The corrected calculations and updates of the associated SI memorandums are provided in Enclosure 2. These calculations and memorandums are provided for informational purposes only, and do not provide the technical basis for the enclosed proposed alternative.

Structural Evaluation Using Finite Element Analysis Methodology

The technical basis for the proposed alternative is provided in Attachment 2 of this enclosure, which includes the following report and calculations:

SI Report No. 1400669.401.R0, "Evaluation of the Palisades Nuclear Plant Branch Line Nozzles for Primary Water Stress Corrosion Cracking," Revision 0, dated May 14, 2015.

SI Calculation, File No. 1400669.313, "Crack Growth Analysis of the Hot Leg Drain Nozzle," Revision 0, dated May 11, 2015.

SI Calculation, File No. 1400669.323, "Crack Growth Analysis of the Cold Leg Bounding Nozzle," Revision 0, dated May 11, 2015.

SI Calculation, File No. 1400669.310, "Finite Element Model for Hot Leg Drain Nozzle," Revision 0, dated March 9, 2015.

SI Calculation, File No. 1400669.320, "Finite Element Model Development for the Cold Leg Drain, Spray, and Charging Nozzles," Revision 0, dated April 3, 2015.

SI Calculation, File No. 1400669.312, "Hot Leg Drain Nozzle Weld Residual Stress Analysis," Revision 0, dated May 5, 2015.

ENCLOSURE 1 PROPOSED ALTERNATIVE

SI Calculation, File No. 1400669.322, "Cold Leg Bounding Nozzle Weld Residual Stress Analysis," Revision 0, dated May 5, 2015.

In these calculations, SI used a finite element analysis (FEA) approach to evaluate postulated flaws in the hot leg and cold leg nozzles. These models were used to perform weld residual stress evaluations and calculations of stress intensity factors in the DM welds. Utilizing these new stress intensity factor distributions for postulated circumferential and axial flaws in the DM welds, crack growth due to PWSCC was evaluated for both the hot leg and cold leg configurations. Crack growth durations were then plotted on charts to show the service life of the hot leg and cold leg configurations based on crack growth from an assumed initial flaw depth of 0.025 inch. It should be noted that PWSCC was the only crack growth mechanism considered in this evaluation (i.e., PWSCC growth of a postulated axial and circumferential flaw in the weld).

The FEA approach is a more sophisticated approach for evaluating a postulated flaw than the SmartCrack closed-form solution approach used to support relief request number RR 4-18. Using a FEA approach, such as the ANSYS FEA software, enables a more realistic and accurate representation of the cracks in a nozzle as it grows. The FEA approach is a detailed numerical method that uses the actual residual stresses directly within the model, without having to make assumptions concerning model geometry and without transitioning the stress inputs into a separate program, like the assumptions made in SmartCrack.

Using the FEA approach, the calculations determined that, for the hot leg drain nozzle, the time for an initial 0.025 inch deep flaw to grow to 75% through-wall was calculated to be 30.5 years for the bounding axial flaw (36.7 years to go 95% through-wall) and 33.9 years for the circumferential flaw (42.1 years to go 95% through-wall).

For the cold leg drain nozzle, the time for an initial 0.025 inch deep flaw to grow to 75% through-wall is 64.5 years for the bounding axial flaw (77 years to go 95% through-wall) and 55.6 years for the circumferential flaw (66.2 years to go 95% through-wall).

By the 1R24 refueling outage, PNP will have operated for 27.4 effective full power years (Reference 21).

The SI report in Attachment 2 discusses a benefit in crack growth rate when Alloy 182 weld metal underwent post weld heat treatment (PWHT). This benefit ranged from a factor of two to four. Dominion Engineering recommended that crack growth rates be reduced by a conservative factor of two based on this data. Using this factor for the nozzles at PNP will increase the crack growth times previously discussed. For comparison, only the bounding crack growth life will be discussed here. This is the axial flaw for the hot leg drain nozzle, and the circumferential flaw for the cold leg nozzles. A factor of two will increase the limiting hot leg drain nozzle duration to 61.0 years, and the bounding cold leg nozzle to 111.2 years, for flaws to grow 75% through wall. Similarly, the durations for 95% through-wall flaws would increase to 73.4 years for the hot leg drain nozzle and 132.4 years for the cold leg nozzle.

Attachment A of the SI report in Attachment 2 includes a calculation of the initiation time for the hot leg drain nozzle and cold leg bounding nozzle using one of the models in the xLPR program that was developed by Electric Power Research Institute (EPRI). The calculation of initiation time based on the PNP results shows that the time to initiation for the hot leg drain nozzle is approximately 130 years. If the crack initiation time is combined with the PWHT

ENCLOSURE 1 PROPOSED ALTERNATIVE

reduction in crack growth rate, the time for a flaw to grow to 75% through-wall would approach 200 years for the hot leg drain nozzle and would exceed 200 years for 95% through-wall. Using the crack initiation value for the cold leg nozzles, the time for a flaw to grow to 75% through-wall would exceed 600 years. For both the hot leg and cold leg nozzles, the time for a flaw to grow to 75% through-wall is well beyond the life of the plant.

Additional Information

Post Weld Heat Treatment

All welds referenced in this relief request were post weld heat treated at the vendor's facility during original fabrication. Per Combustion Engineering detail weld procedure (MA-41, Revision 0), heat treatment of the hot leg nozzle weld (weld number 5-675) consisted of an intermediate post weld heat treatment at 1100°F, - 0°F/+ 50°F, for 15 minutes. Final heat treatment at the hot leg nozzle consisted of 1150°F, +/- 25°F, for one hour per inch thickness of weld. No heat treatment was performed at the site for the subject welds. See Reference 2.

The post weld heat treatment was applied to the nozzle welds by heating the affected nozzle/weld as part of the hot leg pipe assembly in a furnace. The hot leg drain nozzle (piece number 675-03) was installed into the hot leg pipe (pipe assembly 673-04) by cutting a hole into the hot leg piping and then fitting and welding the hot leg drain nozzle in place using an intermediate heat treat of 1100°F + 50°F for 15 minutes. The backing ring for the weld was removed, the weld was dye penetrant tested, and then back welded. The back weld was dye penetrant tested, and any indications were repaired, and then a final dye penetrant test was performed. The weld was then back clad and dye penetrant tested. Any indications were removed and dye penetrant tested again. The hot leg drain nozzle weld was radiographed and any defects were removed, weld repaired, and then dye penetrant tested and radiographed. The pipe assembly with the hot leg drain nozzle installed was post weld heat treated in a furnace using a post weld heat treat of 1150°F ± 25°F, holding this temperature for one hour/inch thickness of weld. See Reference 5.

Weld Repair History

The manufacturing/quality plan provided in the specification for the PCS piping provides instructions for performing weld repairs based on the results of NDE testing. Any defects identified in the nozzle welds would have been removed prior to final furnace heat treatment of the assembly. PNP is unable to locate post-fabrication documentation other than the weld radiographs taken after the final furnace heat treatment. These radiographs represent the condition of the subject welds at the time of installation at the site. A search of PNP records did not identify any repairs performed on the subject welds since installation. See Reference 2.

ENCLOSURE 1 PROPOSED ALTERNATIVE

Weld and Cladding Geometry

The hot leg weld is ½ inch wide at the ID and then increases in width at a 7-½° (+2°/-0°) angle to the OD of the hot leg pipe. The thickness of the hot leg pipe is 3-¾ inches. See Reference 2.

The thickness of the alloy 182/82 cladding on the inside surface of the weld is 1/4 inch nominal thickness with a minimum thickness of 5/32 inch. The inner radius at the hot leg drain is 21.34 inches measured from the inside surface of the cladding to the centerline of the hot leg pipe. See Reference 5.

Detailed information concerning the weld geometry is provided in References 2 and 5.

Basis for Assuming No Weld Repair

The presence of an initial weld repair from plant construction (e.g., extending 50% of the wall thickness from the inside diameter (ID)) is often assumed when modeling Alloy 82/182 piping butt welds. Often for piping butt welds, the residual stress calculated for the ID is a small tensile value, or even compressive, in the absence of an assumed weld repair. In such cases, the possibility of a significant weld repair being present on the weld ID can have a relatively large effect on the calculated stresses, especially on and near the ID surface.

However, for the Alloy 82/182 branch connection welds at PNP, there are two reasons why it is not necessary to include a weld repair assumption in the analysis. First, the design for this weldment specifies a 360° backweld on the ID surfaces of the pipe that is about 0.25 inch thick. This design feature results in elevated residual stress levels at the ID surface prior to the PWHT being applied. The residual stress levels at the inside surface due to the presence of the backweld are similar to what would be expected due to the presence of a weld repair on the ID surface.

Second, any weld repairs would have been made prior to PWHT being applied, and would be expected to extend over a relatively limited circumferential portion of the original weld. Similar to the situation for the elevated residual stresses due to the presence of the backweld, the PWHT would relax the residual stresses in the weld repair area, including the substantial relaxation expected at the surface exposed to primary coolant. Moreover, in the unlikely case that initiation occurred in the area of a weld repair, the weld repair would be an additional source of non-axisymmetric crack loading that would tend to drive crack growth through-wall over a relatively local circumferential region, ultimately resulting in detection of leakage prior to the possibility of unstable pipe rupture.

See Reference 2.

Basis for Five-Cycle Shakedown Assumption

Operational cycles are frequently included in welding residual stress calculations as a part of determining the operating stress condition. In particular, the standard modeling practice adopted by the xLPR (Extremely Low Probability of Rupture) welding residual stress team, which includes the NRC, national laboratories, and industry participants, specifies that the welded configuration should be cycled between operating conditions and residual conditions to shake down the nonlinear material hardening behavior. Typically, three to five cycles are used to shake down the material's behavior.

ENCLOSURE 1 PROPOSED ALTERNATIVE

Since the primary interest from the residual stress analysis is to provide residual stresses for calculating stress corrosion crack growth under normal operating conditions, it is desirable to determine a stabilized residual stress state that will not change under normal operating cycles. The as-welded residual stresses usually contain localized peak stresses at some nodal locations. Applying a few operating cycles will stabilize the stress peaks and valleys due to the slight stress redistribution at elevated temperatures. It has been determined through experience that the residual stresses will stabilize after three to five cycles. Five cycles was used for conservatism.

See Reference 2.

Operating Conditions

The operating temperature of a component is a primary factor influencing the initiation of PWSCC. Research by EPRI (Reference 17) indicates that the difference in the operating temperature between hot leg locations and cold leg locations is sufficient to significantly influence the time to initiation of PWSCC, with the susceptibility increasing with temperature. The research reports PWSCC is less likely to occur in cold leg temperature penetrations.

All but one of the welds covered by this relief are found in lower temperature regions of the system, typically at temperatures near to T_{cold} , which is approximately 537°F. This means, for these welds, there is a lower probability of crack initiation, and a slower crack growth rate (Reference 18).

Leakage Detection Capabilities

The leak detection methodology presently used by industry is very sensitive. After a number of recent operating events, the industry imposed an NEI 03-08, "Guideline for the Management of Materials Issues," requirement to improve leak detection capability. As a result, virtually all pressurized water reactors (PWRs) in the United States, including PNP, have a leak detection capability of less than or equal to 0.1 gpm (Reference 16). All plants, including PNP, also monitor seven-day moving averages of reactor coolant system leak rates.

Action response times following a detected primary coolant system leak vary, based on the action level exceeded and whether containment entry is required to identify the source of the leak.

Action levels have been standardized for all PWRs, and are based on deviations from:

- the seven day rolling average,
- specific values, and
- the baseline mean.

Leak rate action levels are identified in Pressurized Water Reactor Owners Group (PWROG) report, WCAP-16465, and are stated below:

Each PWR utility is required to implement the following standard action levels for reactor coolant system (RCS) inventory balance in their RCS leakage monitoring program.

ENCLOSURE 1 PROPOSED ALTERNATIVE

Action levels on the absolute value of unidentified RCS inventory balance (from surveillance data):

Level 1 - One seven day rolling average of unidentified RCS inventory balance values greater than 0.1 gpm.

Level 2 - Two consecutive unidentified RCS inventory balance values greater than 0.15 gpm.

Level 3 - One unidentified RCS inventory balance value greater than 0.3 gpm.

Note: Calculation of the absolute RCS inventory balance values must include the rules for the treatment of negative values and missing observations.

Action levels on the deviation from the baseline mean:

Level 1 - Nine consecutive unidentified RCS inventory balance values greater than the baseline mean $[\mu]$ value.

Level 2 - Two of three consecutive unidentified RCS inventory balance values greater than $[\mu + 2\sigma]$, where σ is the baseline standard deviation.

Level 3 - One unidentified RCS inventory balance value greater than $[\mu + 3\sigma]$.

These action levels have been incorporated into PNP procedures.

A small steam leak from a weld flaw would, over time, result in a rise in containment sump level rate of increase. Containment sump level is continually monitored, and if a rise in the rate of containment sump level increase is observed, plant procedures direct plant operators to identify the source of the leakage. Operators may also be alerted to a leak from a flaw by containment radiation monitoring instrumentation. This instrumentation, required by the Technical Specifications, is capable of detecting a 100 cm³/min leak in 45 minutes, based on 1% failed fuel. Periodic system leakage tests are performed in accordance with ASME Section XI. Operator walkdowns of containment are periodically performed during power operations at lower levels of containment to detect leakage.

Therefore, with the periodic system leakage tests, the visual and surface examinations performed during 2012 and 2014 refueling outages, the results of the SI evaluation, containment monitoring activities, and the testing, examination, and PCS leakage requirements in the proposed alternative, an acceptable level of quality and safety is provided for identifying degradation from PWSCC prior to a safety-significant flaw developing.

5. DURATION OF PROPOSED ALTERNATIVE

The duration of the proposed alternative is until refueling outage 1R24, which is currently scheduled to begin in fall 2015.

ENCLOSURE 1
PROPOSED ALTERNATIVE

6. REFERENCES

1. Entergy Nuclear Operations, Inc. letter PNP 2014-015, "Relief Request Number RR 4-18 Proposed Alternative, Use of Alternate ASME Code Case N-770-1 Baseline Examination," dated February 25, 2014 (ADAMS Accession No. ML14056A533).
2. Entergy Nuclear Operations, Inc. letter PNP 2014-021, "Response to Request for Additional Information dated February 26, 2014, for Relief Request Number RR 4-18 – Proposed Alternative, Use of Alternate ASME Code Case N-770-1 Baseline Examination," dated March 1, 2014 (ADAMS Accession No. ML14072A361).
3. Entergy Nuclear Operations, Inc. letter PNP 2014-022, "Response to Second Request for Additional Information dated February 27, 2014, for Relief Request Number RR 4-18 – Proposed Alternative, Use of Alternate ASME Code Case N-770-1 Baseline Examination," dated March 4, 2014 (ADAMS Accession No. ML14063A089).
4. Entergy Nuclear Operations, Inc. letter PNP 2014-028, "Supplemental Response to Request for Additional Information dated February 26, 2014, for Relief Request Number RR 4-18 – Proposed Alternative, Use of Alternate ASME Code Case N-770-1 Baseline Examination," dated March 6, 2014 (ADAMS Accession No. ML14066A409).
5. Entergy Nuclear Operations, Inc. letter PNP 2014-029, "Response to Third Request for Additional Information dated March 5, 2014, for Relief Request Number RR 4-18 – Proposed Alternative, Use of Alternate ASME Code Case N-770-1 Baseline Examination," dated March 6, 2014 (ADAMS Accession No. ML14070A182).
6. Entergy Nuclear Operations, Inc. letter PNP 2014-030, "Second Supplemental Response to Request for Additional Information dated February 26, 2014, for Relief Request Number RR 4-18 – Proposed Alternative, Use of Alternate ASME Code Case N-770-1 Baseline Examination," dated March 9, 2014 (ADAMS Accession No. ML14069A004).
7. Entergy Nuclear Operations, Inc. letter PNP 2014-031, "Response to Fourth Request for Additional Information dated March 11, 2014, for Relief Request Number RR 4-18 – Proposed Alternative, Use of Alternate ASME Code Case N-770-1 Baseline Examination," dated March 11, 2014 (ADAMS Accession No. ML14070A477).
8. NRC Electronic Mail, "Palisades Nuclear Plant – Verbal Authorization for Relief Request RR 4-18 - MF3508," March 13, 2014 (ADAMS Accession No. ML14073A274).
9. NRC letter, "Palisades Nuclear Plant – Proposed Alternative, Use of Alternate ASME Code Case N-770-1 Baseline Examination (TAC No. MF3508)," dated September 4, 2014 (ADAMS Accession No. ML14223B226).
10. 10 CFR 50.55a, "Codes and standards," December 11, 2014.
11. ASME Section XI, "Rules For Inservice Inspection of Nuclear Power Plant Components," 2001 Edition with Addenda through 2003.
12. ASME Section XI, Division 1, Code Case N-460, "Alternative Examination Coverage for Class 1 and Class 2 Welds, Section XI, Division 1."

**ENCLOSURE 1
PROPOSED ALTERNATIVE**

13. Material Reliability Program: Primary System Piping Butt Weld Inspection and Evaluation Guideline (MRP-139), Revision 1, EPRI, Palo Alto, CA, 2008 (ADAMS Accession No. ML1009700671).
14. Nondestructive Evaluation: Procedure for Manual Phased Array Ultrasonic Examination of Dissimilar Metal Welds, EPRI-DMW-PA-1, Revision 3, 1016645, EPRI Palo Alto, CA, 2008.
15. "Changing the Frequency of Inspections for PWSCC Susceptible Welds at Cold Leg Temperatures", in Proceedings of 2011 ASME Pressure Vessels and Piping Conference, July 17-21, 2011, Baltimore, MD.
16. WCAP-16465-NP, Rev. 0, "Pressurized Water Reactor Owners Group Standard RCS Leakage Action Levels and Response Guidelines for Pressurized Water Reactors," Westinghouse Electric Co., September 2006 (ADAMS Accession No. ML070310082).
17. Electric Power Research Institute: PWSCC of Alloy 600 Materials in PWR Primary System Penetrations, EPRI, Palo Alto, CA, 1994, TR-103696 (ADAMS Accession No. ML013110446).
18. Materials Reliability Program Crack Growth Rates for Evaluating Primary Water Stress Corrosion Cracking (PWSCC) of Alloy 82, 182, and 132 Welds (MRP-115), EPRI, Palo Alto, CA, 2004, 1006696 (ADAMS Accession No. ML051100204).
19. PNP Technical Specification Surveillance Procedure RT-71A, "Primary Coolant System, Class 1 System Leakage Test," Revision 18.
20. Pressurized Water Reactor (PWR) Owner's Group Letter OG-12-89, "Transmittal of 'Final Relief Request Framework' under Relief Request for Large Diameter Cold Leg Locations with Obstructions (PA-MS-0934)," March 8, 2012.
21. WCAP-15353-Supplement 1-NP, Palisades Reactor Pressure Vessel Fluence Evaluation, Revision 0, May 2010 (ADAMS Accession Number ML110060692).

7. ATTACHMENTS

Attachment 1

Table 1 - Weld Examination History

Figure 1 - Nozzle Assembly Materials

Figure 2 - Hot Leg Drain Nozzle Configuration (Representative)

**ENCLOSURE 1
PROPOSED ALTERNATIVE**

Attachment 2

1. Structural Integrity Associates, Inc. Report No. 1400669.401.R0, "Evaluation of the Palisades Nuclear Plant Branch Line Nozzles for Primary Water Stress Corrosion Cracking," Revision 0, dated May 14, 2015.
2. Structural Integrity Associates, Inc. Calculation, File No. 1400669.313, "Crack Growth Analysis of the Hot Leg Drain Nozzle," Revision 0, dated May 11, 2015.
3. Structural Integrity Associates, Inc. Calculation, File No. 1400669.323, "Crack Growth Analysis of the Cold Leg Bounding Nozzle," Revision 0, dated May 11, 2015.
4. Structural Integrity Associates, Inc. Calculation, File No. 1400669.310, "Finite Element Model for Hot Leg Drain Nozzle," Revision 0, dated March 9, 2015.
5. Structural Integrity Associates, Inc. Calculation, File No. 1400669.320, "Finite Element Model Development for the Cold Leg Drain, Spray, and Charging Nozzles," Revision 0, dated April 3, 2015.
6. Structural Integrity Associates, Inc. Calculation, File No. 1400669.312, "Hot Leg Drain Nozzle Weld Residual Stress Analysis," Revision 0, dated May 5, 2015.
7. Structural Integrity Associates, Inc. Calculation, File No. 1400669.322, "Cold Leg Bounding Nozzle Weld Residual Stress Analysis," Revision 0, dated May 5, 2015.

**ENCLOSURE 1
ATTACHMENT 1**

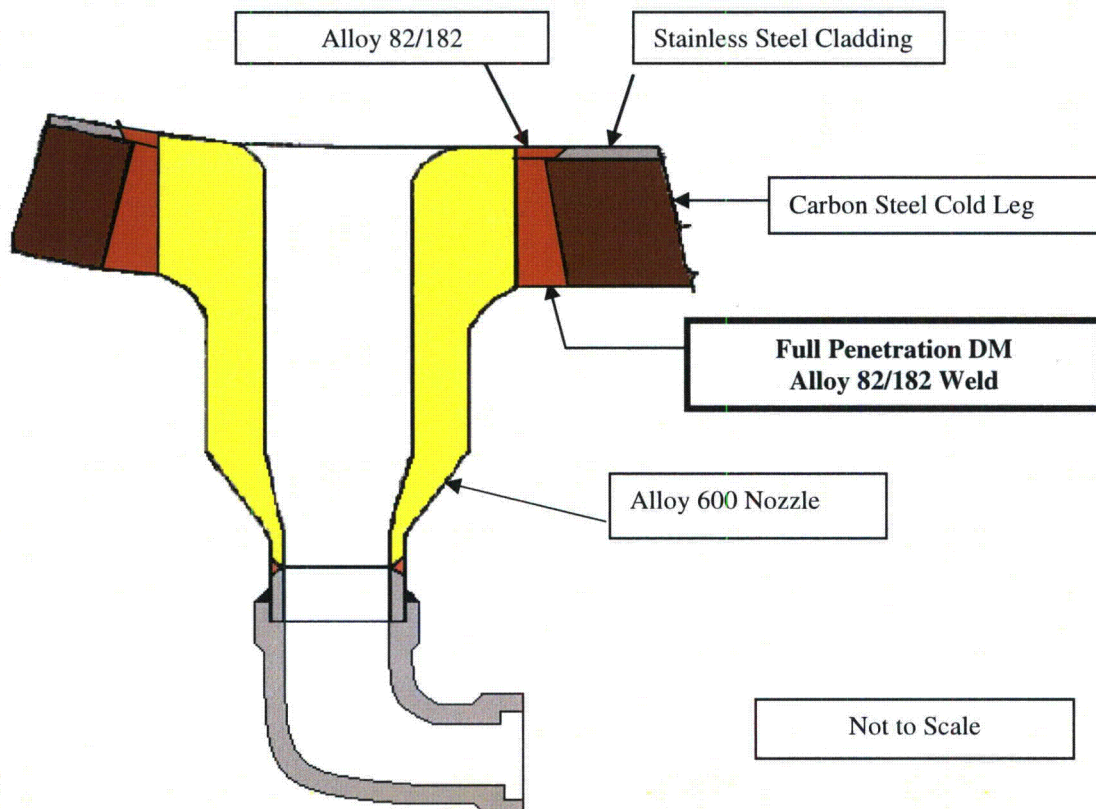
**Table 1
Weld Examination History**

No.	Description	ISI Weld ID	Location	1R19 Examinations	1R20 Examinations	1R21 Examinations	1R22 Examinations	1R23 Examinations
1.	2 inch Cold Leg Charging Nozzle	PCS-30-RCL-1A- 11/2	P-50A Discharge Leg	Visual (Report# 4046 Exam number 06-26)				Surface (Report# 1R23- PT-14-025)
2.	2 inch Cold Leg Drain Nozzle	PCS-30-RCL-1A- 5/2	P-50A Suction Leg	Visual (Report# 4047 Exam number 07-28.1)				Surface (Report# 1R23- PT-14-031)
3.	3 inch Cold Leg Pressurizer Spray Nozzle	PCS-30-RCL-1B- 10/3	P-50B Discharge Leg			Visual (Report# VT-10- 069)	Surface (Report# 1R22- PT-12-039)	
4.	2 inch Cold Leg Drain Nozzle	PCS-30-RCL-1B- 5/2	P-50B Suction Leg			Visual (Report# VT-10- 048)		Surface (Report #1R23- PT-14-032)
5.	2 inch Cold Leg Charging Nozzle	PCS-30-RCL-2A- 11/2	P-50C Discharge Leg		Visual (Report# VT-09- 083)			Surface (Report# 1R23- PT-14-019)
6.	3 inch Cold Leg Pressurizer Spray Nozzle	PCS-30-RCL-2A- 11/3	P-50C Discharge Leg		Visual (Report# VT-09- 035)		Surface (Report# 1R22- PT-12-032)	
7.	2 inch Cold Leg Drain Nozzle	PCS-30-RCL-2A- 5/2	P-50C Suction Leg		Visual (Report# VT-09- 038)			
8.	2 inch Cold Leg Drain and Letdown Nozzle	PCS-30-RCL-2B- 5/2	P-50D Suction Leg			Visual (Report# VT-10- 071)		Surface (Report# 1R23- PT-14-020)
9.	2 inch Hot Leg Drain Nozzle	PCS-42-RCL-1H- 3/2	A Hot Leg	Visual (Report# 4047 Exam number 07-23.1)	Visual (Report# VT-09- 062)	Visual (Report# VT-10- 022)	Visual (Report# 1R22- VT-12-076)	Visual (Report# 1R23- VT-14-059)

**ENCLOSURE 1
ATTACHMENT 1**

Figure 1

Nozzle Assembly Materials

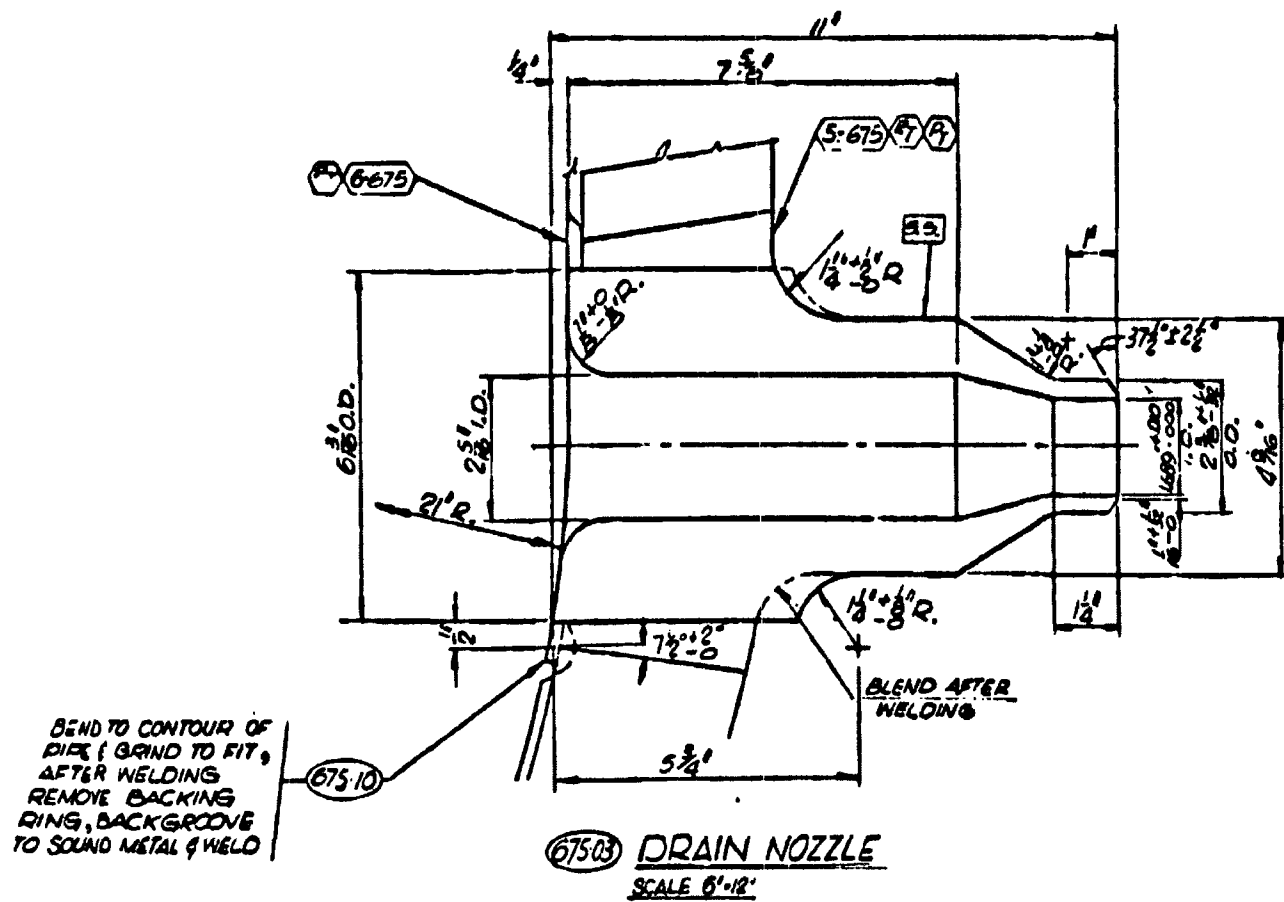


ENCLOSURE 1
ATTACHMENT 1

Figure 2

Hot Leg Drain Nozzle Configuration (Representative)

(excerpt from PNP vendor drawing VEN-M1-D Sheet 108, Revision 8)

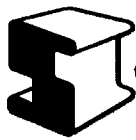


ENCLOSURE 1
ATTACHMENT 2

The attached Structural Integrity Associates, Inc. report and calculations provide the technical basis for the proposed alternative.

1. Structural Integrity Associates, Inc. Report No. 1400669.401.R0, "Evaluation of the Palisades Nuclear Plant Branch Line Nozzles for Primary Water Stress Corrosion Cracking," Revision 0, dated May 14, 2015.
2. Structural Integrity Associates, Inc. Calculation, File No. 1400669.313, "Crack Growth Analysis of the Hot Leg Drain Nozzle," Revision 0, dated May 11, 2015.
3. Structural Integrity Associates, Inc. Calculation, File No. 1400669.323, "Crack Growth Analysis of the Cold Leg Bounding Nozzle," Revision 0, dated May 11, 2015.
4. Structural Integrity Associates, Inc. Calculation, File No. 1400669.310, "Finite Element Model for Hot Leg Drain Nozzle," Revision 0, dated March 9, 2015.
5. Structural Integrity Associates, Inc. Calculation, File No. 1400669.320, "Finite Element Model Development for the Cold Leg Drain, Spray, and Charging Nozzles," Revision 0, dated April 3, 2015.
6. Structural Integrity Associates, Inc. Calculation, File No. 1400669.312, "Hot Leg Drain Nozzle Weld Residual Stress Analysis," Revision 0, dated May 5, 2015.
7. Structural Integrity Associates, Inc. Calculation, File No. 1400669.322, "Cold Leg Drain Nozzle Weld Residual Stress Analysis," Revision 0, dated May 5, 2015.

213 pages follow



5215 Hellyer Ave.
Suite 210
San Jose, CA 95138-1025
Phone: 408-978-8200
Fax: 408-978-8964
www.structint.com
clhse@structint.com

May 14, 2015

Report No. 1400669.401.R0

Quality Program: ☒ Nuclear (Safety-related) ☐ Commercial

Mr. Keith Smith
Entergy Nuclear Operations, Inc.
Palisades Nuclear Plant
27780 Blue Star Memorial Highway
Covert, MI 49043

Subject: Evaluation of the Palisades Nuclear Plant Branch Line Nozzles for Primary Water Stress Corrosion Cracking

Dear Keith:

In Relief Request RR 4-18 [1], Entergy Nuclear Operations (Entergy) committed to volumetrically examine a total of nine (9) pressure retaining dissimilar metal welds (DMWs) containing Alloy 600 nozzles and Alloy 182 weld material at the Palisades Nuclear Plant (Palisades) during the upcoming 1R24 refueling outage (Fall of 2015). Of the nine weld locations, eight are cold leg nozzles (three 2-inch diameter drain nozzles, one 2-inch diameter letdown nozzle, two 2-inch diameter charging nozzles, and two 3-inch diameter spray nozzles) and one 2-inch diameter hot leg drain nozzle.

On December 1, 2014, Entergy contracted with Structural Integrity Associates, Inc. (SI) [2] to support a flaw readiness evaluation for the 1R24 examinations of the nine reactor coolant system (RCS) branch connection Alloy 600 nozzle boss welds at Palisades. SI began working in earnest on this project in early January 2015. The base work scope involved performing flaw evaluations for the hot leg and cold leg branch line DMWs. SI's work was interrupted in mid-February 2015 to support a possible relief request to defer inspections for the upcoming outage.

To support Entergy's new Relief Request, SI was requested to provide a technical basis for deferral of inspection of the hot leg drain nozzle and eight cold leg branch line nozzle DMWs. In order to perform the necessary flaw evaluations, finite element models were developed for the hot leg and cold leg nozzles. These models were used to perform weld residual stress evaluations and calculations of stress intensity factors in the DMWs. Utilizing these new stress intensity factor distributions for postulated circumferential and axial flaws in the DMWs, crack growth due to primary water stress corrosion cracking (PWSCC) was evaluated for both the hot

Toll-Free 877-474-7693

Chicago, IL
877-474-7693

Akron, OH
330-899-9753
Denver, CO
303-792-0077

Austin, TX
512-533-9191
San Diego, CA
858-455-6350

Charlotte, NC
704-597-5554
San Jose, CA
408-978-8200

Chattanooga, TN
423-553-1180
State College, PA
814-954-7776

Toronto, Canada
905-829-9817

Evaluation of the Palisades Nuclear Plant Branch Line Nozzles for Primary Water Stress
Corrosion Cracking

leg and cold leg configurations. Crack growth durations were then plotted on charts to show the service life of the hot leg and cold leg configurations based on crack growth from an assumed initial flaw depth of 0.025 inch.

This report summarizes the evaluation results. It should be noted that PWSCC was the only crack growth mechanism considered in this evaluation (i.e., PWSCC growth of a postulated axial and circumferential flaw in the weld). The overall goal of SI's evaluation was to show that it takes considerable time to grow postulated flaws to allowable flaw sizes in both the hot leg drain nozzle and the cold leg nozzle configurations, and that the crack growth time for these locations is quite significant.

Finite Element Analyses

For the hot leg drain nozzle, a three-dimensional (3-D) finite element model was developed using the ANSYS software [3]. The area of interest was the nozzle-to-hot leg DMW. The model used elastic-plastic material properties intended for weld residual stress analysis. The model included a local portion of the hot leg pipe and cladding, the drain nozzle, and the nozzle-to-hot leg DMW, including the inside diameter (ID) patch weld, as shown in Figure 1. As depicted in the figure, a single 90° quadrant of the drain nozzle penetration is modeled due to geometric symmetry. The included portion of the hot leg piping measured 36 inches longitudinally and 180 degrees circumferentially. The mesh of the finite element model is shown in Figure 2.

For the cold leg nozzles, one bounding 3-D finite element model was developed using the ANSYS software [4]. All three nozzle configurations (i.e., drain/letdown, charging, and spray) are of similar size (diameter) near the forging boss area (within 1/16 inch). Therefore, the largest ID and smallest outside diameter (OD) of the three nozzle types was chosen for the bounding model. The spray and drain/letdown nozzles have identical nozzle and boss OD dimensions of 4-9/16 inches and 6-3/16 inches, respectively, which are slightly smaller than the charging nozzle OD dimensions of 4-5/8 inches and 6-1/4 inches. For the nozzle ID, the charging nozzle was bored out to 2-5/8 inches in the first 1.5 inches to accommodate a thermal sleeve. For conservatism, it was assumed that the entire nozzle ID is 2-5/8 inches. Therefore, the ID of the bored out charging nozzle and the OD of the spray/drain/letdown nozzles were used for the bounding cold leg nozzle configuration.

For the cold leg nozzles, the area of interest was the nozzle-to-cold leg DMW. The model used elastic-plastic material properties intended for weld residual stress analysis. The model included a local portion of the cold leg pipe and cladding, the nozzle, and the nozzle-to-cold leg DMW, including the ID patch weld, as shown in Figure 3. As depicted in the figure, a single 90° quadrant of the nozzle penetration is modeled due to geometric symmetry. The included portion of the cold leg piping measured 36 inches longitudinally and 180 degrees circumferentially. The mesh of the finite element model is shown in Figure 4.

Weld Residual Stress Analyses

Weld residual stress analyses were performed for the hot leg drain nozzle [5] and bounding cold leg nozzle [6], and the following steps of initial construction were simulated in the analyses:

1. Deposit cladding on hot leg/cold leg pipe inside surface.
2. Install nozzle, backing ring, and deposit boss weld.
3. Remove backing ring and deposit ID patch weld.
4. Post weld heat treatment (PWHT), including creep effects based upon experimental data.
5. Subject the configuration to a hydrostatic test.
6. Impose five cycles of “shakedown” at normal operating temperature and pressure to stabilize the residual stress fluctuations due to stress redistribution.

For the hot leg drain nozzle, the boss weld connects the drain nozzle to the hot leg piping. As shown in Figure 5, the weld is composed of 40 nuggets deposited in 20 weld layers. As depicted in Figure 6, the ID patch weld is composed of 6 nuggets deposited in 2 layers. Stabilized stress results normal to a circumferential flaw are shown in Figure 7, and those normal to an axial flaw are shown in Figure 8. They represent the operating conditions of the hot leg, and include the residual stresses due to welding plus the operating pressure of 2085 psig and steady-state temperature of 583°F.

For the cold leg nozzles, the boss weld connects the bounding nozzle to the cold leg piping. As shown in Figure 9, the weld is composed of 40 nuggets deposited in 20 weld layers. As depicted in Figure 10, the ID patch weld is composed of 6 nuggets deposited in 2 layers. Stabilized stress results normal to a circumferential flaw are shown in Figure 11, and those normal to an axial flaw are shown in Figure 12. They represent the operating conditions of the cold leg, and include the residual stresses due to welding plus the operating pressure of 2085 psig and steady-state temperature of 537°F.

Crack Growth Evaluations

Crack growth evaluations were performed for the hot leg drain nozzle [7] and the bounding cold leg nozzle [8]. For both the hot leg drain nozzle and bounding cold leg nozzle, stress intensity factors (Ks) at five depths for a 360° inside surface connected, part-through wall circumferential flaw as well as two axial thumbnail flaws, at the 0- and 90-degree azimuthal locations of the nozzle, were calculated using finite element analysis techniques. For the circumferential flaw, the maximum K values around the nozzle circumference for each flaw depth were extracted and used as input for performing the PWSCC growth analyses. For the axial flaws, the K at the deepest point of the thumbnail shape was used as input for performing the PWSCC growth analyses.

For the crack growth analyses, a small initial flaw size of 0.025 inch was chosen. This is based on the expected flaw size that would be possible since the crack growth evaluation is assumed to

start on day one of plant operation. The final flaw size for these analyses is 75% of the wall thickness. This final depth is chosen as it is the maximum allowable flaw depth per Section XI of the ASME Code for pipe flaw evaluations. The 75% requirement is driven by the tables and equations in Appendix C, Article C-5000 of Section XI of the ASME Code. The equations and tables are limited to 75% of the pipe thickness. The values for a through-wall flaw (95% depth) are also calculated to explore the time for a flaw to grow through-wall. In response to Nuclear Regulatory Commission RAI's [12] pertaining to Relief Request RR 4-18 [1], SI performed limit load analyses to show that the hot leg/cold leg/nozzle structures remained structurally stable for both circumferential and axial through-wall flaws.

The key parameters used in the crack growth calculations included:

- Initial flaw depth = 0.025" for both hot and cold leg configurations
- Temperature = 583°F (hot leg) and 537°F (cold leg)
- Wall thickness = 4" (hot leg pipe thickness) and 3" (cold leg pipe thickness)

An example of the 360° circumferential flaw is shown in Figure 13 for the hot leg nozzle and Figure 18 for the bounding cold leg nozzle. A total of five circumferential flaw depths were modeled. Similarly, five axial flaw depths were modeled at the 0- and 90-degree azimuths. Figure 14 shows the axial flaws modeled at the 0-degree azimuth for the hot leg nozzle, and Figure 19 shows the comparable axial flaws modeled for the bounding cold leg nozzle.

Stress intensity factors, K_s , were calculated for the 360° circumferential flaws as well as the axial flaws at the 0° and 90° locations. The stress intensity factors were calculated using the stress distributions for residual stress plus normal operating conditions shown in Figures 7 and 8 for the hot leg drain nozzle, and Figures 11 and 12 for the bounding cold leg nozzle. In addition, a far field in-plane bending moment is applied to the free end of the hot leg and cold leg run piping to account for piping moments in the main loop piping. This combined loading is used for the determination of the stress intensity factors for both the circumferential and axial flaws. Figures 15 and 16 show the calculated stress intensity factors for the hot leg drain nozzle for the circumferential and axial flaws, respectively. Figures 20 and 21 show the calculated stress intensity factors for the bounding cold leg nozzle for the circumferential and axial flaws, respectively.

Crack growth evaluations were performed for all three flaws. For the hot leg drain nozzle, Figure 17 shows that the time for an initial 0.025" deep flaw to grow to 75% through wall is 30.5 years for the bounding axial flaw (on the 0° plane) and 33.9 years for the circumferential flaw. For the 100% through wall flaw (growth up to 95%) the bounding axial flaw takes 36.7 years (on the 0° plane) and the circumferential flaw takes 42.1 years as shown in Figure 17.

For the bounding cold leg nozzle, Figure 22 shows that the time for an initial 0.025" deep flaw to grow to 75% through wall is 64.5 years for the bounding axial flaw (on the 0° plane) and 55.6 years for the circumferential flaw. For the 100% through wall flaw (growth up to 95%) the

Evaluation of the Palisades Nuclear Plant Branch Line Nozzles for Primary Water Stress
Corrosion Cracking

bounding axial flaw takes 77.0 years (on the 0° plane) and the circumferential flaw takes 66.2 years as shown in Figure 22.

Potential Additional Margin Due to PWHT

Dominion Engineering documented in Reference 9 that industry papers [10, 11] note a benefit in fatigue crack growth rate when Alloy 182 weld metal underwent PWHT. This benefit ranged from a factor of two to four. There was a recommendation that crack growth rates be reduced by a factor of two based on this data. If such a factor were used for the nozzles at Palisades, it would increase the crack growth times previously discussed. For comparison, only the bounding crack growth life will be discussed here. This is the axial flaw for the hot leg drain nozzle, and the circumferential flaw for the cold leg nozzles. A factor of two would increase the limiting hot leg drain nozzle duration to 61.0 years, and the bounding cold leg nozzle to 111.2 years for flaws to grow 75% through wall. Similarly, the durations for 100% through wall flaws (growth up to 95%) would increase to 73.4 years for the hot leg drain nozzle and 132.4 years for the cold leg nozzle.

Crack Initiation Time

The original relief request [1] did not include any consideration for crack initiation. Attachment A of this report includes a calculation of the initiation time for the hot leg drain nozzle and cold leg bounding nozzle using one of the models in the xLPR program that was developed by EPRI. The calculation of initiation time based on the Palisades results shows that the time to initiation for the hot leg drain nozzle is approximately 130 years. Attachment A contains additional details regarding the calculation. Combining crack initiation time with the PWHT reduction in crack growth rate, the time for a flaw to grow to 75% through wall will approach 200 years for the hot leg drain nozzle. Using the crack initiation value for the cold leg nozzles, the time for a flaw to grow to 75% through wall would exceed 600 years.

Conclusions

Based on the assessments and calculations documented herein, it is concluded that these welds do not experience fast growing flaws due to PWSCC. The hot leg drain nozzle limiting crack growth life, not considering the benefits of PWHT or crack initiation time, is 30.5 years for a flaw to grow to 75% through wall, and 36.7 years for a flaw to grow to 100% through wall (95% through wall). Similarly, the cold leg nozzles take 55.6 years for the limiting flaw to grow to 75% through wall, and 66.2 years for 100% through wall (95% through wall). The cold leg nozzles lag the hot leg nozzle by roughly a factor of two.

It should be noted that the resulting crack growth times are specified as the duration during which the reactor is at operating pressure and temperature and not simply years since the reactor was licensed to operate. Per Reference 13, the total Effective Full Power Years (EFPY) at the end of the following refueling outage (1R25) is expected to be 28.8, which is less than the 75% through-wall crack growth time for both the hot leg nozzle and bounding cold leg nozzle.

Evaluation of the Palisades Nuclear Plant Branch Line Nozzles for Primary Water Stress
Corrosion Cracking

These crack growth lives do not consider the potential additional margin on PWSCC growth rate for PWHT or crack initiation time. Taking into account these margins would increase the time for a crack to grow to 75% or 100% through wall to almost 200 years or more. Based on this information, deferring inspections on these locations for one more plant operating cycle will not represent a decrease in nuclear safety.


References

1. Relief Request Number RR 4-18, "Proposed Alternative, Use of Alternate ASME Code Case N-770-1 Baseline Examination," PNP 2014-015, February 25, 2014.
2. Entergy Nuclear Operations, Inc. Contract Order No. 10426669, Effective Date January 1, 2015.
3. Structural Integrity Associates Calculation 1400669.310, Rev. 0, "Finite Element Model for Hot Leg Drain Nozzle."
4. Structural Integrity Associates Calculation 1400669.320, Rev. 0, "Finite Element Model Development for the Cold Leg Drain, Spray, and Charging Nozzles."
5. Structural Integrity Associates Calculation 1400669.312, Rev. 0, "Hot Leg Drain Nozzle Weld Residual Stress Analysis."
6. Structural Integrity Associates Calculation 1400669.322, Rev. 0, "Cold Leg Bounding Nozzle Weld Residual Stress Analysis."
7. Structural Integrity Associates Calculation 1400669.313, Rev. 0, "Crack Growth Analysis of the Hot Leg Drain Nozzle."
8. Structural Integrity Associates Calculation 1400669.323, Rev. 0, "Crack Growth Analysis of the Cold Leg Bounding Nozzle."
9. Letter from G. White (Dominion Engineering, Inc.) to W. Sims (Entergy), "Effect of Post-Weld Heat Treatment Applied to Alloy 82/182 Full-Penetration Branch Pipe Connection Welds at Palisades," DEI Letter L-4199-00-01, Rev. 0, dated February 25, 2014.
10. T. Cassagne, D. Caron, J. Daret, and Y. Lefèvre, "Stress Corrosion Crack Growth Rate Measurements in Alloys 600 and 182 in Primary Water Loops under Constant Load," *Proceedings of 9th International Symposium on Environmental Degradation of Materials in Nuclear Systems—Water Reactors*, The Minerals, Metals & Materials Society, Warrendale, PA, 1999, pp. 217–224.
11. S. Le Hong, J. M. Boursier, C. Amzallag, and J. Daret, "Measurements of Stress Corrosion Cracking Growth Rates in Weld Alloy 182 in Primary Water of PWR," *Proceedings of 10th International Conference on Environmental Degradation of Materials in Nuclear Power Systems—Water Reactors*, NACE International, 2002.
12. Entergy Nuclear Operation, Inc. letter PNP 2014-028, "Supplemental Response to Request for Additional Information, dated February 26, 2014, for Relief Request Number RR 4-18, Proposed Alternative, Use of Alternate ASME Code Case N-770-1 Baseline Examination," dated March 6, 2014.
13. Email from Daniel Depuydt (Entergy) to Norman Eng (SI), dated May 13, 2015, "Subject: Palisades EFPY at 1R25," includes attached file "WCAP-15353-Suppl 1 Excerpt.pdf," SI File No. 1400669.205.

Evaluation of the Palisades Nuclear Plant Branch Line Nozzles for Primary Water Stress
Corrosion Cracking

Very truly yours,

Preparer:

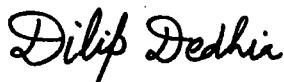


Chris S. Lohse, P.E.
Senior Consultant

5/14/2015

Date

Reviewer:



Dilip Dedhia
Senior Associate

5/14/2015

Date

Reviewer:



Norman Eng
Associate

5/14/2015

Date

Approver:



Richard A. Mattson, P.E.
Senior Associate

5/14/2015

Date

Attachment A – Crack Initiation Study

cc: R. Bax
M. Fong
C. Fourcade
F. Ku
G. Mukhim
W. Wong

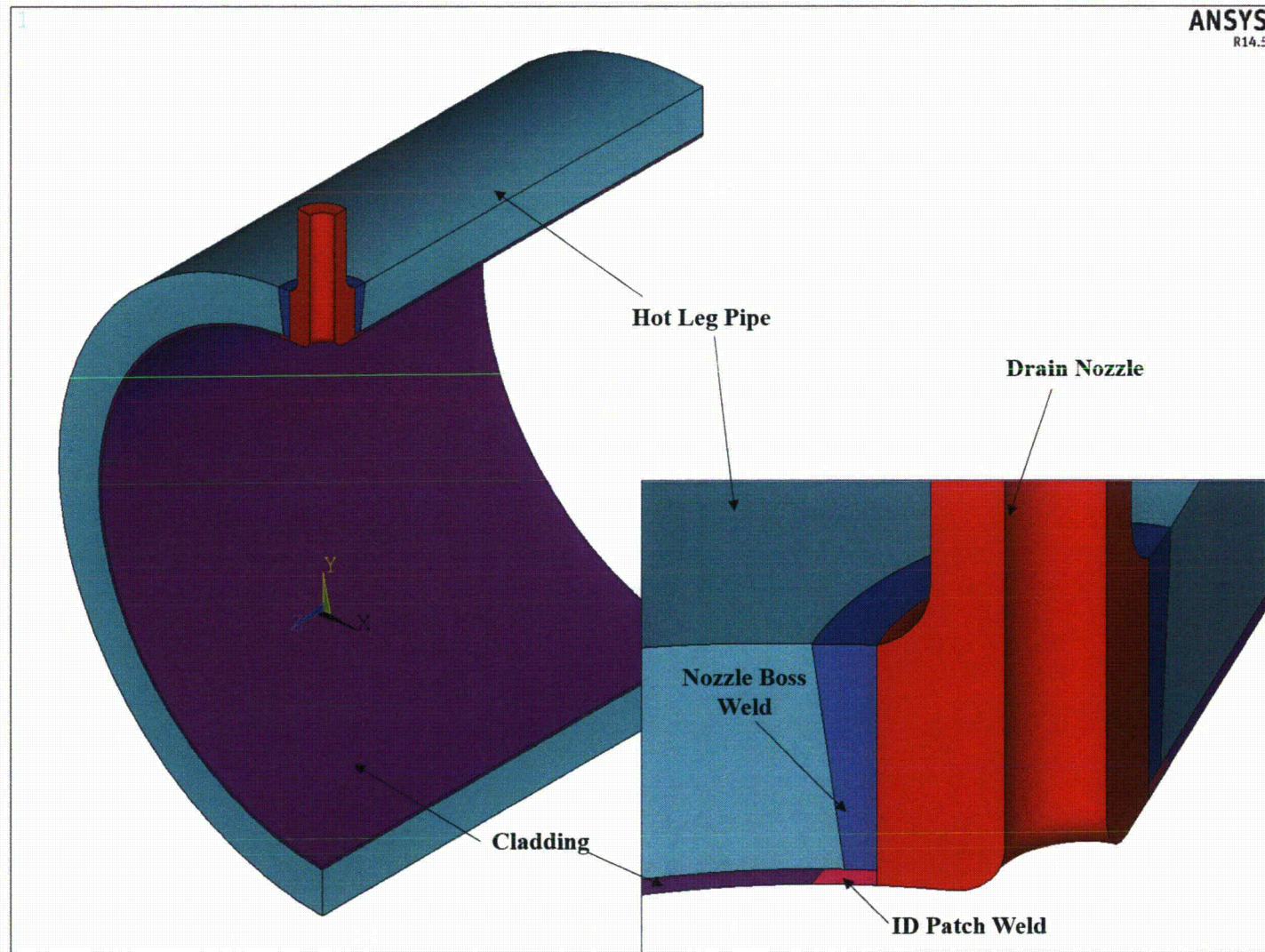


Figure 1. Components Included in the Hot Leg Drain Nozzle Finite Element Model

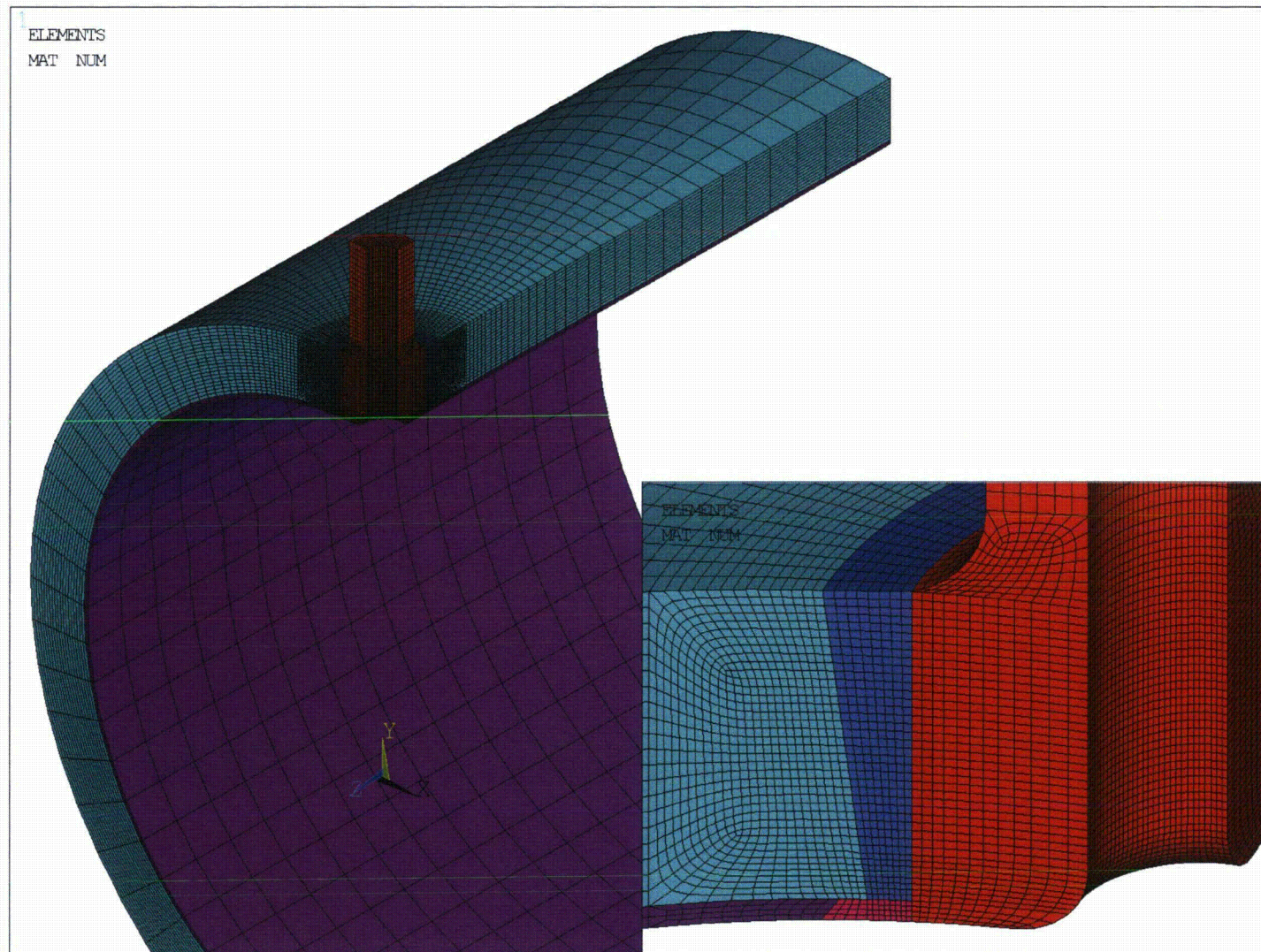


Figure 2. Isometric View of the Hot Leg Drain Nozzle Finite Element Model

Note: Nozzle weld detail is shown in the bottom right corner.

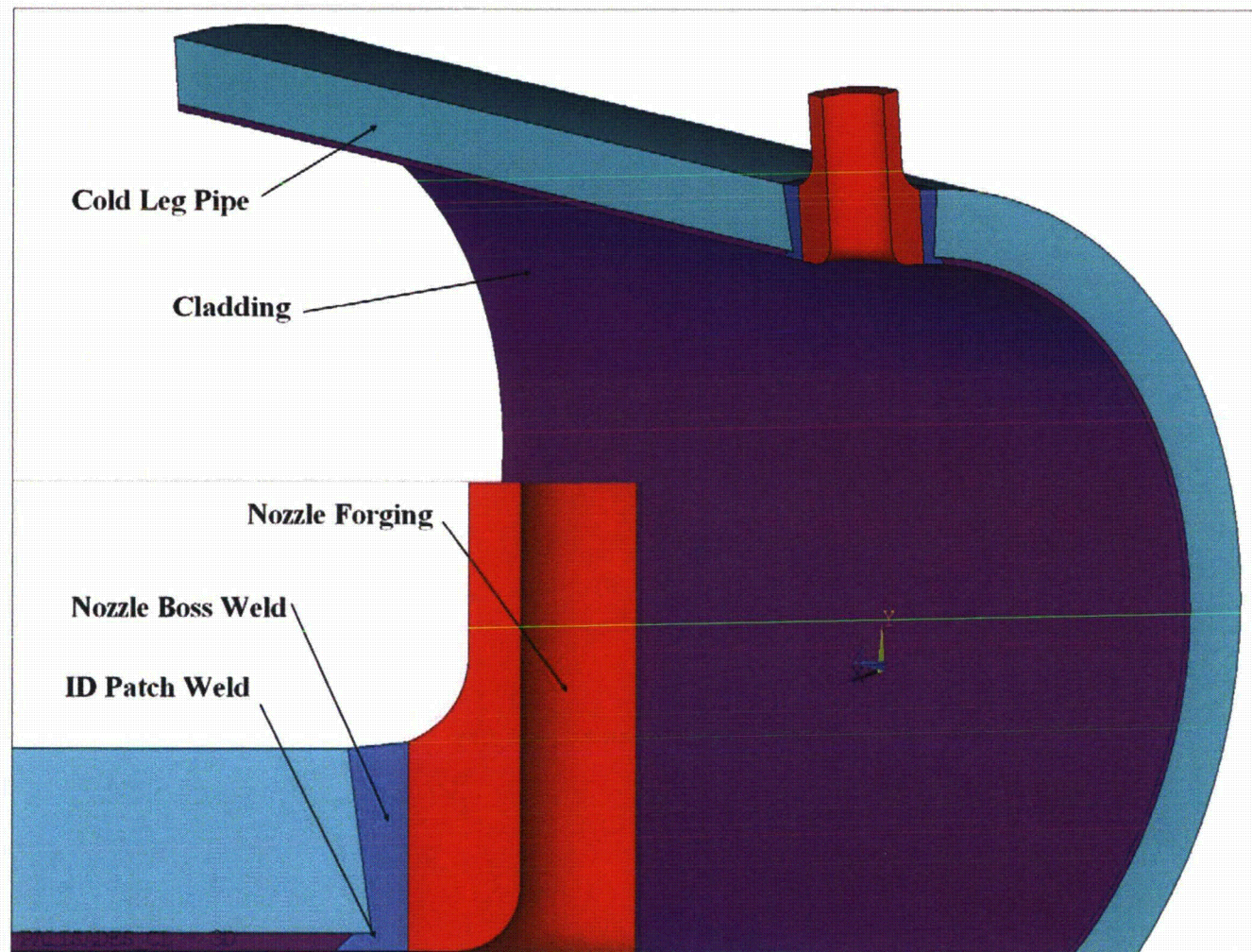


Figure 3. Components Included in the Bounding Cold Leg Nozzle Finite Element Model

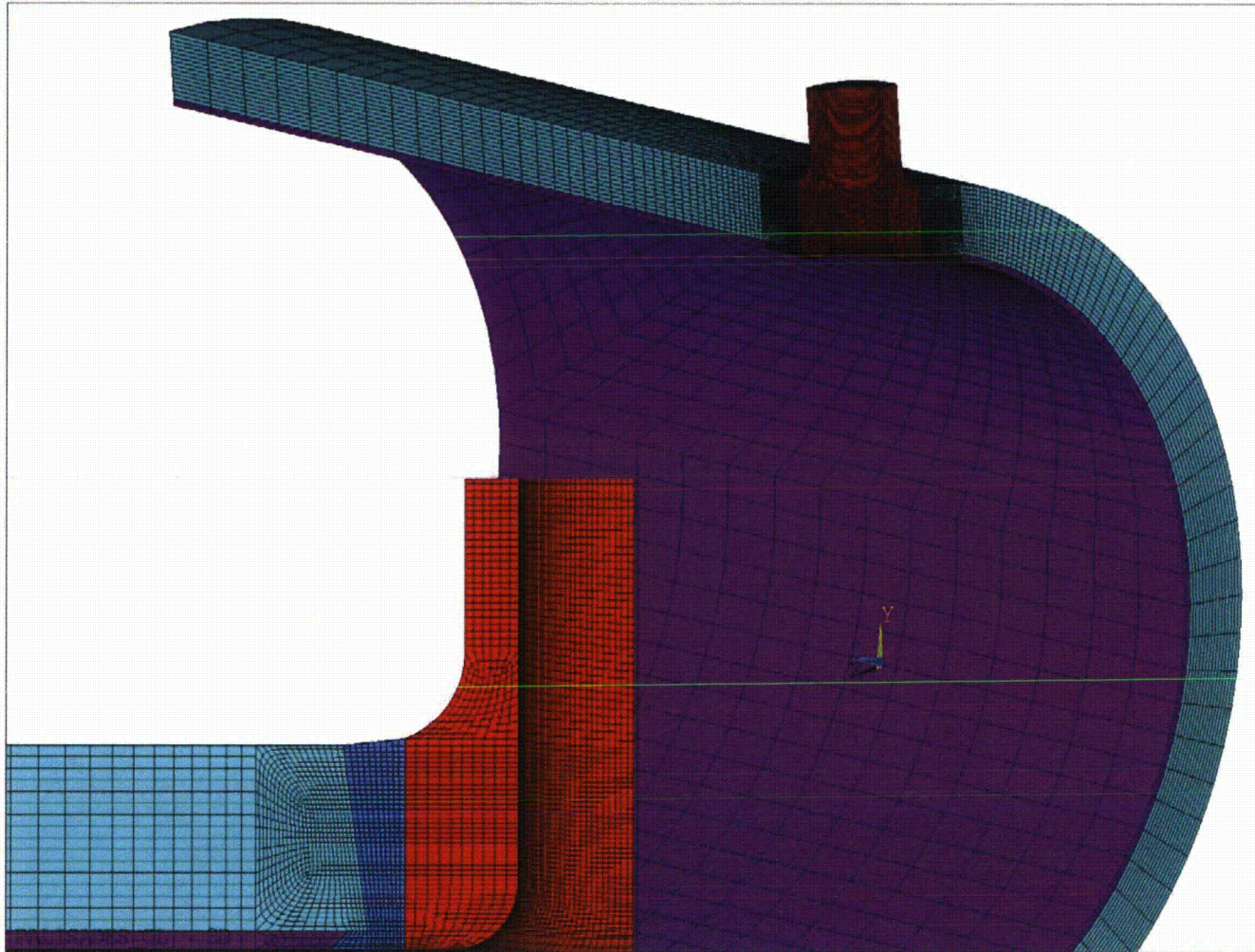


Figure 4. Isometric View of the Bounding Cold Leg Nozzle Finite Element Model

Note: Nozzle weld detail is shown in the bottom left corner.

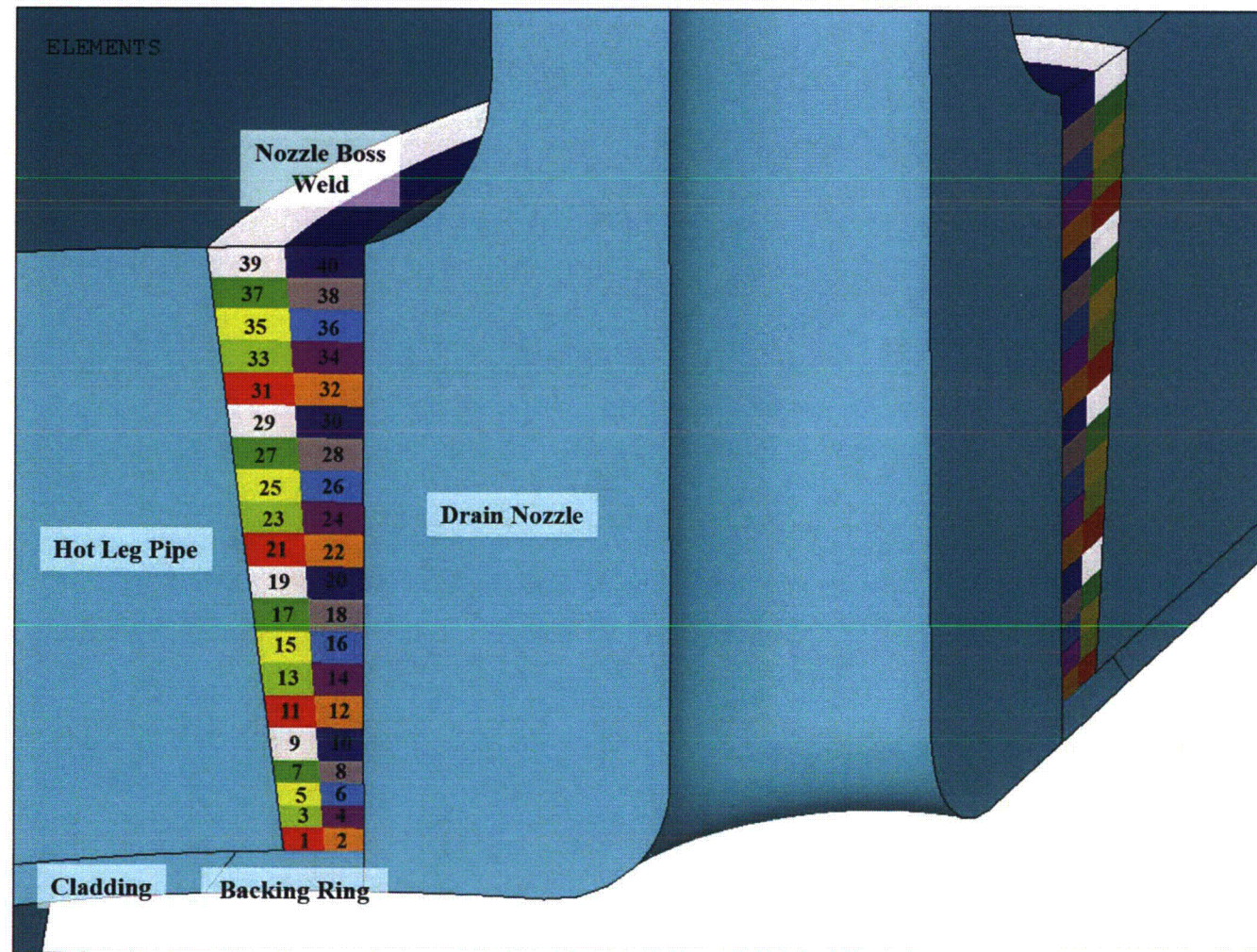


Figure 5. Weld Nugget Definitions for the Hot Leg Drain Nozzle Boss Weld

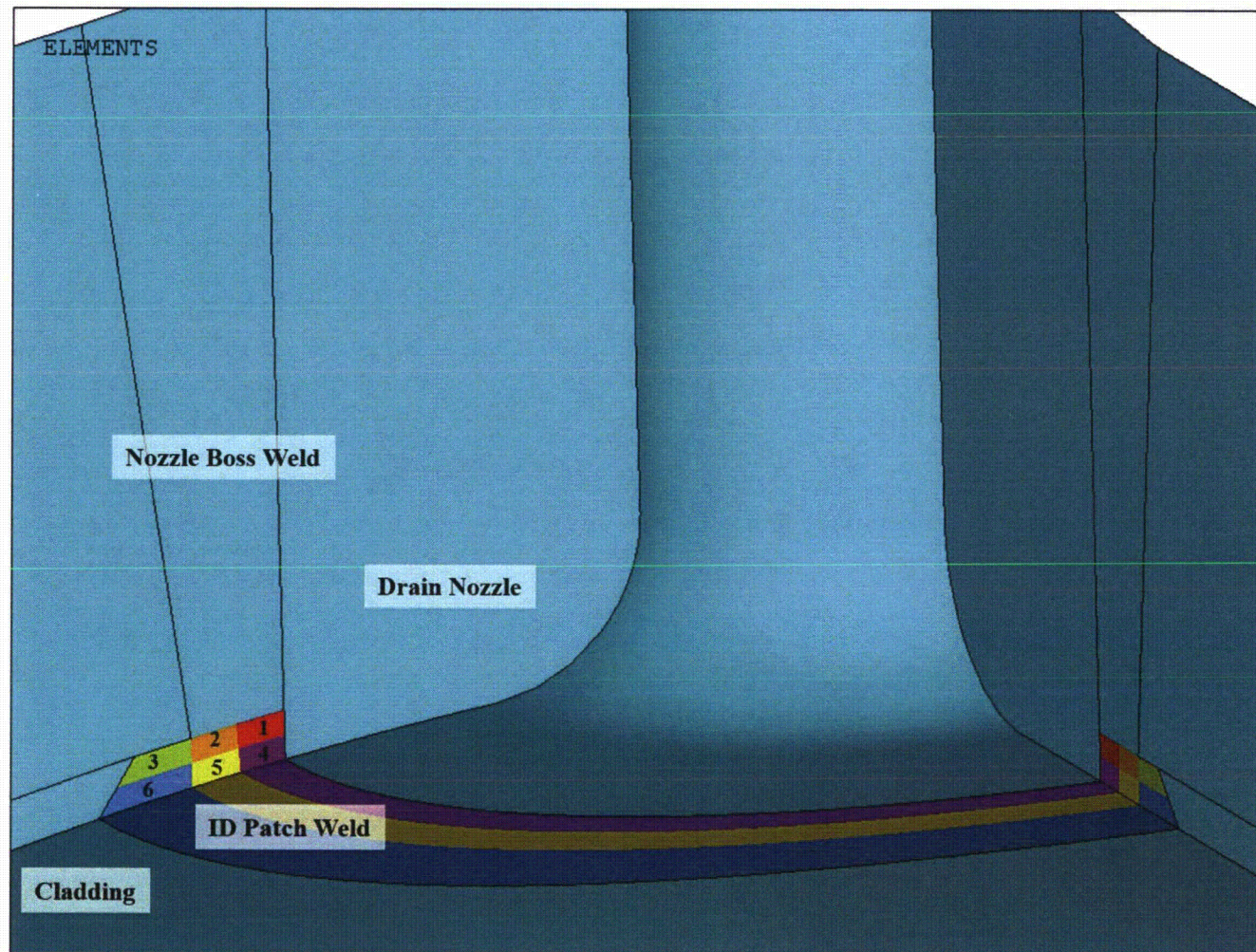


Figure 6. Weld Nugget Definitions for the Hot Leg Drain Nozzle ID Patch Weld

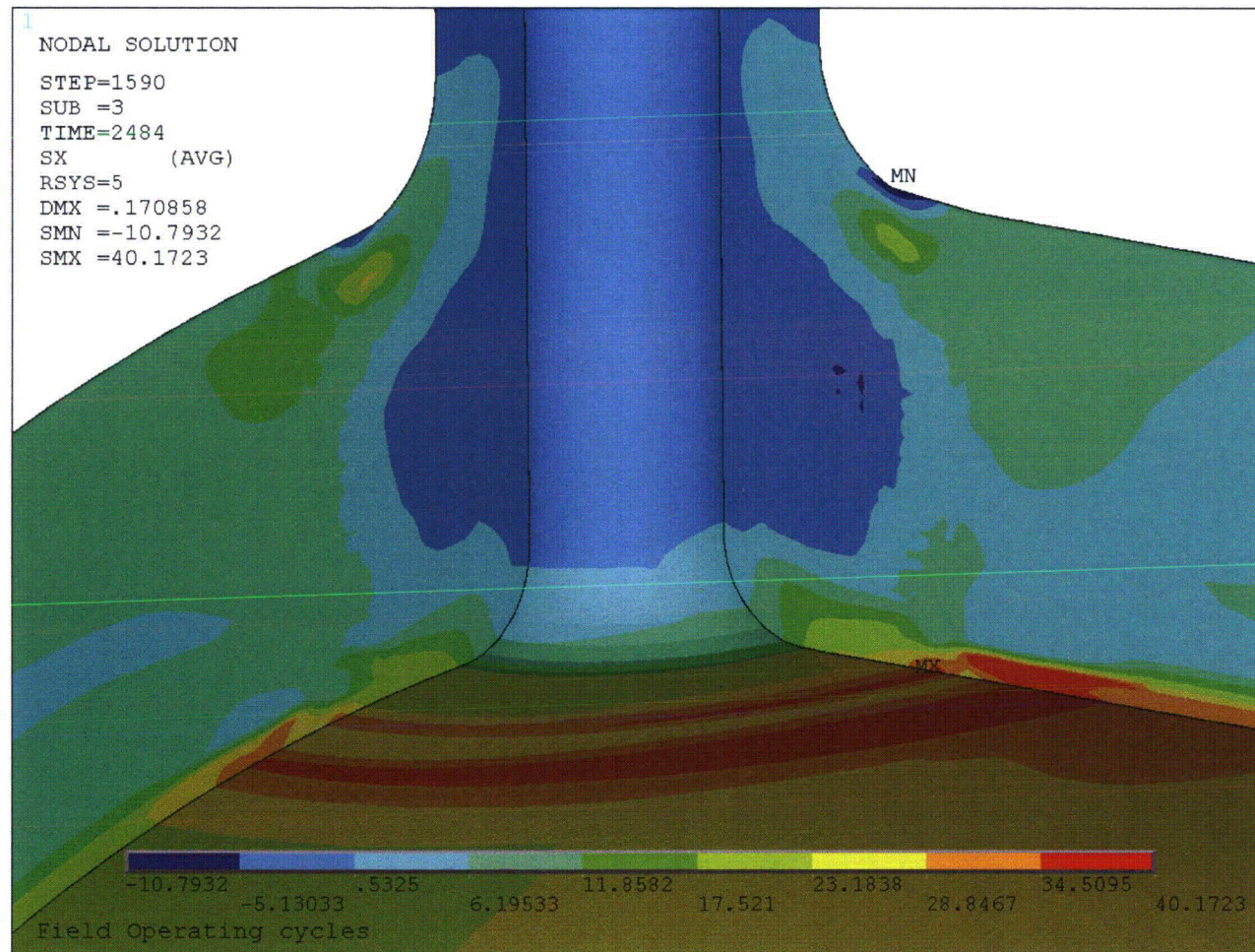


Figure 7. Radial Stresses at Operating Conditions for the Hot Leg Drain Nozzle

Note: Radial stresses are shown in the nozzle axis radial direction and units are in ksi.

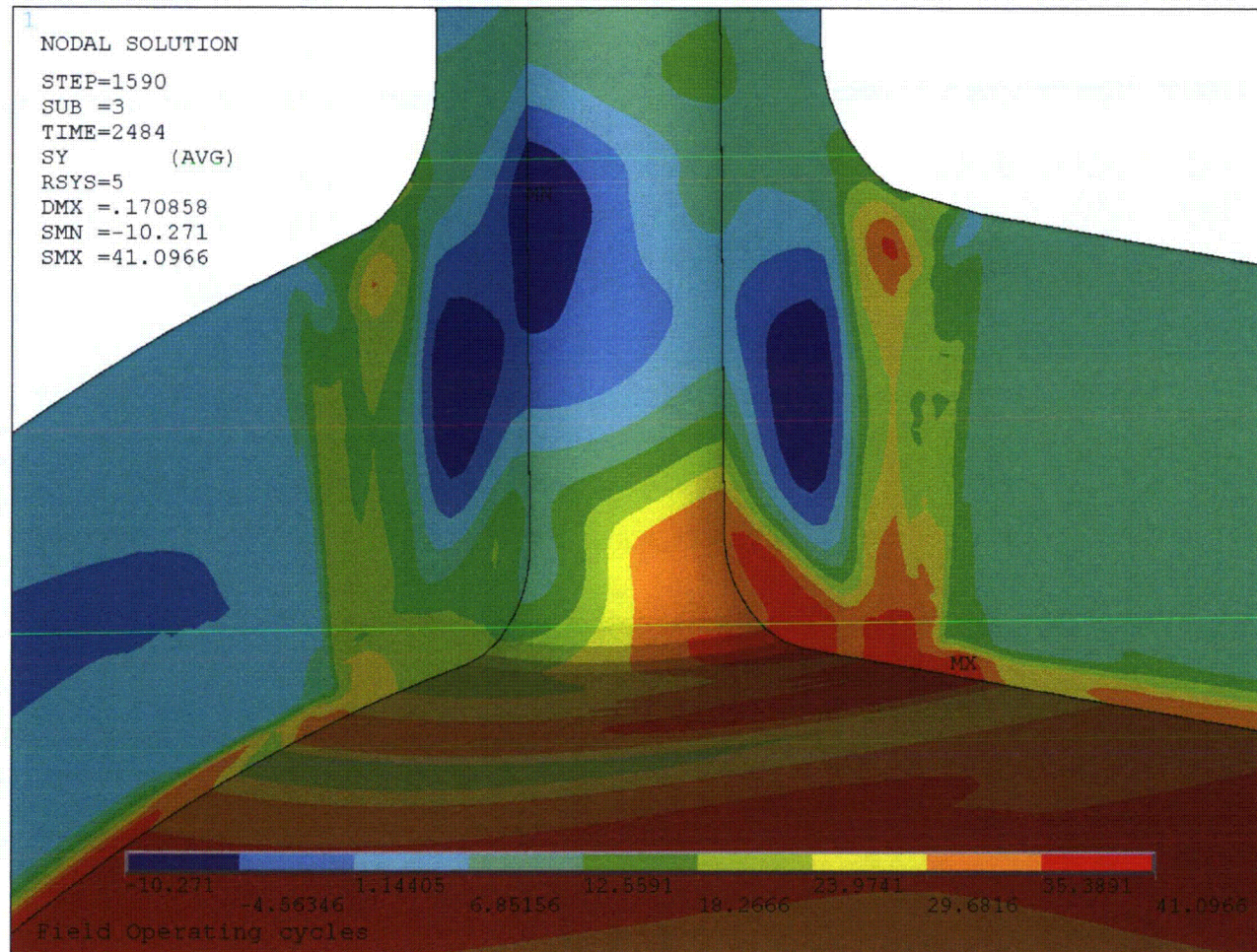


Figure 8. Circumferential Stresses at Operating Conditions for the Hot Leg Drain Nozzle

Note: Circumferential stresses are shown in the nozzle axis circumferential direction and units are in ksi.

Evaluation of the Palisades Nuclear Plant Branch Line Nozzles for Primary Water Stress Corrosion Cracking

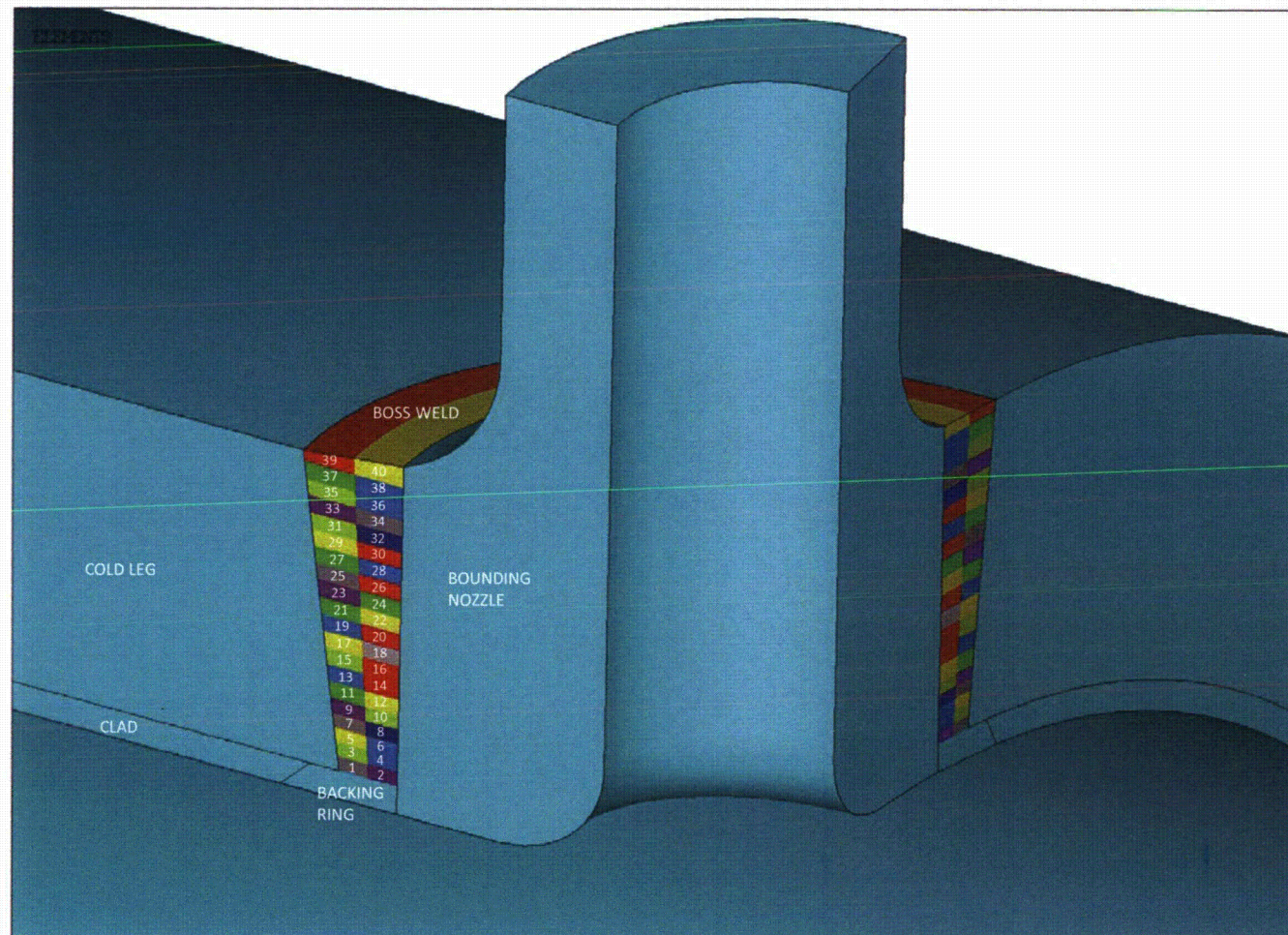


Figure 9. Weld Nugget Definitions for the Bounding Cold Leg Nozzle Boss Weld

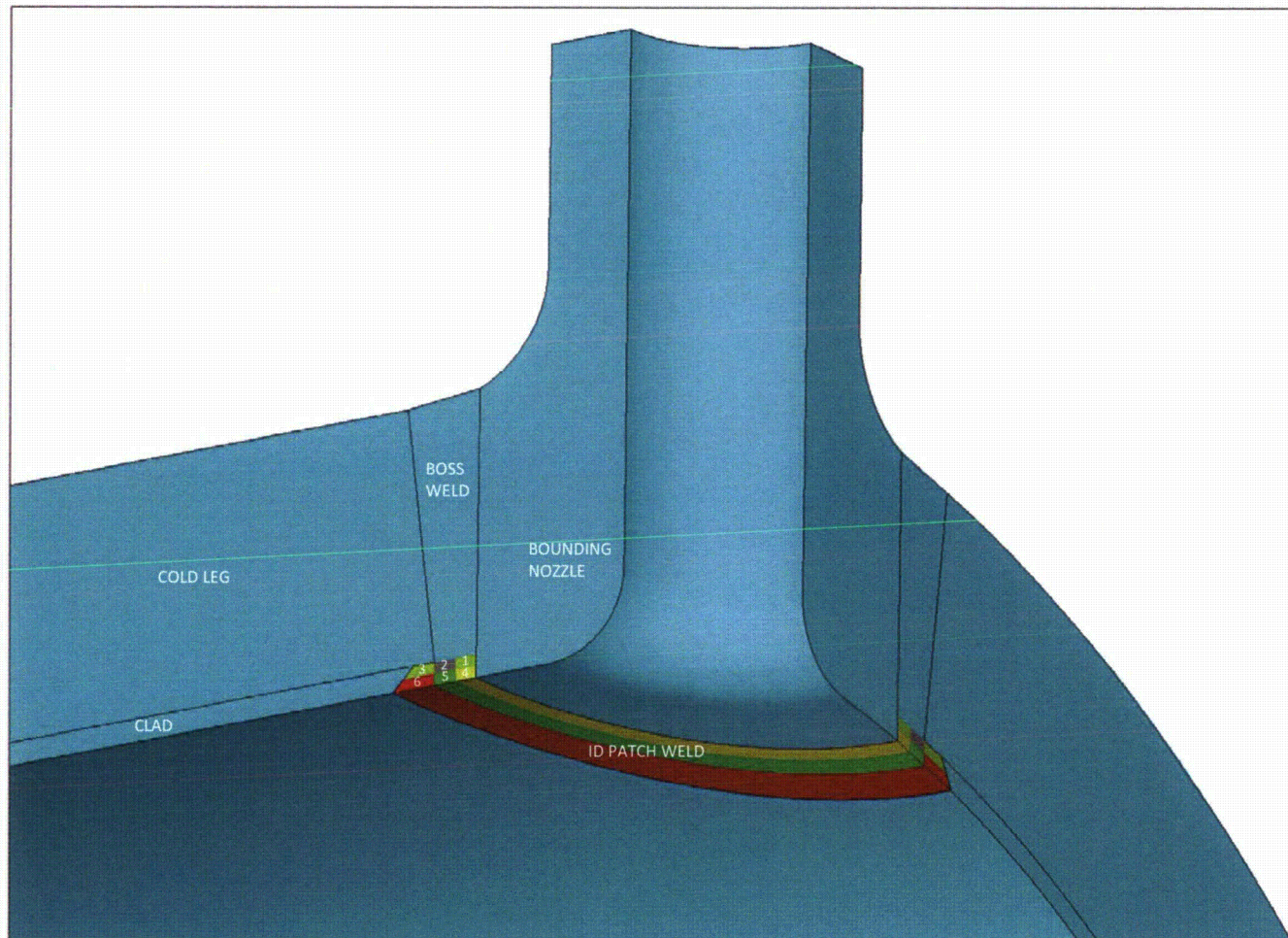


Figure 10. Weld Nugget Definitions for the Bounding Cold Leg Nozzle ID Patch Weld

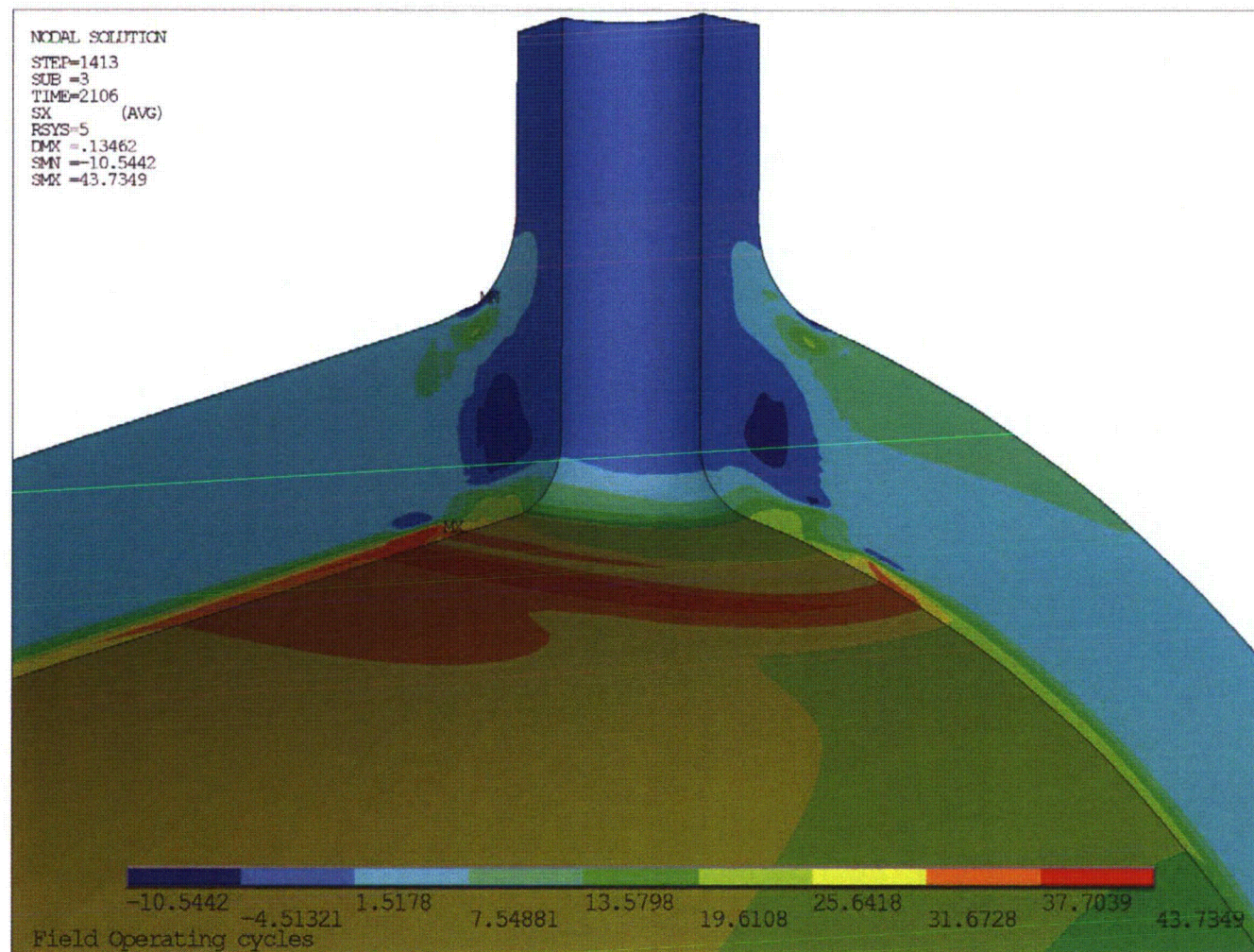


Figure 11. Radial Stresses at Operating Conditions for the Bounding Cold Leg Nozzle

Note: Radial stresses are shown in the nozzle axis radial direction and units are in ksi.

Evaluation of the Palisades Nuclear Plant Branch Line Nozzles for Primary Water Stress Corrosion Cracking

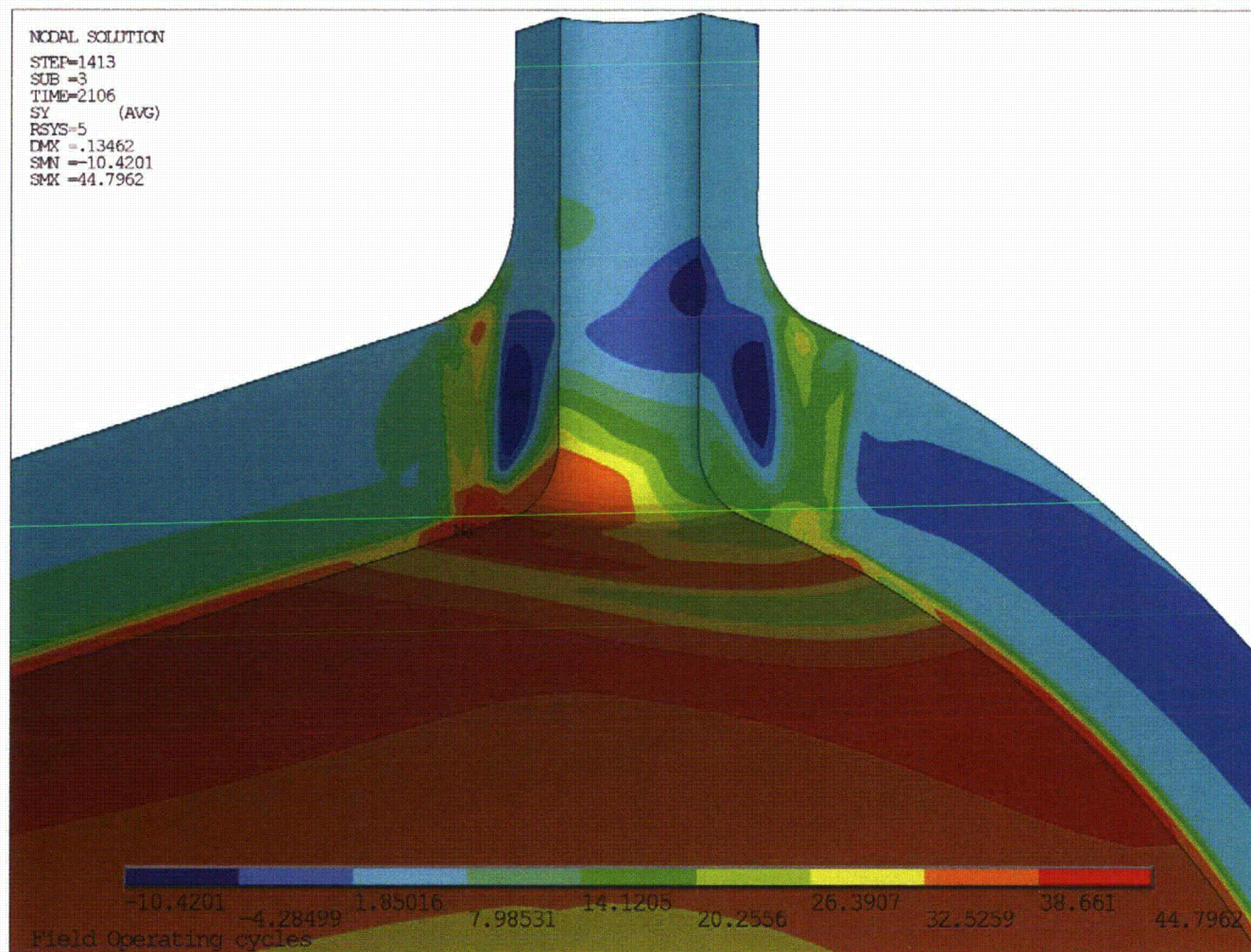


Figure 12. Circumferential Stresses at Operating Conditions for the Bounding Cold Leg Nozzle
Note: Circumferential stresses are shown in the nozzle axis circumferential direction and units are in ksi.

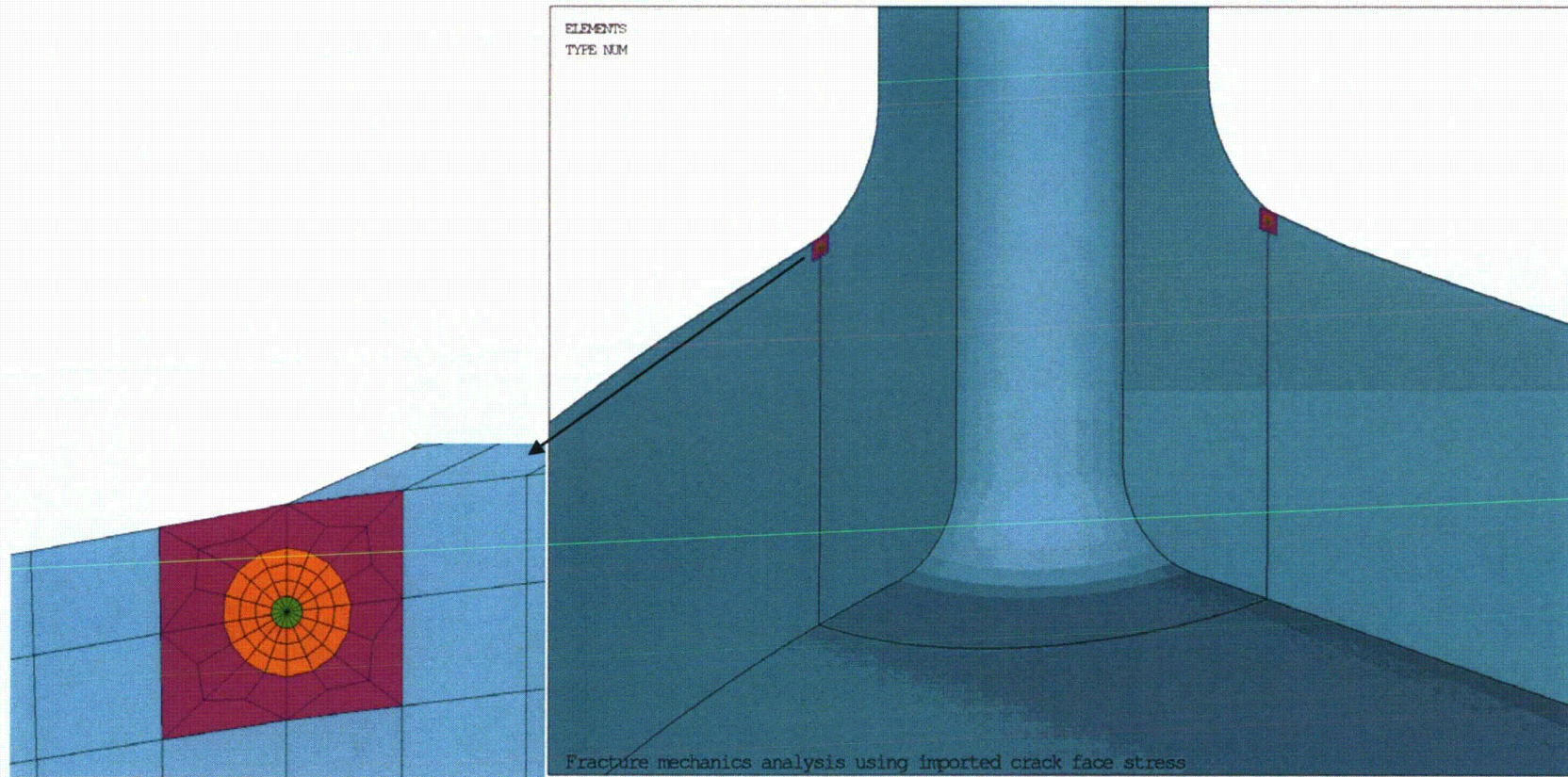


Figure 13. Circumferential Flaw with Crack Tip Elements Inserted for the Hot Leg Drain Nozzle

Note: Deepest circumferential flaw is shown as an example.

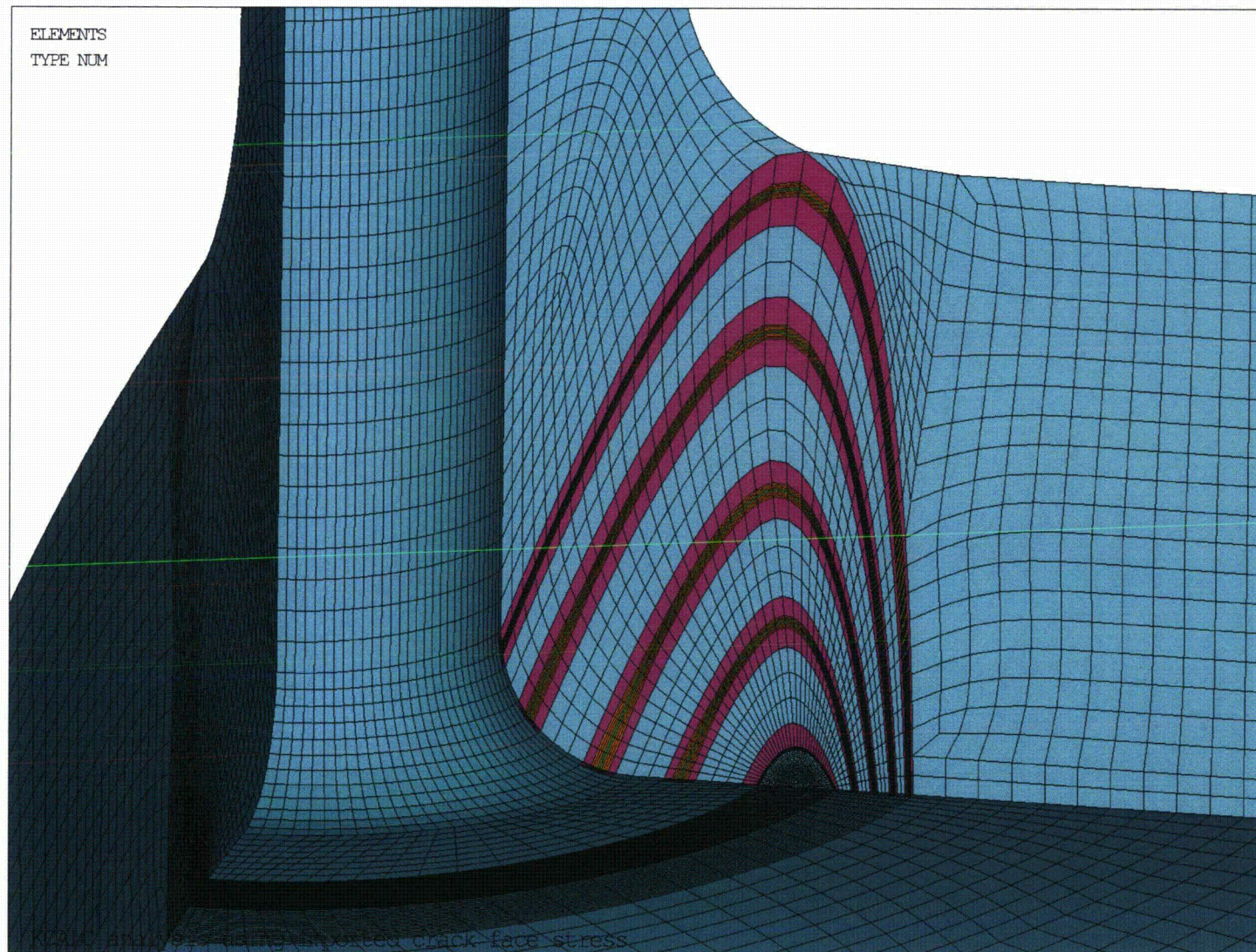


Figure 14. Axial Flaws on the 0° Face with Crack Tip Elements Inserted for the Hot Leg Drain Nozzle

Note: Only the 0° axial flaws are shown. The 90° flaws are similar.

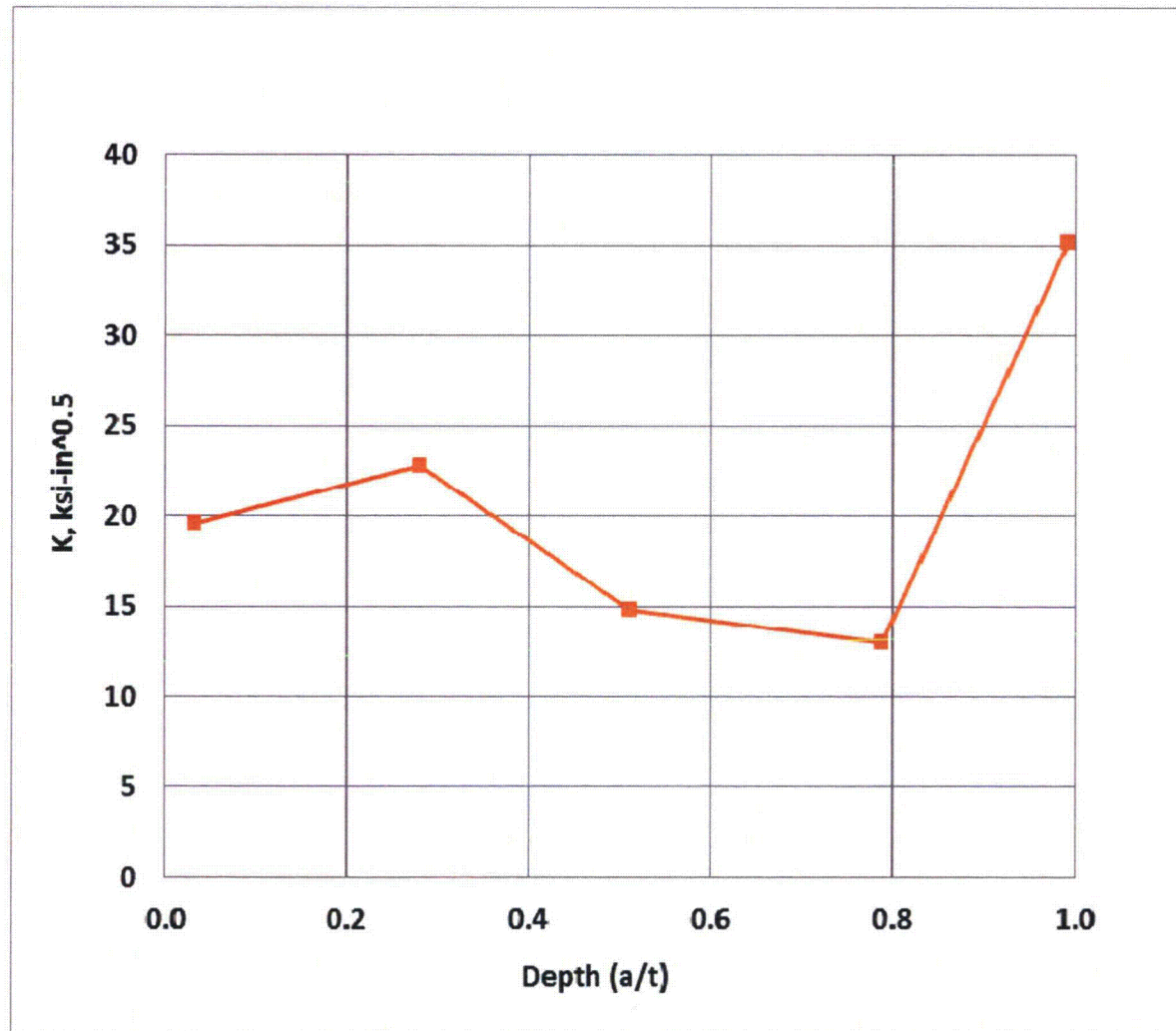


Figure 15. Stress Intensity Factors as a Function of Depth for the Hot Leg Drain Nozzle Circumferential Flaws

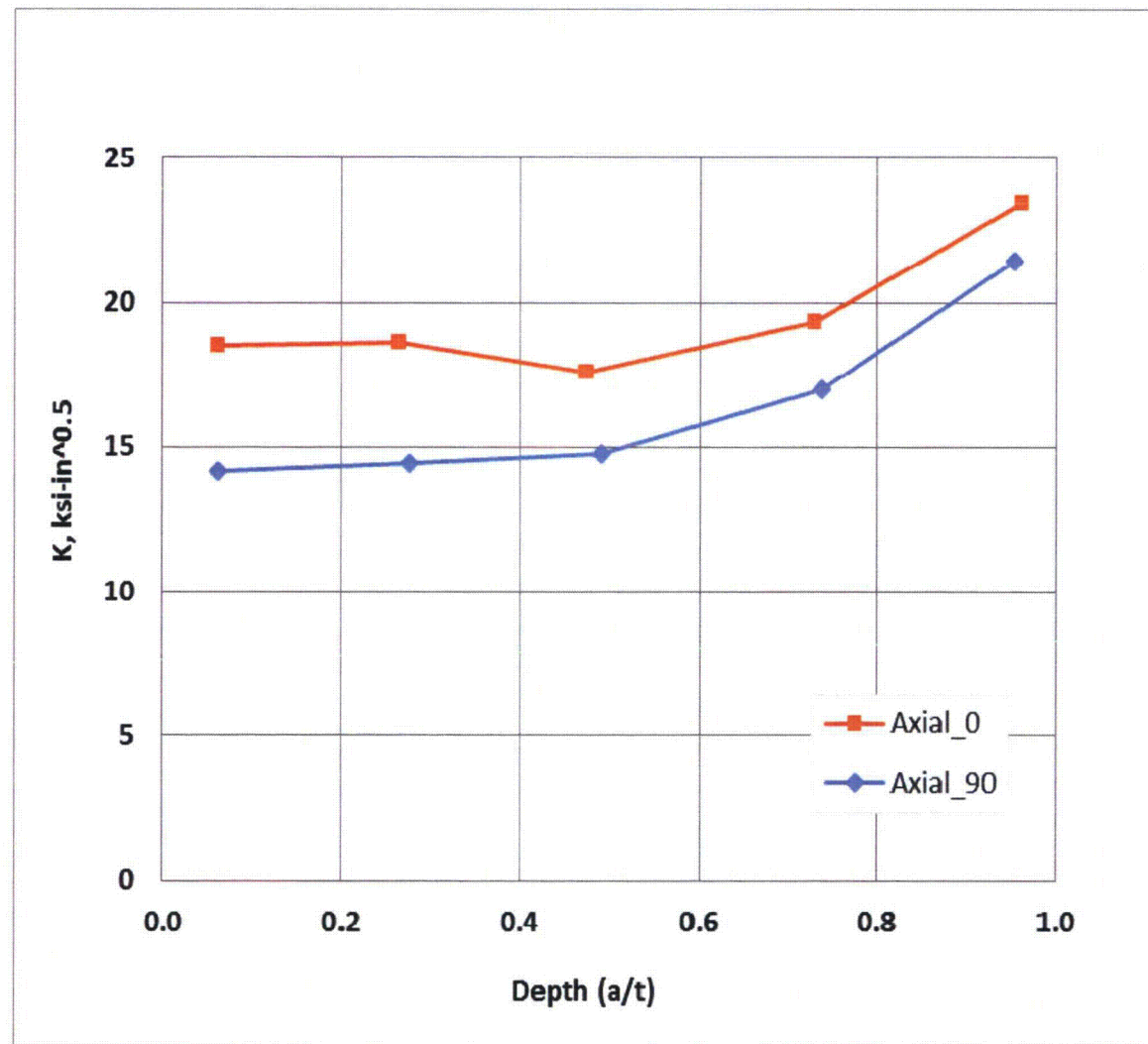


Figure 16. Stress Intensity Factors as a Function of Depth for the Hot Leg Drain Nozzle Axial Flaws

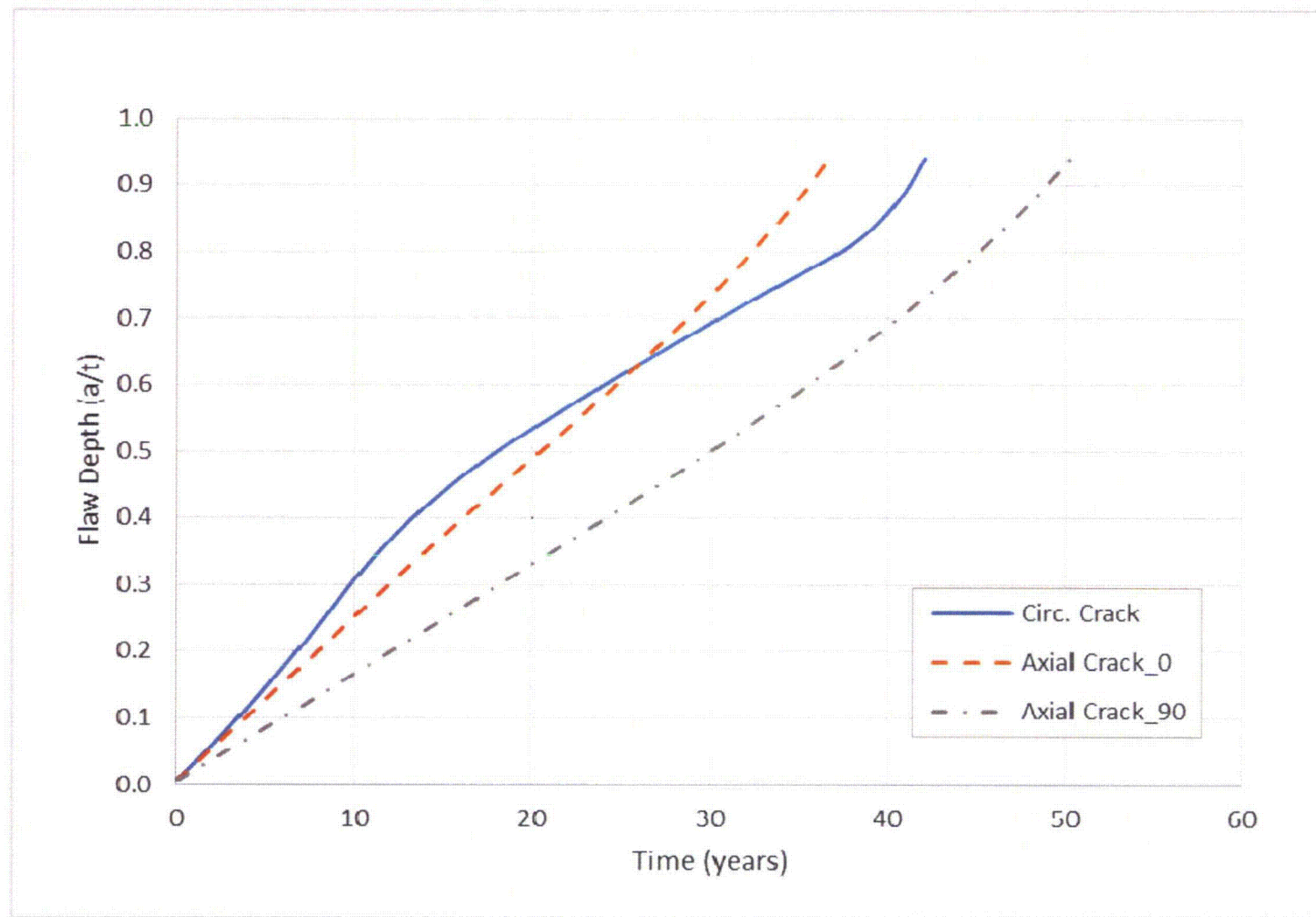


Figure 17. Crack Growth for All Flaw Types in the Hot Leg Drain Nozzle (Initial Flaw of 0.025")

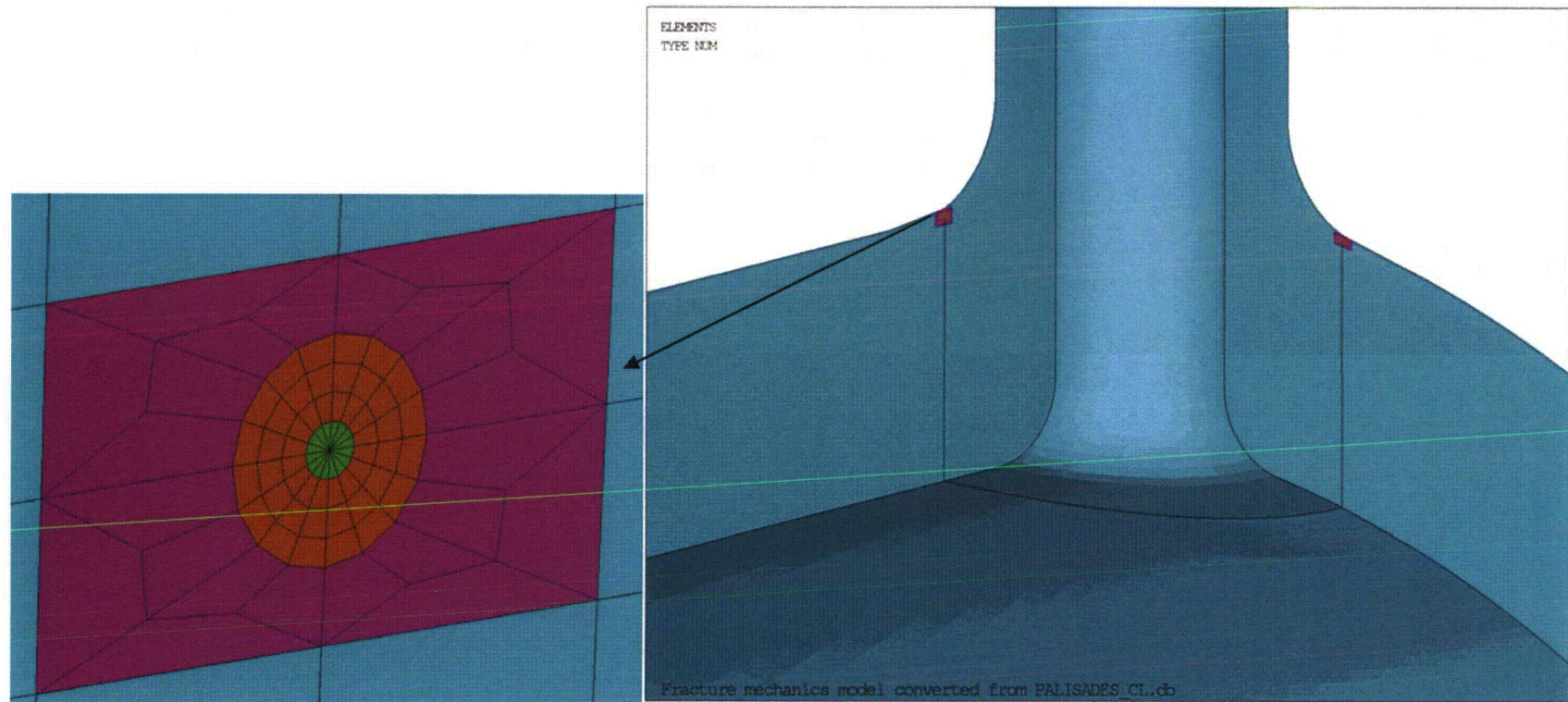


Figure 18. Circumferential Flaw with Crack Tip Elements Inserted for the Bounding Cold Leg Nozzle

Note: Deepest circumferential flaw is shown as an example.

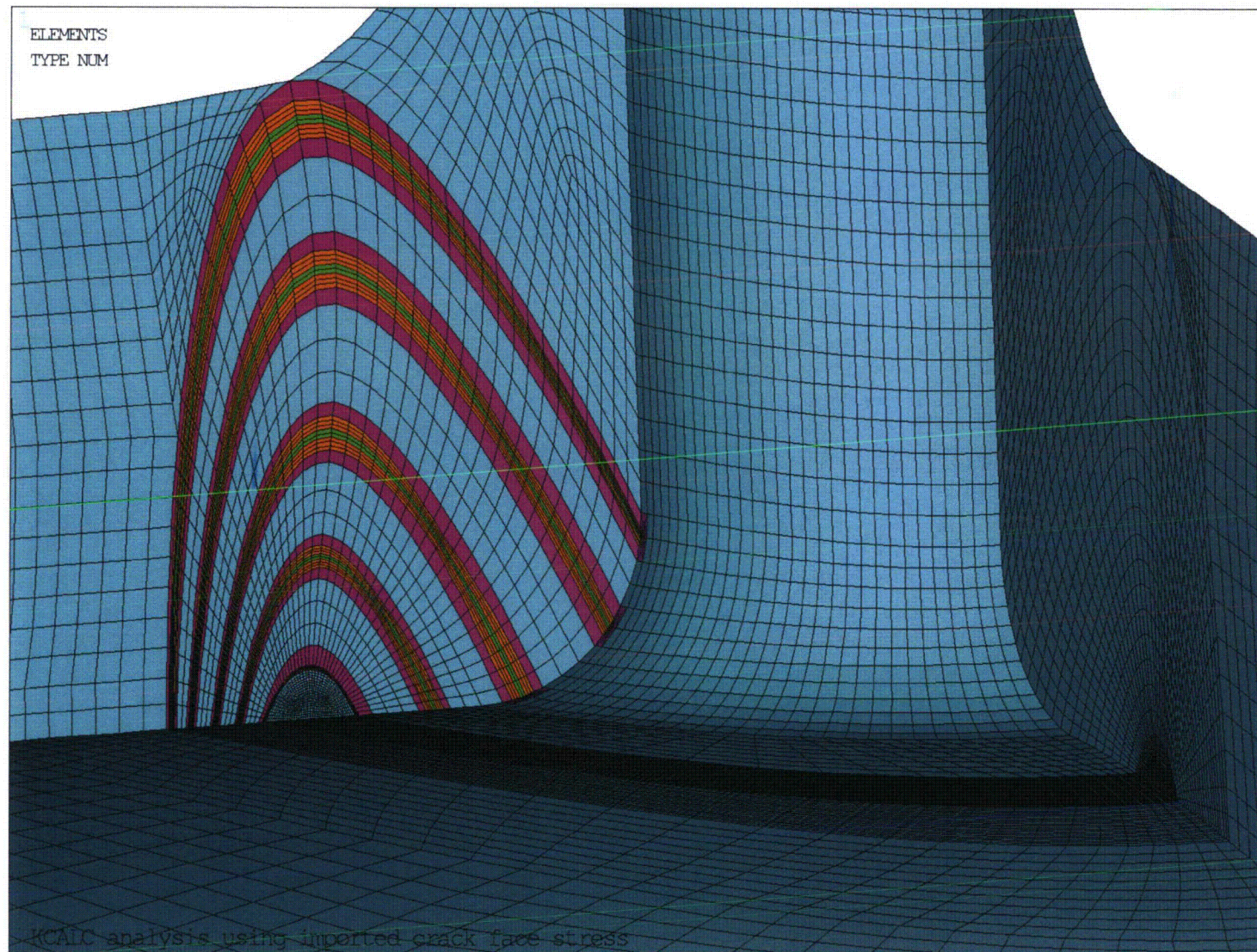


Figure 19. Axial Flaws on the 0° Face with Crack Tip Elements Inserted for the Bounding Cold Leg Nozzle

Note: Only the 0° axial flaws are shown. The 90° flaws are similar.

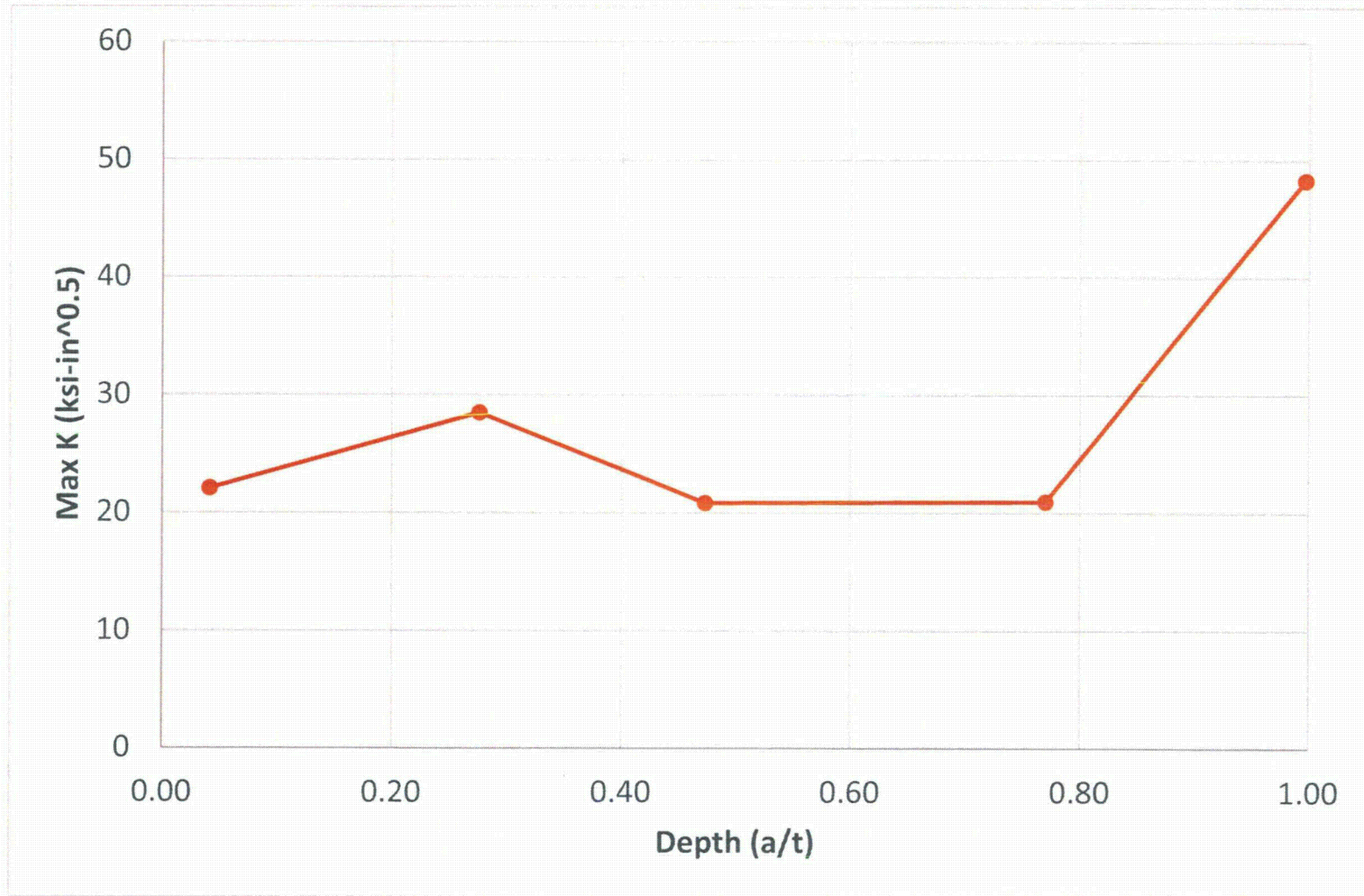


Figure 20. Stress Intensity Factors as a Function of Depth for the Bounding Cold Leg Nozzle Circumferential Flaws

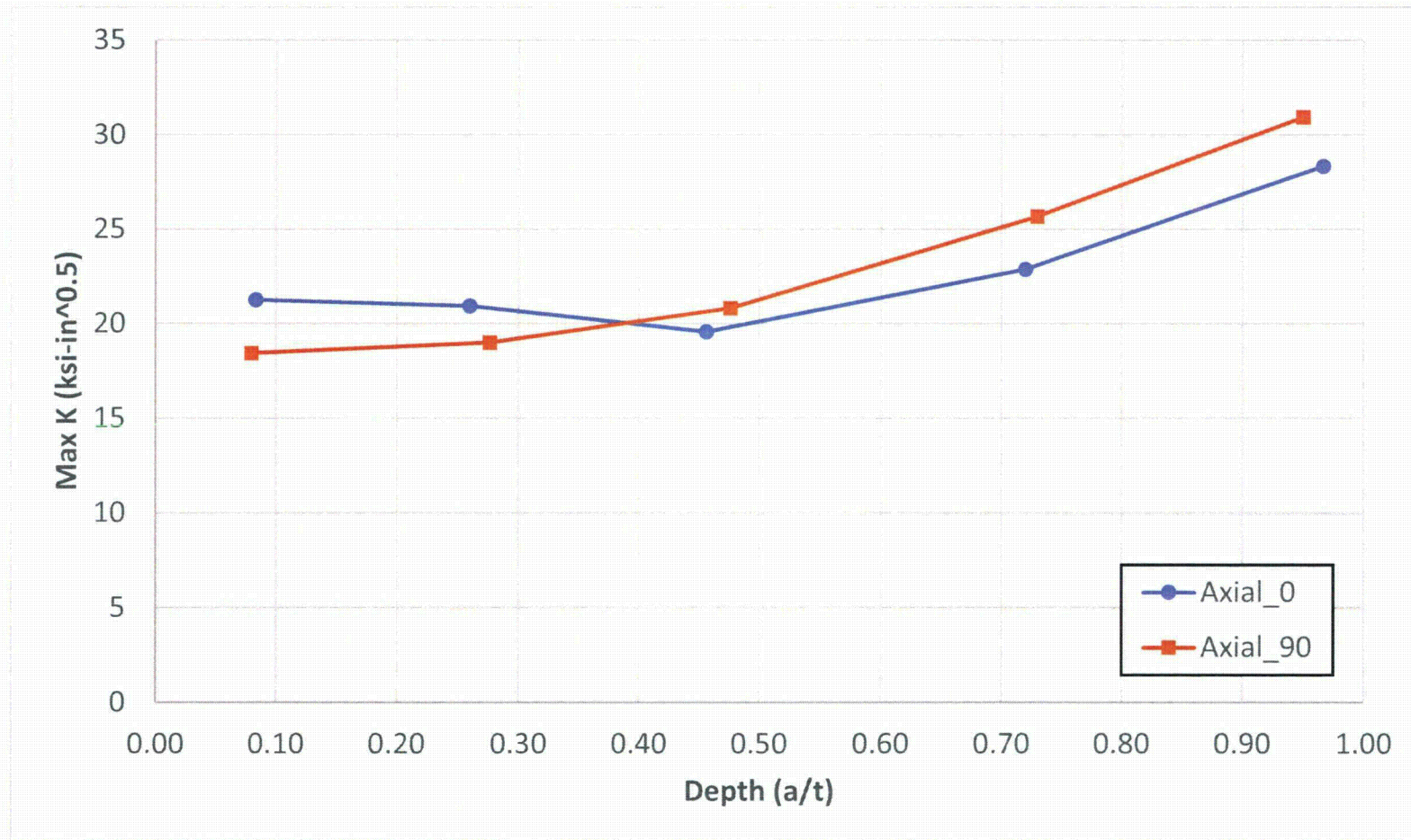


Figure 21. Stress Intensity Factors as a Function of Depth for the Bounding Cold Leg Nozzle Axial Flaws

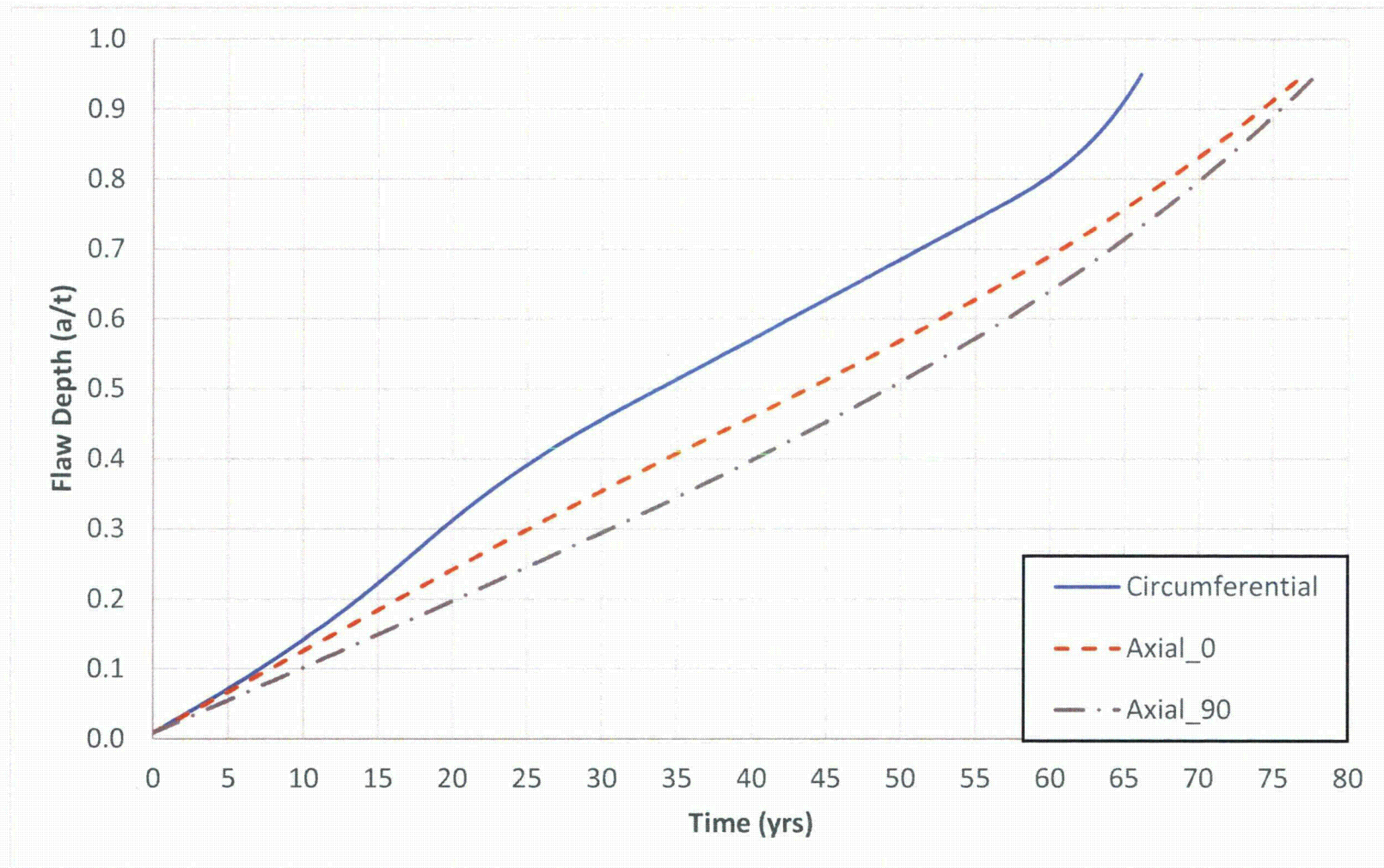


Figure 22. Crack Growth for All Flaw Types in the Bounding Cold Leg Nozzle (Initial Flaw of 0.025")

Attachment A Crack Initiation Study

Introduction

The crack growth evaluations performed for relief request RR 4-18 did not include any calculation of initiation times for the hot leg drain nozzle. The evaluations only included a crack growth evaluation starting from day one of operation of the plant. This is conservative as some time is required for cracks to initiate prior to PWSCC growth occurring. This section calculates initiation time for the hot leg drain nozzle and the bounding cold leg nozzle using the module developed for the xLPR program. The xLPR program is a joint venture between the industry and the NRC to address the extreme low probability of rupture for Alloy 82/182 piping welds in PWR plants.

Initiation Model

xLPR reviewed a number of initiation models as part of the program. The xLPR Version 1.0 code used one model that was benchmarked for use on Alloy 82/182 weld material. The model used was named Direct Model 2 and was developed by EPRI in Report No. 1019032 [2]. It was benchmarked for use for Alloy 82/182 material and the inputs for use are in the xLPR Version 1.0 report by EPRI [1]. The model calculates the initiation time based on the material properties (yield and ultimate strength), temperature, and surface stress. The model also has two threshold stresses. The first is the stress initiation threshold (σ_{th}) where if the surface stress is less, no initiation will be predicted. The equations below calculate this initiation threshold. All equations presented in this section are rearranged from those provided in Reference 2 for ease of use and presentation.

$$\begin{aligned}\sigma_{th} &= z\sigma_{ys} \\ z &= z_1 + z_2 \ln(\xi) \\ \xi &= \frac{\sigma_{ult}}{\sigma_{ys}}\end{aligned}$$

where

$$\begin{aligned}\sigma_{ys} &= \text{local yield stress (input)} \\ \sigma_{ult} &= \text{local ultimate stress (input)} \\ z_1, z_2 &= \text{CW-SCC threshold parameters (input)}\end{aligned}$$

Additionally, there is a maximum stress (σ_{max}) where initiation would occur instantly. This value is calculated using the following equations.

$$\sigma_{\max} = D\sigma_{ys}$$

$$D = v \cdot e^{w\zeta}$$

$$\zeta = \frac{\sigma_{ult}}{\sigma_{ys}}$$

where

v, w = cold work microcracking resistance parameters (input)

For the evaluation documented herein, the stresses are between the minimum and maximum threshold values. Therefore, the time to initiation is calculated using the following equations.

$$t_{INI,nom} = BGe^{Q/RT} \ln \left[\frac{D-z}{\frac{\sigma}{\sigma_{ys}} - z} \right]$$

where

$$G = m^{-q} \frac{\ln(D)}{\ln\left(\frac{D-z}{1-z}\right)}$$

$$D = v \cdot e^{w\zeta}$$

$$z = z_1 + z_2 \ln(\zeta)$$

$$m = k \left(\frac{\sigma_{ys}}{E} \right)^a (\zeta - 1)^b (\zeta)^c$$

$$\zeta = \frac{\sigma_{ult}}{\sigma_{ys}}$$

and

$$\begin{aligned} t_{INI,nom} &= \text{initiation time under fixed set of conditions (output)} \\ T &= \text{temperature (input)} \end{aligned}$$

σ	=	surface stress (input)
E	=	local elastic modulus (input)
Q	=	activation energy for initiation (input)
R	=	universal gas constant (input)
B	=	proportionality constant (input)
q	=	environment-cold-work exponent (input)
a, b, c, k	=	general cold work parameters (input)

The inputs for the Palisades specific configurations are given below. Note that approximate values are taken for some of the physical properties of the material (E , yield strength, and ultimate strength). The actual values are close, and the differences here lead to insignificant changes in the results. The B value is a distribution in the Reference 1 report as xLPR is a probabilistic program. For this deterministic analysis, a conservative value was taken by using the 95% lower bound based on the inputs in Reference 1 (Appendix D).

The B value is a log normal distribution with values given below [1, Appendix D]:

Mean = $1.20\text{e-}9$ hours $\rightarrow 1.37\text{e-}13$ years (is equal to $e^{-29.62}$)

Standard deviation (heat to heat) = 1.607

Standard deviation (within heat) = 0.555

Overall standard deviation = $\sqrt{1.607^2 + 0.555^2} = 1.70$

The 95% percentile is 1.65 standard deviations away from the mean.

$95^{\text{th}} = -29.62 - (1.65 \cdot 1.70) = -32.425 \rightarrow e^{-32.425} = 8.3\text{e-}15$ (in units of years)

$T = 583^\circ\text{F}$ (hot leg) (from body of report)

$T = 537^\circ\text{F}$ (cold leg) (from body of report)

Hot Leg Circumferential Surface Stress = ~ 41 ksi (see Figure 8 in the body of this report)

Cold Leg Circumferential Surface Stress = ~ 45 ksi (see Figure 12 in the body of this report)

$E = 29\text{e}6$ psi [3, at approximately 583°F (Hot Leg) and 537°F (Cold Leg)] the actual value at the operating temperatures are slightly below $29\text{e}6$ psi. The difference will have an insignificant impact on the results.

$Q/R = 22,000$ K [1, Appendix D]

$B = 8.3\text{e-}15$ years (calculated above)

$q = 0.375$ [2, Table 5-4]

$a = 0.25$ [2, Table 5-4]

$b = -0.75$ [2, Table 5-4]

$c = -0.25$ [2, Table 5-4]

$k = 10$ [2, Table 5-4]

$z_1 = 0.35$ [2, Table 5-4]

$z_2 = 0.333$ [2, Table 5-4]

$v = 0.66$ [2, Table 5-4]

$w = 0.5$ [2, Table 5-4]

Yield Strength = 32,000 psi used (30,000 psi is the approximate value at 583°F (Hot Leg) [3] and 30,200 psi is the approximate value at 537°F (Cold Leg) [3]). Using 32,000 psi is conservative as it reduces the time to initiation.

Ultimate Strength = 80,000 psi [3, at approximately 583°F (Hot Leg) and 537°F (Cold Leg)]

Calculations

The model was used with Palisades' specific information to calculate the time to initiation. For the hot leg drain nozzle, the surface stress of 41 ksi (shown in Figure 8, page 15 of this report) and the hot leg temperature are used in the model to calculate the time to initiation. Figure A-1 shows the plot for this case. The plot shows the initiation time for a given surface stress. For the 41 ksi stress of the hot leg drain nozzle, the initiation time is roughly 130 years.

For the bounding cold leg nozzle, the surface stress of 45 ksi (shown in Figure 12, page 19 of this report) and the cold leg temperature are used in the model to calculate the time to initiation. Figure A-2 shows the plot for this case. The plot shows the initiation time for a given surface stress. For the 45 ksi stress of the bounding cold leg nozzle, the initiation time is roughly 600 years, 4.6 times longer than the hot leg drain nozzle despite the slightly higher surface stress.

For comparison, various different temperatures are considered to put the hot leg drain nozzle and bounding cold leg nozzle in perspective with other typical PWR plant components that have seen actual cracking in the industry.

The Palisades hot leg temperature is fairly low when compared to other PWR plants in the industry. Other PWR plants typically operate at a hot leg temperature above 600°F. For comparison, a hot leg temperature of 604°F is evaluated and compared to the hot leg drain nozzle at Palisades. The results of this comparison are presented in Figure A-3. Additionally, the hottest plant components are more susceptible to cracking. For PWR plants, susceptible locations exist in the pressurizer that operates at around 653°F. Figure A-4 shows the plot for initiation at the pressurizer temperature.

It should also be noted that most locations that have experienced cracking in the industry did not receive a PWHT. Therefore, the residual stresses for these other locations would have higher residual stresses, on the order of ~50 – 60 ksi. Looking at these higher stresses from the hot leg or pressurizer initiation plots shows that the time to initiation for these locations would be roughly 30 and 5 years for the hot leg and pressurizer, respectively (approximate values taken at 55 ksi surface stress).

Using the Palisades hot leg drain nozzle surface stress (41 ksi) for comparison, the higher hot leg temperature of 604°F would reduce the time to initiation by a factor of over 2 when compared to the Palisades temperature (~130 years vs. ~60 years). Comparing the Palisades hot leg drain nozzle results to a pressurizer temperature shows a factor of ~10 for time to initiation (~130 years vs. ~12 years). This shows the extreme temperature dependence related to initiation. For the Palisades hot leg drain nozzle, the lower temperature gives the location at least a factor of 2 over other hot leg locations in PWR plants.

References

1. *Materials Reliability Program: Models and Inputs Selected for Use in the xLPR Pilot Study (MRP-302)*, EPRI, Palo Alto, CA: 2010, 1022528.
2. *Stress Corrosion Cracking Initiation Model for Stainless Steel and Nickel Alloys: Effects of Cold Work*, EPRI, Palo Alto, CA: 2009, 1019032.
3. ASME Boiler and Pressure Vessel Code, Section II, Part D, "Material Properties," 2004 Editions with no Addenda.

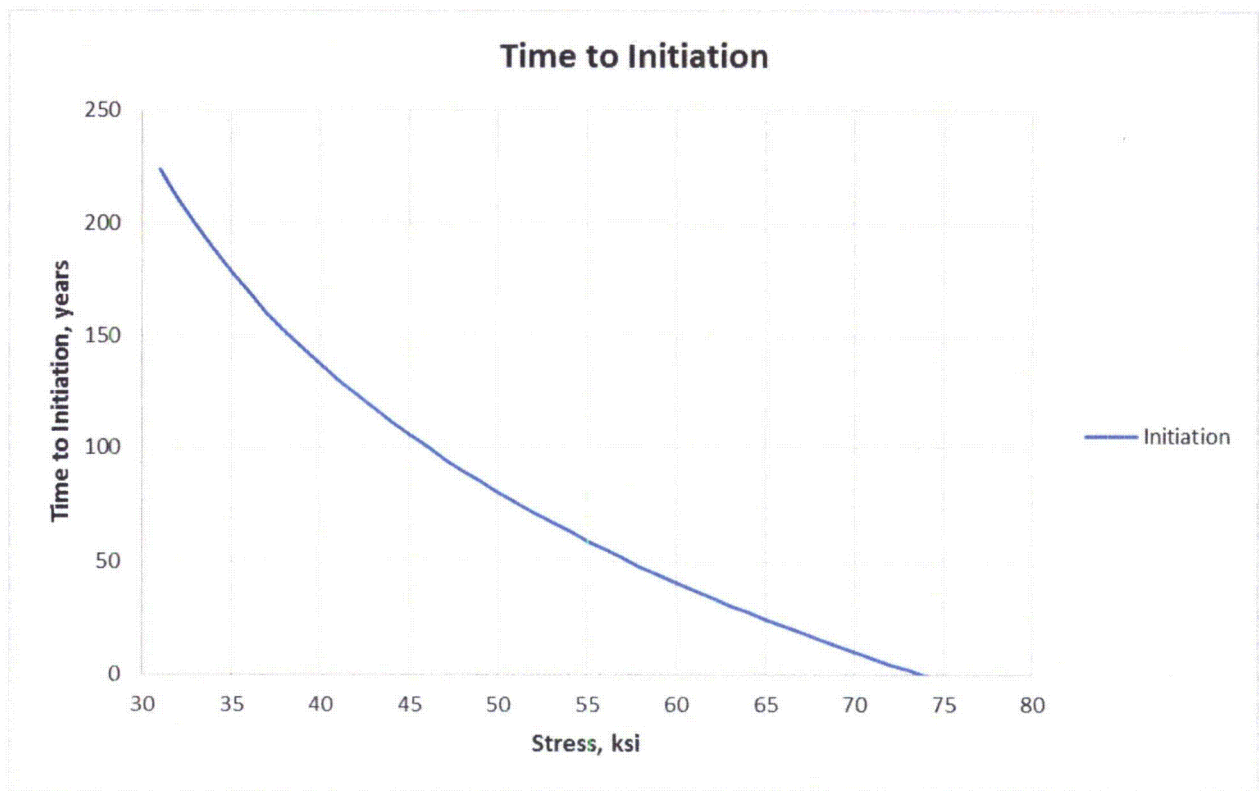


Figure A-1. Initiation Time for Palisades Hot Leg Drain Nozzle at the Hot Leg Temperature of 583°F

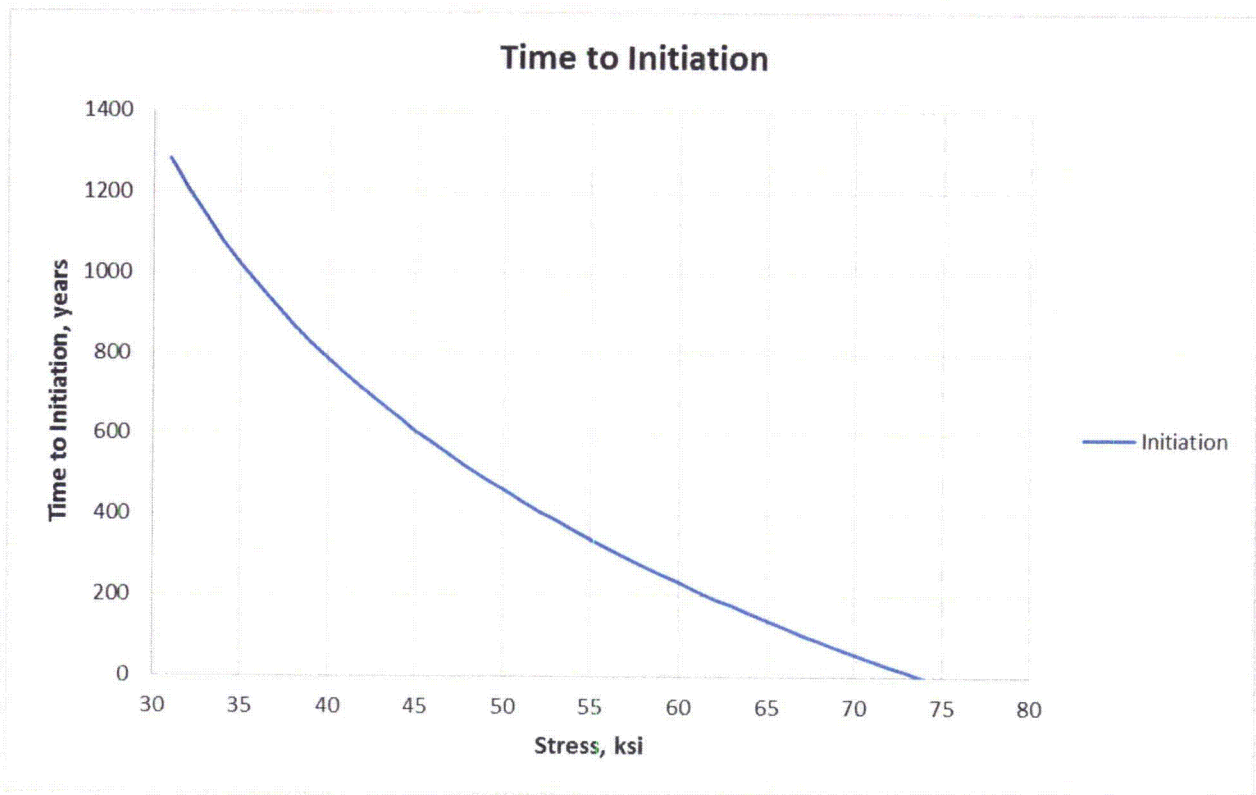


Figure A-2. Initiation Time for Palisades Bounding Cold Leg Nozzle at the Cold Leg Temperature of 537°F

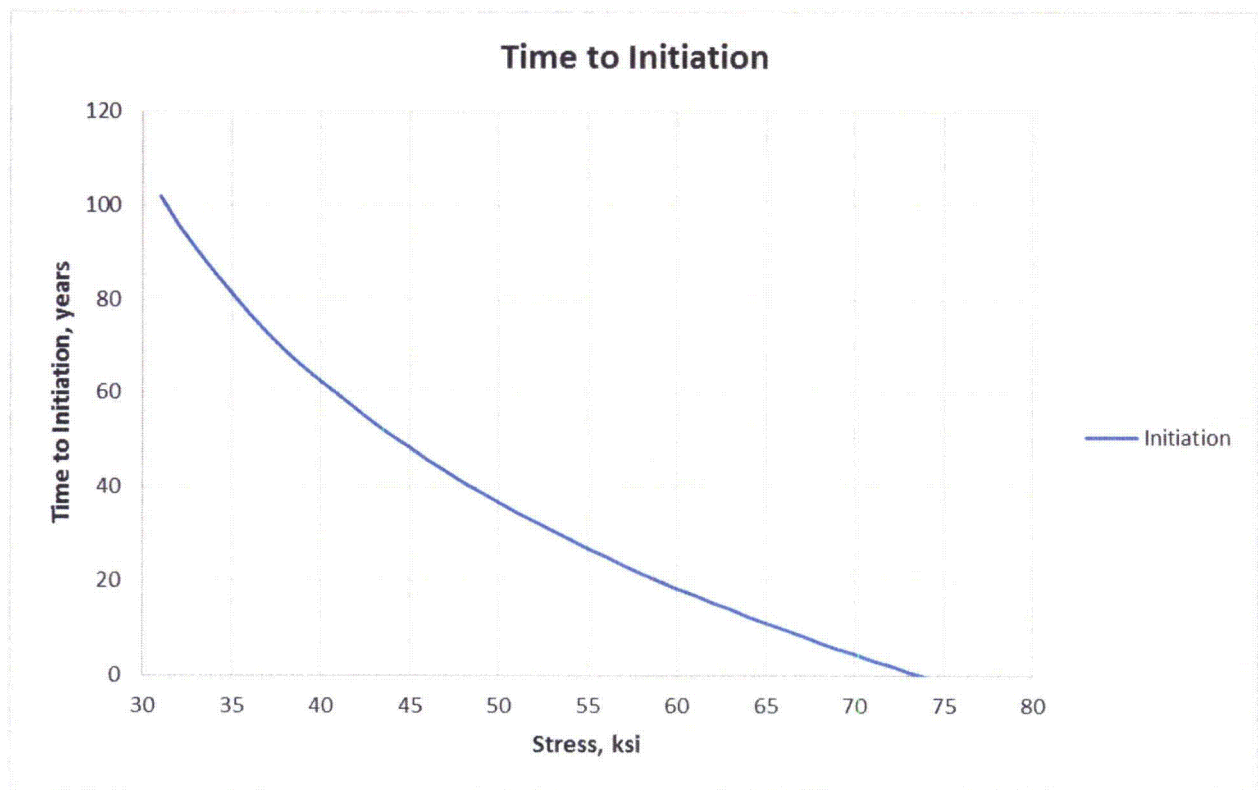


Figure A-3. Initiation Time for Typical Hot Leg Temperature of 604°F

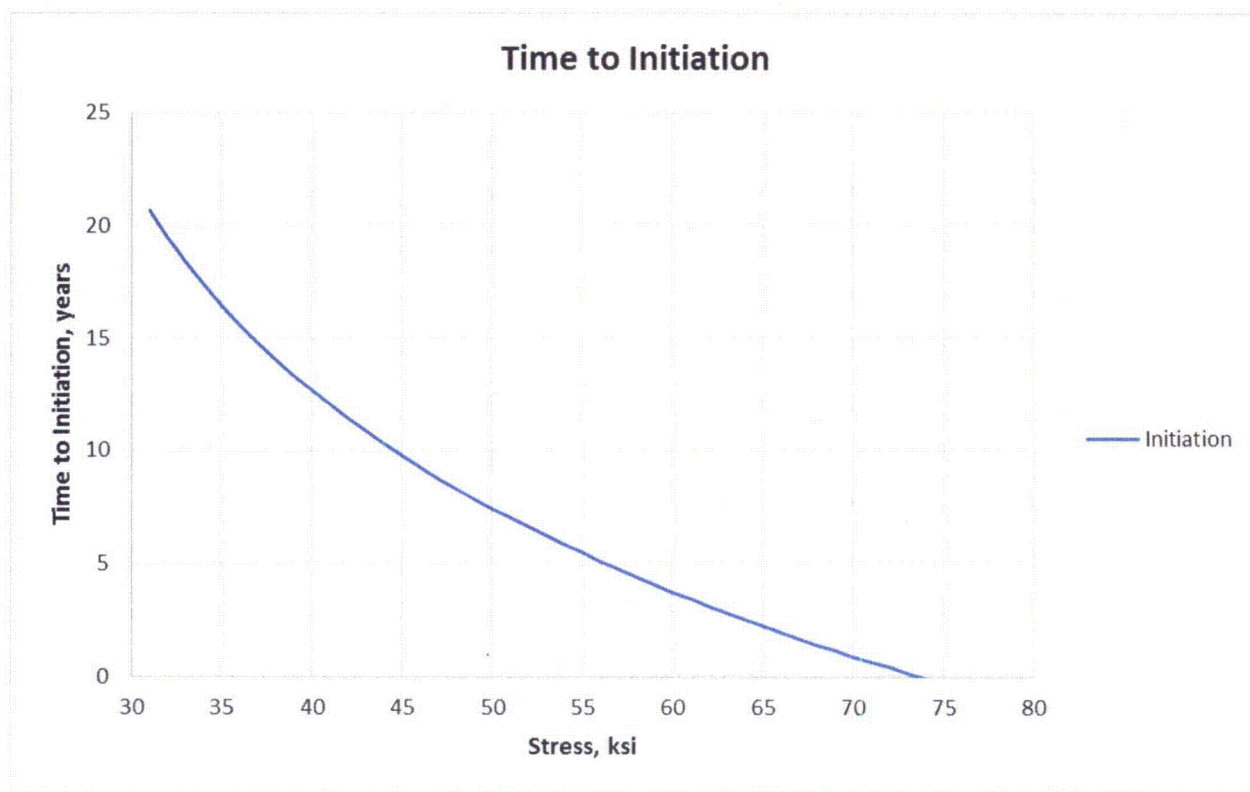


Figure A-4. Initiation Time for Typical Pressurizer Temperature of 653°F



Structural Integrity Associates, Inc.®

CALCULATION PACKAGE

File No.: 1400669.313

Project No.: 1400669

Quality Program Type: ☒ Nuclear ☐ Commercial

PROJECT NAME:

Palisades Flaw Readiness Program for 1R24 NDE Inspection

CONTRACT NO.:

10426669

CLIENT:

Entergy Nuclear Operations, Inc.

PLANT:

Palisades Nuclear Plant

CALCULATION TITLE:

Crack Growth Analysis of the Hot Leg Drain Nozzle

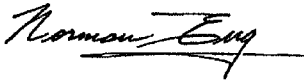
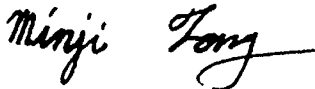
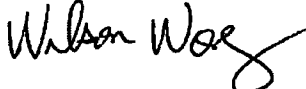

Document Revision	Affected Pages	Revision Description	Project Manager Approval Signature & Date	Preparer(s) & Checker(s) Signatures & Date
0	1 - 23 A-1 - A-3 Computer Files	Initial Issue	 Norman Eng NE 5/11/15	Preparer:  Minji Fong MF 5/11/15 Checkers:  Wilson Wong WW 5/11/15  Gole Mukhim GSM 5/11/15

Table of Contents

1.0	OBJECTIVE	4
2.0	DESIGN INPUTS.....	4
2.1	Piping Interface Loads	4
2.2	Residual Stresses at Normal Operating Temperature and Pressure.....	5
2.3	Mechanical Load Boundary Conditions	5
2.4	Crack Growth Rate	5
3.0	ASSUMPTIONS.....	6
4.0	DETERMINATION OF STRESS INTENSITY FACTOR	6
4.1	Crack Face Pressure Application.....	6
4.2	K Calculation for Circumferential Flaws	7
4.2.1	<i>Finite Element Model with Circumferential Flaws</i>	7
4.2.2	<i>Stress Intensity Factor Results</i>	8
4.3	K Calculation for Axial Flaws.....	8
4.3.1	<i>Finite Element Model with Axial Flaws</i>	8
4.3.2	<i>Stress Intensity Factor Results</i>	8
5.0	CRACK GROWTH CALCULATION.....	9
6.0	CONCLUSIONS	9
7.0	REFERENCES	11
	APPENDIX A COMPUTER FILES LISTING.....	A-1

List of Tables

Table 1: Stress Intensity Factors for Circumferential Flaws	12
Table 2: Stress Intensity Factors for Axial Flaws.....	12
Table 3: Crack Growth Time to 75% Through-Wall.....	12
Table 4: Crack Growth Time to 95% Through-Wall.....	12
Table 5: Allowable Detected Flaw Size	13

List of Figures

Figure 1. Base Finite Element Model Mesh	14
Figure 2. Applied Mechanical Load Boundary Conditions.....	15
Figure 3. Circumferential Flaw with Crack Tip Elements Inserted.....	16
Figure 4. Transferred Residual Stress + NOC + Pressure Stress for Circumferential Flaws .	17
Figure 5. Stress Intensity Factors as a Function of Depth for Circumferential Flaws.....	18
Figure 6. Axial Flaws with Crack Tip Elements Inserted	19
Figure 7. Transferred Residual Stress + NOC + Pressure Stress for Axial Flaws	20
Figure 8. Stress Intensity Factors as a Function of Depth for Axial Flaws	21
Figure 9. Crack Growth for All Flaw Types with 0.025” Initial Flaw Size	22
Figure 10. Crack Growth for All Flaw Types with 0.1” Initial Flaw Size	23

1.0 OBJECTIVE

The objective of this calculation package is to determine maximum allowable flaw sizes for 18 and 36 months of continued operation based on crack growth analyses for a series of postulated flaws in the hot leg drain nozzle boss weld in support of a Primary Water Stress Corrosion Cracking (PWSCC) susceptibility study at the Palisades Nuclear Plant (Palisades). The stresses due to the hot leg pipe interface loads which are determined in this calculation, and residual stresses extracted from a previous analysis [1] are used to calculate stress intensity factors (K) which are used to perform crack growth analyses. The PWSCC crack growth analyses are performed using the **pc-CRACK** [2] program for both circumferential and axial flaws. The allowable detected flaw sizes are determined by back-calculating the predicted growth time to a maximum flaw size of 75% through wall thickness per ASME Code Section XI, IWB-3643.

2.0 DESIGN INPUTS

The finite element model shown in Figure 1 was developed in Reference [3] and is used for the determination of stress intensity factors.

2.1 Piping Interface Loads

Reference 4 (PDF file, page 88) indicates that, for the hot leg, the bounding thermal transient stress of 1.010 ksi is due to case Thermal 002, the deadweight (DW) stress is 0.096 ksi and the friction stress is 1.056 ksi. The hot leg loads are applied as an equivalent bending moment to the axial free end of the modeled hot leg. The equivalent bending moment is based on the combined stress which is assumed to occur at the outside surface of the hot leg. The maximum combined bending stress is:

$$DW + Friction + Thermal = 0.096 + 1.056 + 1.010 = 2.162 \text{ ksi}$$

The moment based on the bending stress is calculated as:

$$M = \frac{\sigma \cdot I}{OR} = \frac{\pi}{4} \cdot \frac{(24.8125^4 - 20.8125^4) \cdot 2.162}{24.8125} = 13099 \text{ in-kips}$$

where,

- M = Moment (in-kips)
- σ = Stress on hot leg pipe free end (ksi)
- I = Moment of Inertia – $(\pi/4)(OR^4 - IR^4)$ (in⁴)
- IR = Inside radius of hot leg pipe (in) = 20.8125" [3]
- OR = Outside radius of hot leg pipe (in) = 24.8125" [3]

Since half the hot leg pipe is modeled, the equivalent moment applied to the model is 6549.5 in-kips (= 13099 in-kips / 2). The moment is applied to the axial end of the hot leg run piping by means of a pilot

node pair to transfer the loading. The pilot node pair is composed of a target node at the center of the pipe (ANSYS TARGE170 element) and a set of surface contact elements on the axial end of the pipe (ANSYS CONTA174 element). The surface elements are bonded to the pilot node in a slave/master coupling relationship, so that the moment load applied to the pilot node is transferred to the end of the pipe. The hot leg drain nozzle piping loads are considered to have negligible effects on the resulting K's for the boss weld, and are therefore not considered.

2.2 Residual Stresses at Normal Operating Temperature and Pressure

Residual stresses at the fifth operating condition cycle (at time = 2484 minutes) are taken from Reference 1. These stresses include the effects of normal operating temperature of 583°F and pressure of 2085 psig [1].

2.3 Mechanical Load Boundary Conditions

The mechanical load boundary conditions for the stress analysis are symmetric boundary conditions at the symmetry planes of the model, axial displacement restraint at the end of the nozzle, and axial displacement restraint on the pilot node, as shown in Figure 2. In the case where axial flaws are modeled on the symmetry planes, the boundary conditions are released at the nodes where the flaw exists.

2.4 Crack Growth Rate

The default PWSCC crack growth rate in **pc-CRACK** [2] is used. This relation is based on expressions in Reference [5, Section 4.3] and the resulting equation for the crack growth rate is as follows:

$$\frac{da}{dt} = C \exp \left[-Q \left(\frac{1}{T + 460} - \frac{1}{T_{ref} + 460} \right) \right] (K - K_{th})^{\beta} \quad \text{for } K > K_{th}$$

For times (t) in hours, temperatures (T and T_{ref}) in °F, crack length (a) in inches and K in ksi-√in, the following reference values are used:

$$T_{ref} = 617^{\circ}\text{F}$$

$$C = 2.47 \times 10^{-7} \text{ (constant)}$$

$$\beta = 1.6 \text{ (constant)}$$

$$Q = 28181.8^{\circ}\text{R (constant)}$$

$$K_{th} = 0 \text{ (threshold stress intensity factor below which there is no crack growth)}$$

$$T = \text{operating temperature at location of crack}$$

3.0 ASSUMPTIONS

The following assumptions are used in this analyses:

- The hot leg drain nozzle piping loads are not considered in calculating stress intensity factors since loads on the drain nozzle do not produce Mode I crack opening stress intensity factors that contribute to crack growth in the boss weld.
- The maximum combined stress on the hot leg piping is assumed to occur at the outside surface of the hot leg.

4.0 DETERMINATION OF STRESS INTENSITY FACTOR

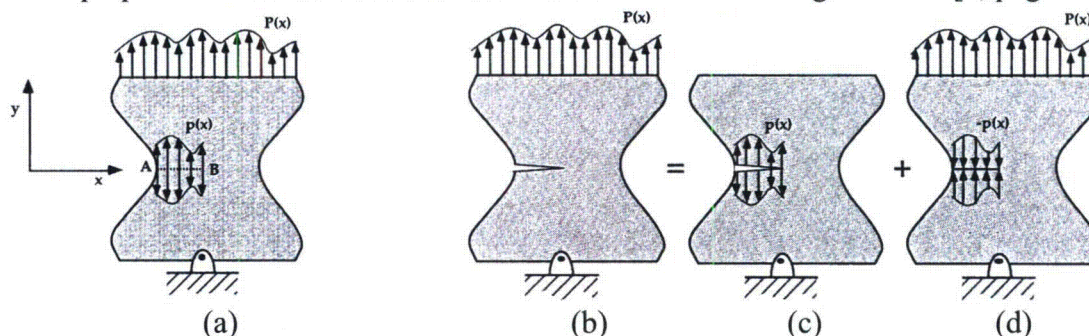
The stresses described in this section are used with a modified version of the finite element model (FEM) developed previously in Reference [3] to determine stress intensity factors. The modification of the FEM consists of adding crack tip elements as addressed in Section 4.2 and 4.3. The stress intensity factors (Ks) are calculated using the KCALC feature in ANSYS [6] which is based on linear elastic fracture mechanics (LEFM) principles. For the LEFM evaluations, only the elastic properties are used in the FEA.

4.1 Crack Face Pressure Application

In order to determine the Ks for the circumferential and axial flaws due to residual stresses, the stresses on the boss weld-to-nozzle interface, at the fifth operating condition (at time = 2484 minutes in the residual stress analysis [1]), are extracted from the residual stress analysis and reapplied on the crack face as surface pressure loading.

This approach is based on the load superposition principle [7], which is utilized to transfer the stresses from the weld residual stress finite element model onto the fracture mechanics finite element model that contains crack tip elements. The superposition technique is based on the principle that, in the linear elastic regime, stress intensity factors of the same mode, which are due to different loads, are additive (similar to stress components in the same direction).

The superposition method can be summarized with the following sketches [7, page 66]:



A load $p(x)$ on an uncracked body, Sketch (a), produces a normal stress distribution $p(x)$ on Plane A-B. The superposition principle is illustrated by Sketches (b), (c), and (d) of the same body with a crack at Plane A-B. The stress intensity factors resulting from these loading cases are such that:

$$K_I(b) = K_I(c) + K_I(d)$$

Thus, $K_I(d) = 0$ because the crack is closed, and:

$$K_I(b) = K_I(c)$$

This means that the stress intensity factor obtained from subjecting the cracked body to a nominal load $p(x)$ is equal to the stress intensity factor resulting from loading the crack faces with the same stress distribution $p(x)$ at the same crack location in the uncracked body.

4.2 K Calculation for Circumferential Flaws

4.2.1 Finite Element Model with Circumferential Flaws

The stress intensity factors for full circumferential flaws in the nozzle boss weld are determined by finite element analysis using deterministic linear elastic fracture mechanics (LEFM) principles. As a result, five fracture mechanics finite element models are derived to include “collapsed” crack meshing that represent full (360°) circumferential flaws surrounding the nozzle at various depths within the boss weld.

The circumferential flaws align with the interface between the boss weld and the nozzle. The modeled crack depths are: 0.13”, 1.17”, 2.05”, 3.13”, and 3.97” as measured at the 0° axial side of the hot leg pipe.

The modeling of the flaws, or cracks, involves splitting the crack plane and then inserting “collapsed” mesh around the crack tips followed by concentrated mesh refinements that surround the “collapsed” mesh, and are referred to as “crack tip elements”. This step is implemented on a source finite element model without the cracks (the FEM developed in Reference 3) where the crack tip elements are inserted by an in-house developed ANSYS macro.

For the fracture mechanics models, 20-node quadratic solid elements (ANSYS SOLID95) are used in the crack tip region, while 8-node solid elements (ANSYS SOLID185) are used everywhere else in the model. The mid-side nodes for the SOLID95 elements around the crack tips are shifted to the “quarter point” locations to properly capture the singularities at the crack tips, consistent with ANSYS recommendations. The finite element model for the 3.97” deep circumferential flaw, with the crack tip mesh, is shown in Figure 3 as an example; the crack tip mesh for the other crack depths follows the same pattern.

The quarter point mid-side nodes combined with the extra layers of concentrated elements around the crack tips provide sufficient mesh refinement to determine the stress intensity factors for the fracture mechanics analyses.

4.2.2 Stress Intensity Factor Results

The radial stresses (radial to the nozzle axis) on the weld/nozzle interface are transferred to the circumferential flaws as crack face pressure per the superposition principle described in Section 4.1.

Figure 4 depicts, as an example, the transferred radial stresses as crack face pressure for the 3.97" circumferential flaw depth. During the crack face pressure transfer, the operating pressure of 2085 psi [1] is added to the crack face pressure to account for the internal pressure acting on the crack face due to cracking. A far field in-plane bending moment per Section 2.1 is also applied to the free end of the hot leg run piping to account for piping moments in the main loop piping.

Each crack model is analyzed as a steady state stress pass at the operating and reference temperature of 583°F [1] in order to use the material properties at the operating temperature, but without inducing additional thermal stresses.

At the completion of each analysis, the ANSYS KCALC post-processing is performed to extract the K's at each crack tip node around the nozzle. The maximum K results are summarized in Table 1 for various crack depth ratios "a/t". Since the crack tip location is same in the circumferential flaw, the maximum K from all locations at each crack size is conservatively used for the K vs. a profile. The "K vs. a/t" trends are then plotted in Figure 5.

4.3 K Calculation for Axial Flaws

4.3.1 Finite Element Model with Axial Flaws

The stress intensity factors for axial flaws are determined using the same methodology as the circumferential flaws. However, the mesh of weld nuggets was removed to insert thumbnail shape flaws in the model. Also, the orientation and shape of the flaws allow all crack depths at the 0° and 90° faces of the symmetric hot leg pipe model to be inserted simultaneously. Figure 6 shows the five modeled crack depths (0.25", 1.06", 1.90", 2.91", and 3.85") on the 0° face (hot leg axial face) and the 90° face with crack tip elements inserted.

The modeling of the axial flaws uses the same crack tip elements as described in Section 4.2.1. The crack tip mesh is the same pattern used in the circumferential flaws and is shown in Figure 6 for the axial flaws at the 0° and 90° faces.

4.3.2 Stress Intensity Factor Results

Similar to the circumferential flaw analyses, the crack opening residual stresses and additional operating pressure are transferred to the axial flaws as crack face pressure. Figure 7 depicts, as an example, the

transferred hoop stresses as crack face pressure for the axial flaws. In addition, a far field in-plane bending moment per Section 2.1 is applied to the free end of the hot leg run piping to account for piping moments in the main loop piping. The K results at the deepest point of the flaws are summarized in Table 2 for various crack depth ratios “a/t” and plotted in Figure 8. Since the deepest point of the postulated axial flaws has the smallest remaining wall thickness, the K at the deepest point is used for the K vs. a profile.

5.0 CRACK GROWTH CALCULATION

Stress intensity factors (Ks) at four depths for 360° inside surface connected, part-through-wall circumferential flaws as well as two axial thumbnail flaws at the 0-and 90-degree azimuthal locations of the nozzle, are calculated using finite element analysis (FEA). For the circumferential flaw, the maximum K values around the nozzle circumference for each flaw depth are extracted and used as input into **pc-CRACK** to perform the PWSCC crack growth analyses. For the axial flaws, the K at the deep point of the thumbnail shape is used as input for performing the PWSCC crack growth analyses. Since the K vs. a profile is used as input, the shape of the component is not relevant.

For the crack growth analyses, two initial flaw sizes are chosen. These are based on expected engineering flaw sizes that could be present for a flaw that would then grow by PWSCC. The final flaw size for these analyses is 75% of the wall thickness. This final depth is chosen as it is the maximum allowable flaw depth per Section XI of the ASME Code for pipe flaw evaluations. Additionally, a final flaw size of 95% of the wall thickness is also considered in this calculation.

The key parameters used in the crack growth calculations included:

Two initial crack depths = 0.025” and 0.1” (assumed)
Temperature = 583°F (operating temperature [1])
Wall thickness = 4.0” (hot leg pipe thickness [3])

The resulting crack depths for the circumferential and axial flaws, as a function of time, as calculated by **pc-CRACK** are shown in Figure 9 for the 0.025” initial flaw size, and Figure 10 for the 0.1” initial flaw size. The time for a flaw to grow from the initial flaw size to 75% and 95% through-wall is tabulated in Table 3 and Table 4 for both circumferential and axial flaw types, respectively. Table 5 shows the maximum allowable detected flaw sizes for the postulated flaws if continued operation for 18 and 36 months is considered.

6.0 CONCLUSIONS

Stress intensity factors were calculated for the 360° circumferential flaws as well as the axial flaws at the 0° and 90° locations. The stress intensity factors were calculated using residual stress distributions for residual stress plus normal operating conditions. In addition, a far field in-plane bending moment is

applied to the free end of the hot leg run piping to account for piping moments in the main loop piping. This combined loading is used for the determination of the stress intensity factors for both the circumferential and axial flaws. Figure 5 and Figure 8, as well as Table 1 and Table 2, show the calculated stress intensity factors for the circumferential and axial flaws.

Crack growth evaluations were performed for circumferential and axial flaw configurations using two different initial flaw sizes. As shown in Figure 9 and Table 3, the shortest time for an initial 0.025" deep flaw to grow to 75% through-wall in all cases is 30.5 years for an axial flaw on the 0° plane. Figure 10 and Table 3 show that the shortest time for an initial 0.1" deep flaw to grow to 75% through-wall in all cases is 29.7 years for an axial flaw on the 0° plane. Table 5 shows the maximum allowable detected flaw sizes for 18 and 36 months continued operation.

7.0 REFERENCES

1. SI Calculation No. 1400669.312, Rev. 0, "Hot Leg Drain Nozzle Weld Residual Stress Analysis."
2. **pc-CRACK 4.1**, Version 4.1 CS, Structural Integrity Associates, December 2013.
3. SI Calculation No. 1400669.310, Rev. 0, "Finite Element Model for Hot Leg Drain Nozzle."
4. Palisades Document, Report No. CENC-1115, "Analytical Report for Consumers Power Piping," SI File No. 1300086.204.
5. *Materials Reliability Program: Crack Growth Rates for Evaluating Primary Water Stress Corrosion Cracking (PWSCC) of Alloy 82, 182 and 132 Welds (MRP-115)*, EPRI, Palo Alto, CA: 2004, 1006696.
6. ANSYS Mechanical APDL and PrepPost, Release 14.5 (w/ Service Pack 1), ANSYS, Inc., September 2012.
7. Anderson, T. L., "Fracture Mechanics Fundamentals and Applications," Second Edition, CRC Press, 1995.

Table 1: Stress Intensity Factors for Circumferential Flaws

Crack Depth (in)	a/t	Max. K (ksi-in ^{0.5})
0.13	0.03	19.61
1.12	0.28	22.76
2.04	0.51	14.78
3.15	0.79	13.03
3.97	0.99	35.15

Table 2: Stress Intensity Factors for Axial Flaws

HL Axial Plane 0°			HL Circ. Plane 90°		
Crack Depth (in)	a/t	K at Deep Pt (ksi-in ^{0.5})	Crack Depth (in)	a/t	K at Deep Pt (ksi-in ^{0.5})
0.25	0.06	18.50	0.25	0.06	14.16
1.06	0.26	18.64	1.10	0.27	14.43
1.90	0.47	17.60	1.96	0.49	14.77
2.91	0.73	19.34	2.95	0.74	16.98
3.85	0.96	23.44	3.81	0.95	21.41

Table 3: Crack Growth Time to 75% Through-Wall

Initial Flaw Size (in)	Axial Crack (0° plane) (years)	Axial Crack (90° plane) (years)	Circ. Crack (years)
0.025	30.5	42.9	33.9
0.100	29.7	41.7	33.1

Table 4: Crack Growth Time to 95% Through-Wall

Initial Flaw Size (in)	Axial Crack (0° plane) (years)	Axial Crack (90° plane) (years)	Circ. Crack (years)
0.025	36.7	50.3	42.1
0.100	36.0	49.2	41.4

Table 5: Allowable Detected Flaw Size

Allowable Detected Flaw Size (a/t) Hot Leg Thickness, t = 4.00"						
Months of Continued Operation	Axial Flaw at 0° plane		Axial Flaw at 90° plane		Circumferential Flaw	
	a/t	a (in)	a/t	a (in)	a/t	a (in)
18	0.7070	2.83	0.7165	2.87	0.7260	2.90
36	0.6690	2.68	0.6785	2.71	0.6975	2.79

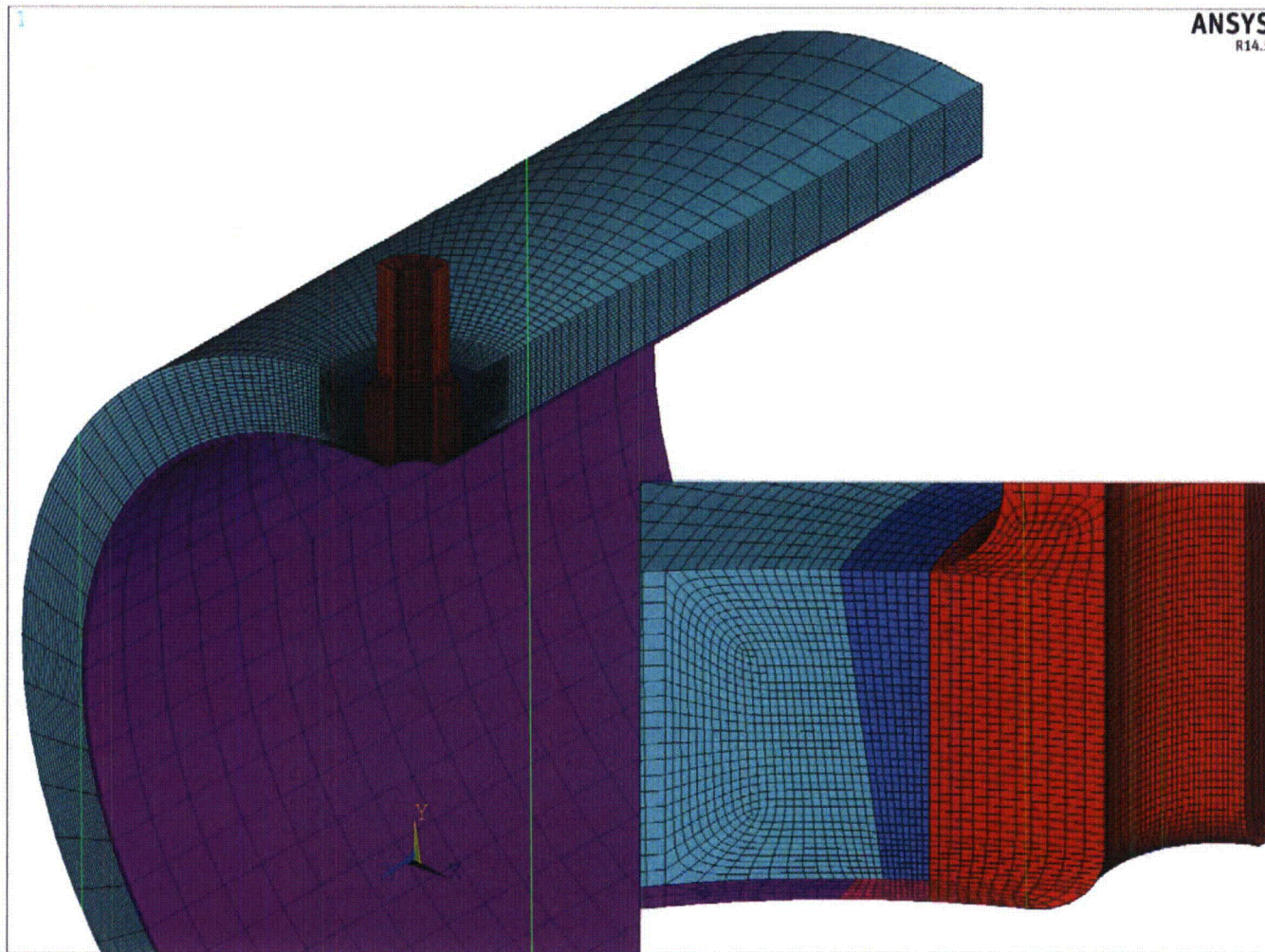


Figure 1. Base Finite Element Model Mesh

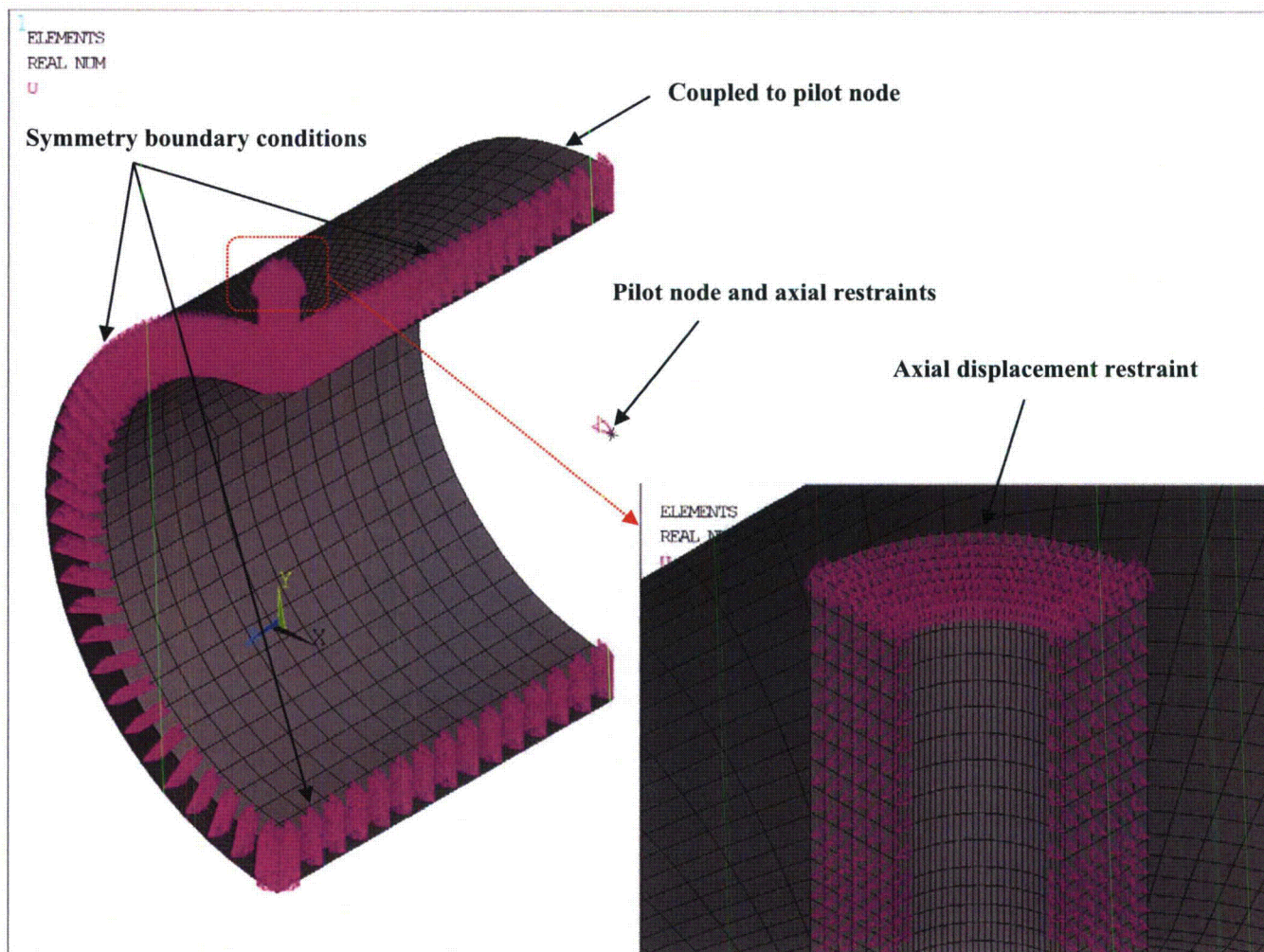


Figure 2. Applied Mechanical Load Boundary Conditions

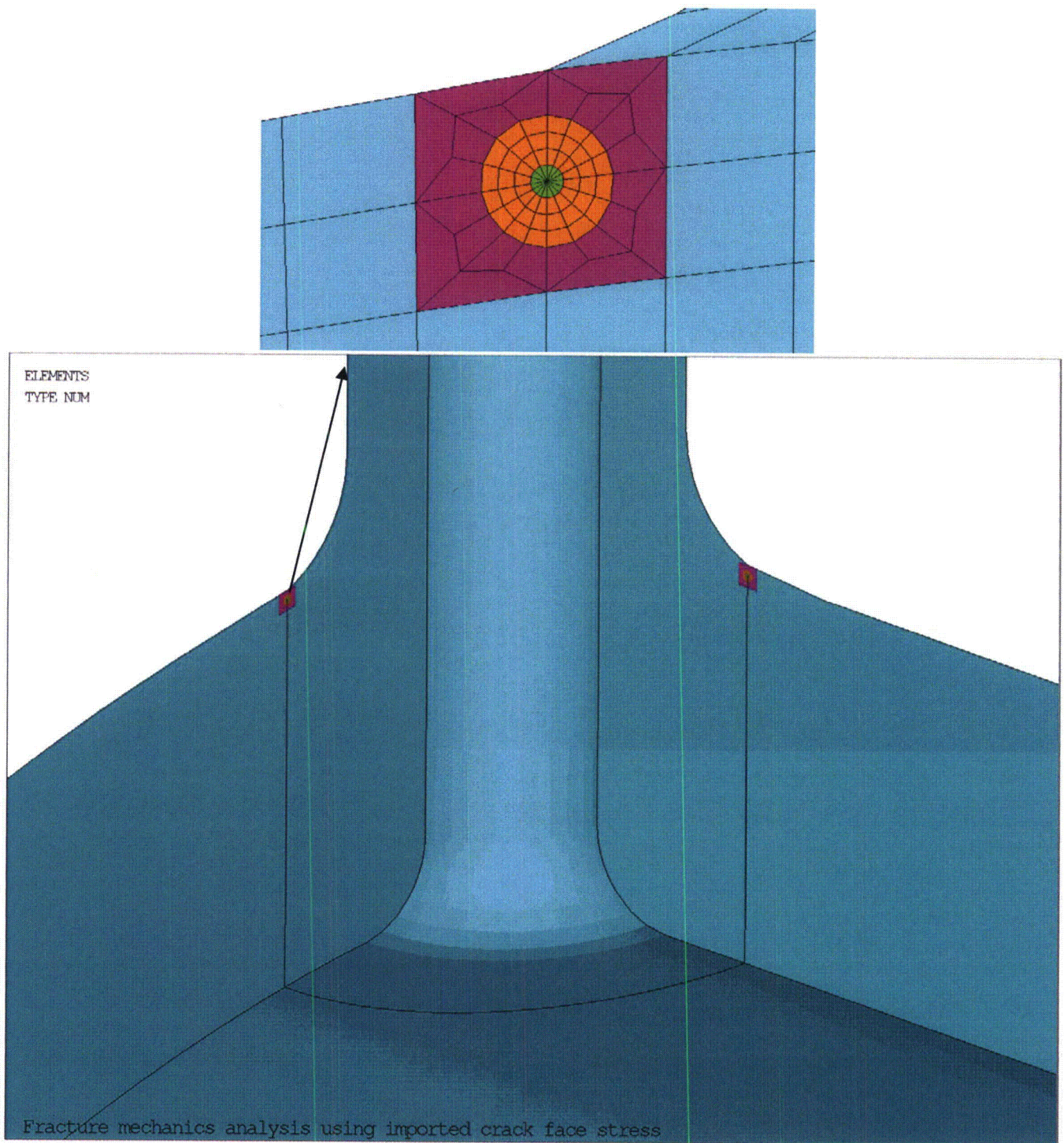


Figure 3. Circumferential Flaw with Crack Tip Elements Inserted

(Note: Deepest circumferential flaw shown for example)

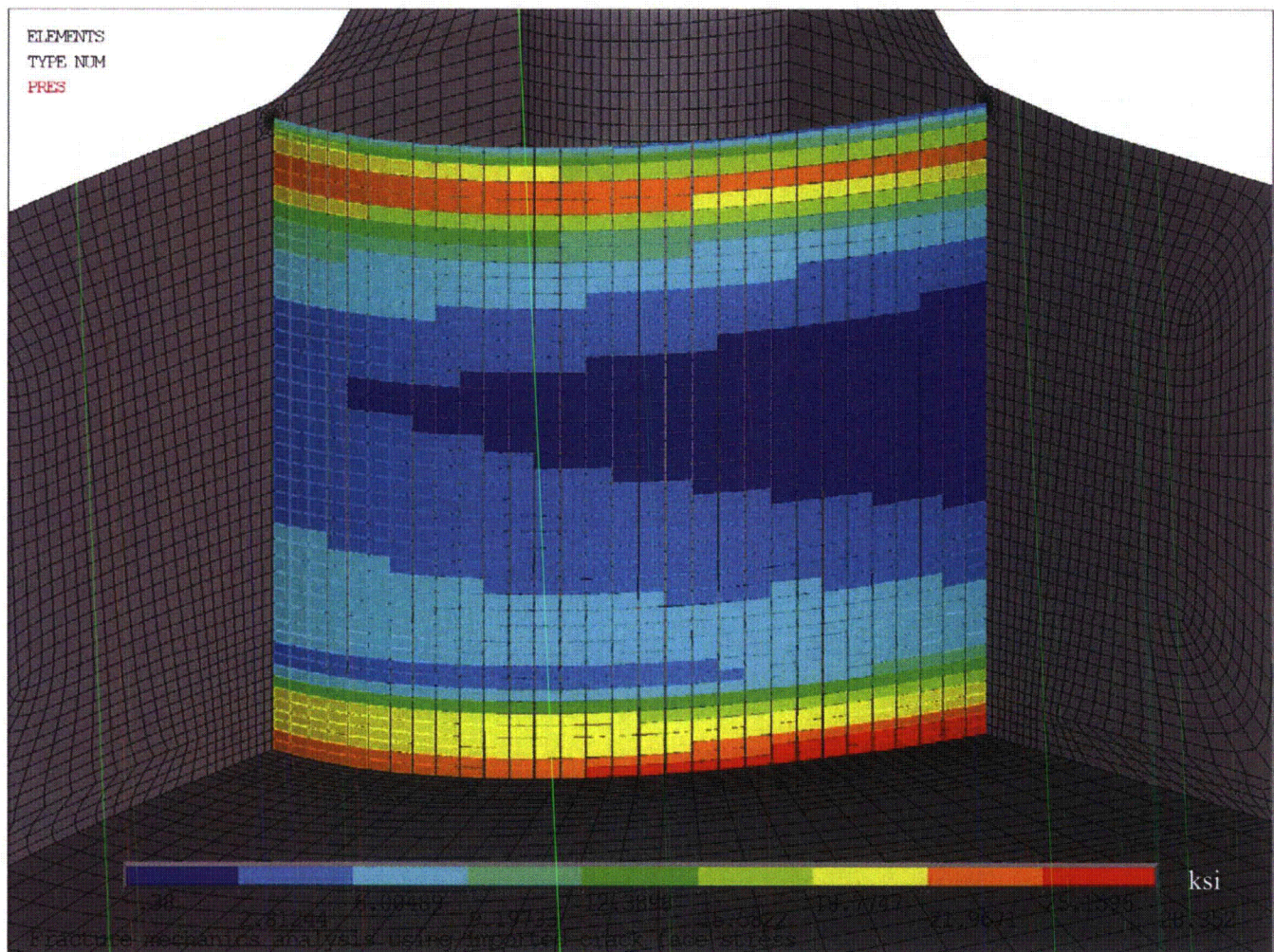


Figure 4. Transferred Residual Stress + NOC + Pressure Stress for Circumferential Flaws

(Note: Deepest circumferential flaw shown for example)

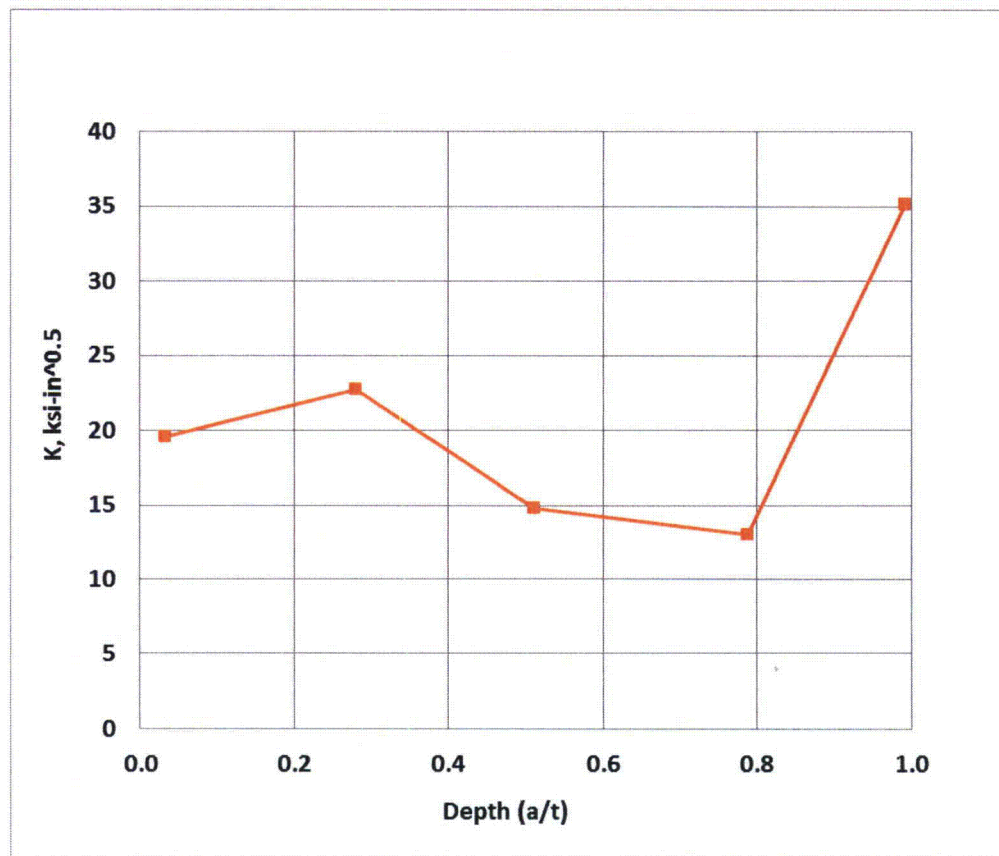


Figure 5. Stress Intensity Factors as a Function of Depth for Circumferential Flaws

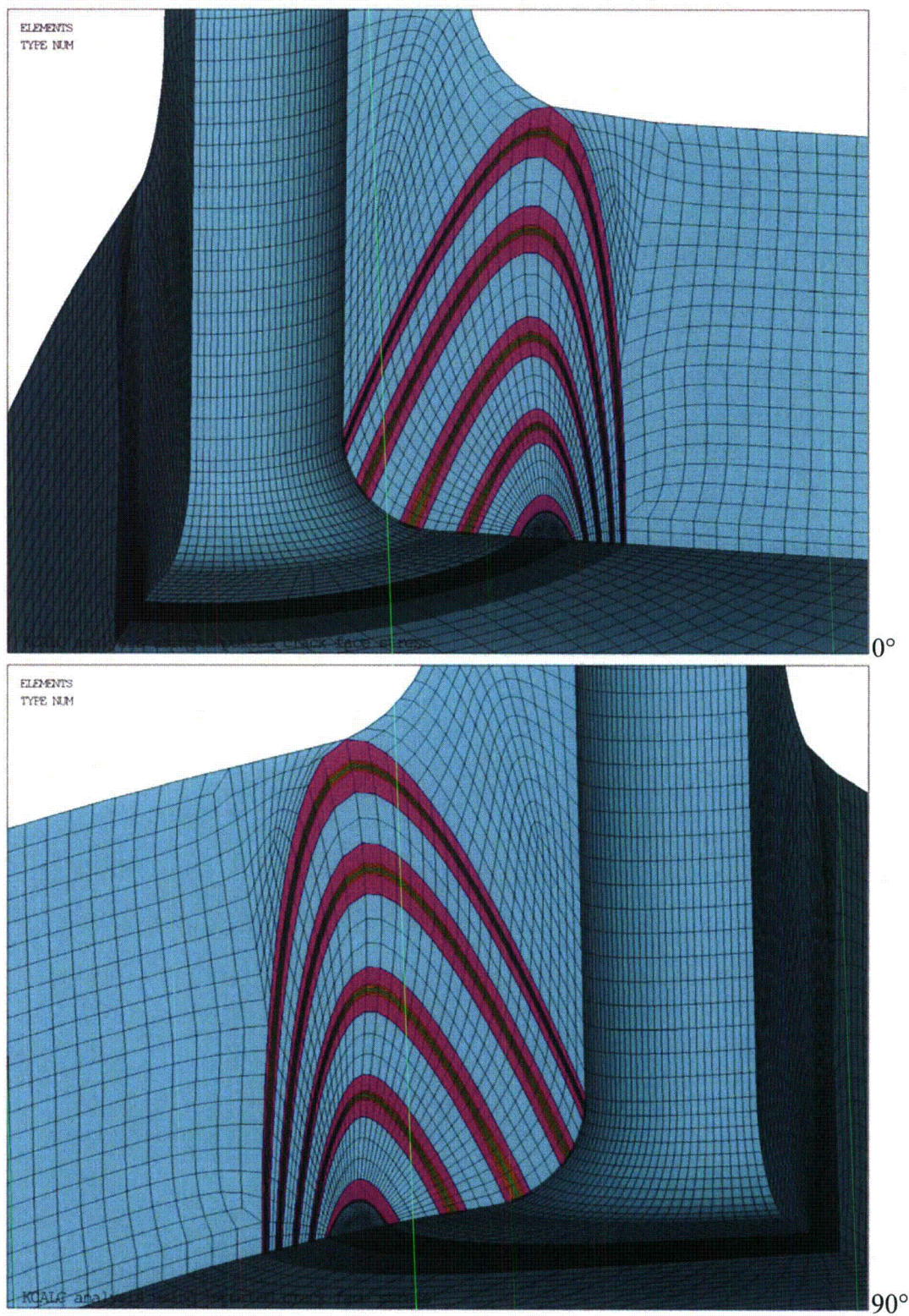


Figure 6. Axial Flaws with Crack Tip Elements Inserted

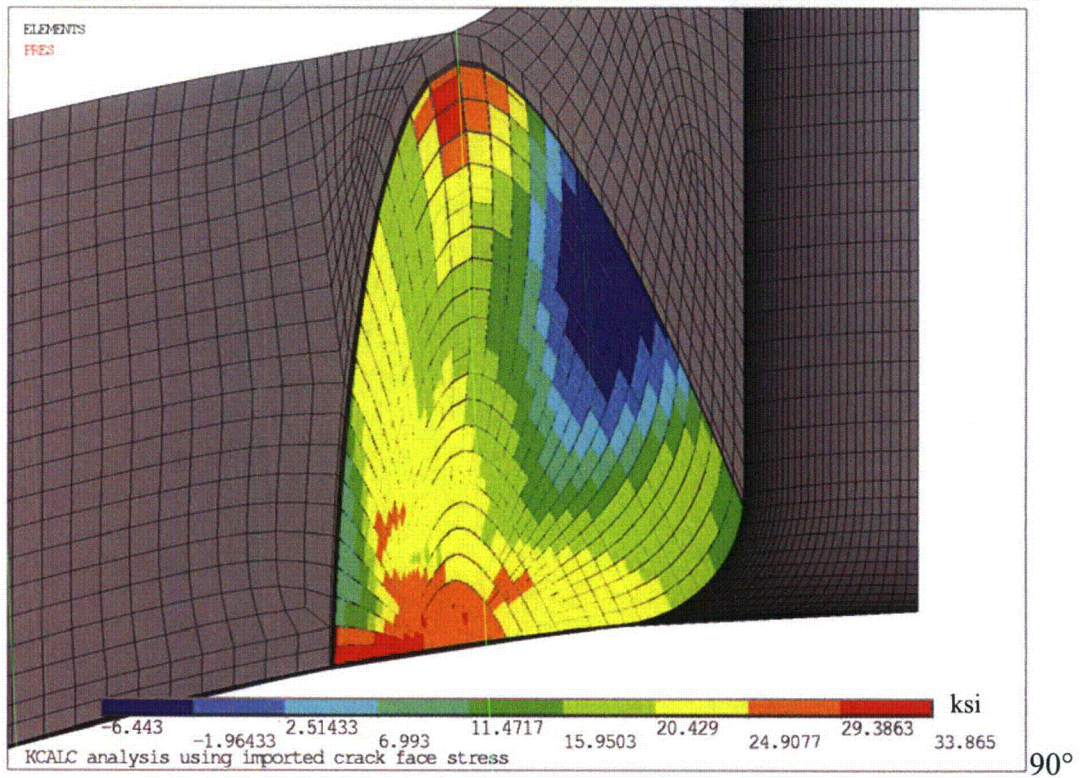
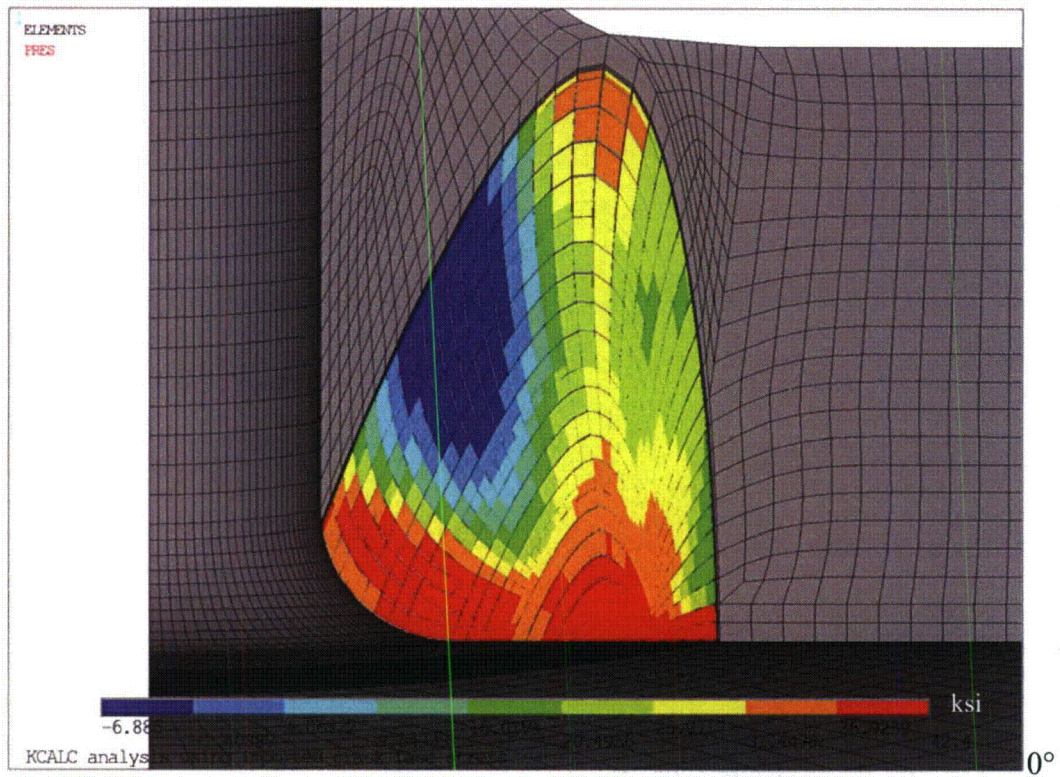


Figure 7. Transferred Residual Stress + NOC + Pressure Stress for Axial Flaws

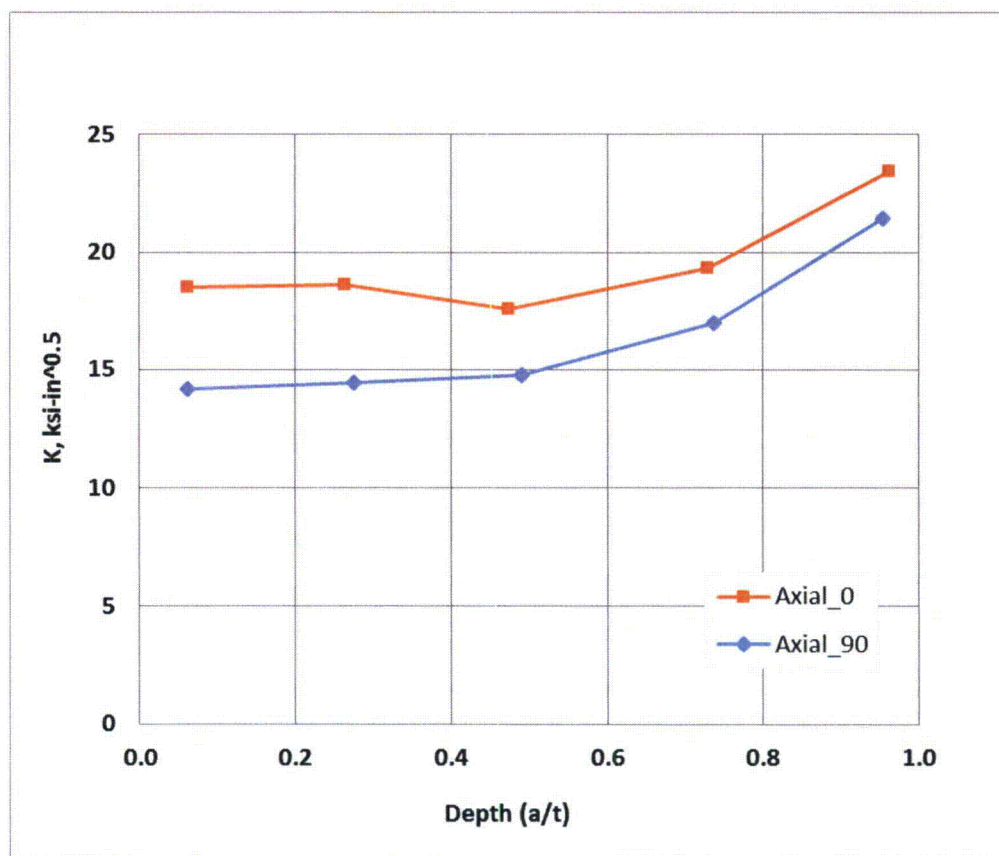


Figure 8. Stress Intensity Factors as a Function of Depth for Axial Flaws

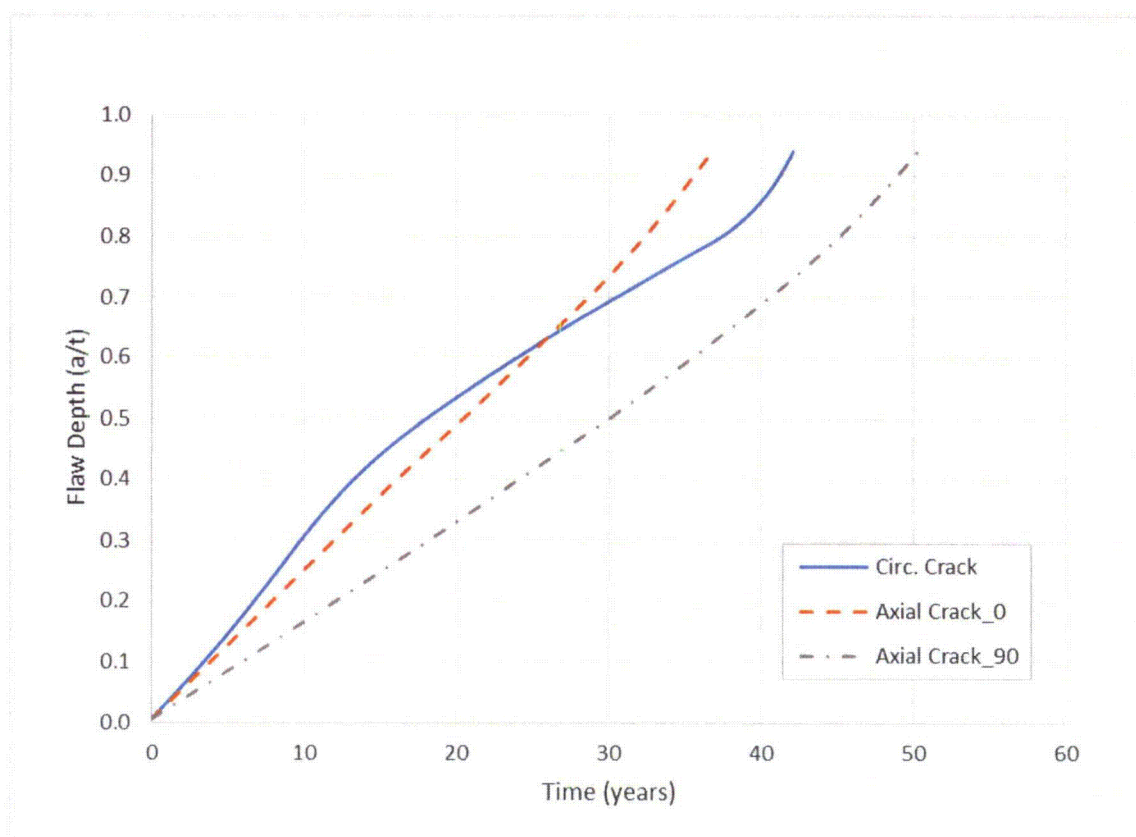


Figure 9. Crack Growth for All Flaw Types with 0.025" Initial Flaw Size

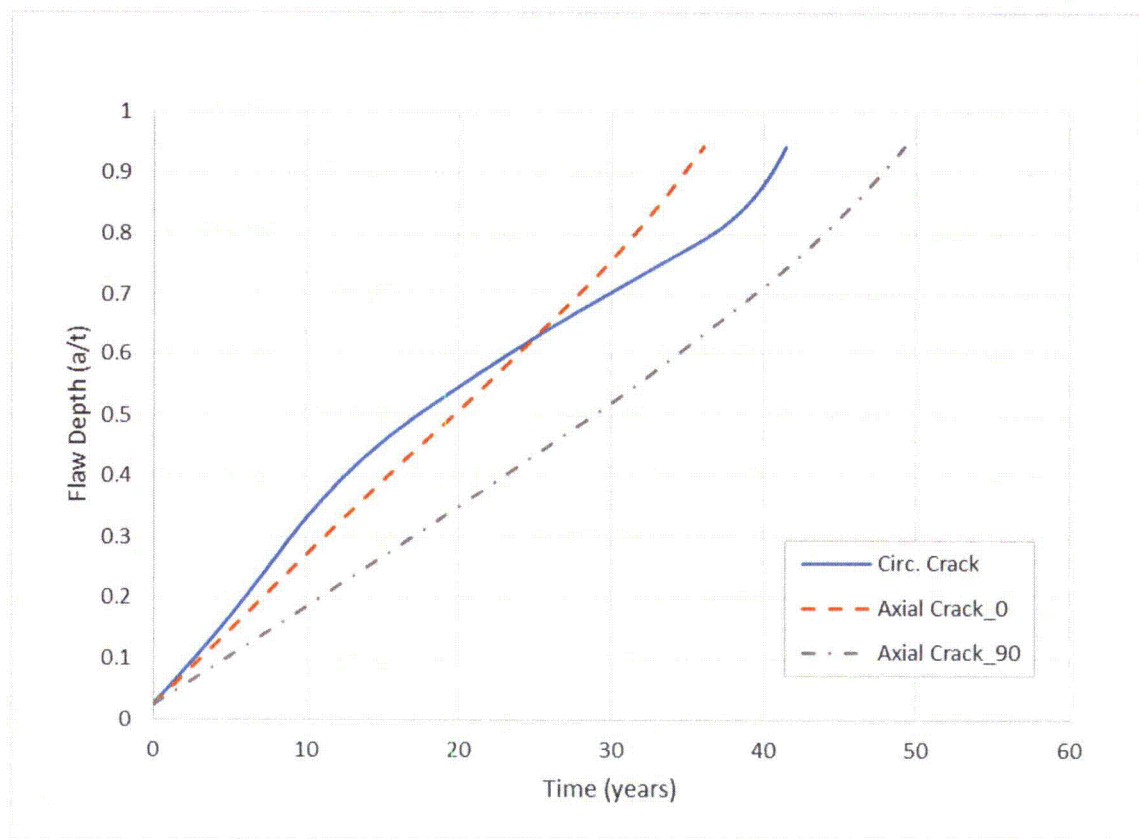


Figure 10. Crack Growth for All Flaw Types with 0.1" Initial Flaw Size

APPENDIX A
COMPUTER FILES LISTING

File Name	Description
Palisades HL Drain.INP	Input file to create base geometry model [3]
MProp_MISO.INP	Elastic-plastic material properties inputs [3]
BCNODES.INP	Component setting for the boundary conditions.
NODESC##.INP	Crack tip node inputs for fracture mechanics model conversion for circumferential flaws. ##=03, 30, 50, 75, and 95 with 03 = 0.13", 30 = 1.17", 50 = 2.05, 75 = 3.13", 95 = 3.97" of flaw size
FM_HL_C##.INP	Geometry input files to create circumferential flaw at specified depth. ##=03, 30, 50, 75, and 95
FM_HL_C##_COORD.INP	Input files to determine circumferential crack face element centroid coordinates. ##=03, 30, 50, 75, and 95
FM_HL_C##_COORD1.txt	Circumferential crack face element centroid coordinate outputs. ##=03, 30, 50, 75, and 95
FM_HL_C##_GETSTR.INP	Input files to extract circumferential crack face stresses from residual stress analysis. ##=03, 30, 50, 75, and 95
STR_FieldOper_C##1.txt	Extracted circumferential crack face stresses from residual stress analysis. ##=03, 30, 50, 75, and 95
FM_HL_C##_IMPORT.INP	Input files to transfer stresses into circumferential crack face pressure (plus operating pressure on crack face and applied pipe moment). ##=03, 30, 50, 75, and 95
FM_HL_C##_IMPORT_K.CSV	Formatted K result outputs for circumferential flaws. ##=03, 30, 50, 75, and 95
HL_AXIAL.INP	Input file to modify base mesh for axial crack tip insertion
Axial**_Nodes.INP	Crack tip node inputs for fracture mechanics model conversion for axial flaws. **=00 and 90 with 00 = 0° plane and 90 = 90° plane
FM_HL_AXL**.INP	Geometry input files to create axial flaws on the plane. **= 00 and 90
FM_HL_AXL**_COORD.INP	Input files to determine axial crack face element centroid coordinates. **=00, and 90
FM_HL_AXL**_COORD1.txt	Axial crack face element centroid coordinate outputs. **=00, and 90
FM_HL_AXL**_GETSTR.INP	Input files to extract axial crack face stresses from residual stress analysis. **=00, and 90
STR_FieldOper_AXL**1.txt	Extracted axial crack face stresses from residual stress analysis. **=00, and 90
FM_HL_AXL**_IMPORT.INP	Input files to transfer stresses into axial crack face pressure (plus operating pressure on crack face and applied pipe moment). **=00, and 90
FM_HL_AXL**_IMPORT_K.CSV	Formatted K result outputs for axial flaws. **=00, and 90
AnTip81_KCALC.INP	KCALC post-processing input file
CirFlaw_\$\$\$\$.pcf	pc-CRACK PWSCC growth input file for circumferential flaw. \$\$\$\$=0.025 and 0.1 with 0.025 = 0.025" and 0.1 = 0.1" initial flaw size

File Name	Description
AxialFlaw_0_\$.pcf	pc-CRACK PWSCC growth input file for axial flaw on 0° plane. \$=0.025 and 0.1
AxialFlaw_90_\$.pcf	pc-CRACK PWSCC growth input file for axial flaw on 90° plane. \$=0.025 and 0.1
CirFlaw_\$.rpt	pc-CRACK PWSCC growth output file for circumferential flaw. \$=0.025 and 0.1
AxialFlaw_0_\$.rpt	pc-CRACK PWSCC growth output file for axial flaw on 0° plane. \$=0.025 and 0.1
AxialFlaw_90_\$.rpt	pc-CRACK PWSCC growth output file for axial flaw on 90° plane. \$=0.025 and 0.1



Structural Integrity Associates, Inc.®

CALCULATION PACKAGE

File No.: 1400669.323

Project No.: 1400669

Quality Program Type: ☒ Nuclear ☐ Commercial

PROJECT NAME:

Palisades Flaw Readiness Program for 1R24 NDE Inspection

CONTRACT NO.:

10426669

CLIENT:

Entergy Nuclear Operations, Inc.

PLANT:

Palisades Nuclear Plant

CALCULATION TITLE:

Crack Growth Analysis of the Cold Leg Bounding Nozzle

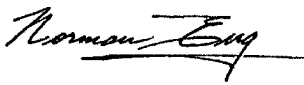
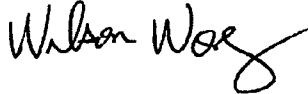
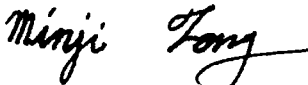

Document Revision	Affected Pages	Revision Description	Project Manager Approval Signature & Date	Preparer(s) & Checker(s) Signatures & Date
0	1 - 23 A-1 - A-2 Computer Files	Initial Issue	 Norman Eng NE 5/11/15	Preparer:  Wilson Wong WW 5/11/15 Checkers:  Minji Fong MF 5/11/15  Gole Mukhim GSM 5/11/15

Table of Contents

1.0	OBJECTIVE	4
2.0	DESIGN INPUTS.....	4
2.1	Piping Interface Loads	4
2.2	Residual Stresses at Normal Operating Temperature and Pressure.....	5
2.3	Mechanical Load Boundary Conditions	5
2.4	Crack Growth Rate	5
3.0	ASSUMPTIONS.....	6
4.0	DETERMINATION OF STRESS INTENSITY FACTOR	6
4.1	Crack Face Pressure Application.....	6
4.2	K Calculation for Circumferential Flaws	7
4.2.1	<i>Finite Element Model with Circumferential Flaws</i>	7
4.2.2	<i>Stress Intensity Factor Results</i>	8
4.3	K Calculation for Axial Flaws	8
4.3.1	<i>Finite Element Model with Axial Flaws</i>	8
4.3.2	<i>Stress Intensity Factor Results</i>	8
5.0	CRACK GROWTH CALCULATION.....	9
6.0	CONCLUSIONS	9
7.0	REFERENCES	11
	APPENDIX A COMPUTER FILE LISTING	A-1

List of Tables

Table 1: Stress Intensity Factors for Circumferential Flaws	12
Table 2: Stress Intensity Factors for Axial Flaws.....	12
Table 3: Crack Growth Time to 75% Through-Wall.....	12
Table 4: Crack Growth Time to 95% Through-Wall.....	12
Table 5: Allowable Detected Flaw Size	13

List of Figures

Figure 1. Base Finite Element Model Mesh	14
Figure 2. Applied Mechanical Load Boundary Conditions.....	15
Figure 3. Circumferential Flaw with Crack Tip Elements Inserted.....	16
Figure 4. Transferred Residual Stress + NOC + Pressure Stress for Circumferential Flaws ..	17
Figure 5. Stress Intensity Factors as a Function of Depth for Circumferential Flaws.....	18
Figure 6. Axial Flaws with Crack Tip Elements Inserted	19
Figure 7. Transferred Residual Stress + NOC + Pressure Stress for Axial Flaws	20
Figure 8. Stress Intensity Factors as a Function of Depth for Axial Flaws	21
Figure 9. Crack Growth for All Flaw Types with 0.025” Initial Flaw Size	22
Figure 10. Crack Growth for All Flaw Types with 0.1” Initial Flaw Size	23

1.0 OBJECTIVE

The objective of this calculation package is to determine maximum allowable flaw sizes for 18 and 36 months of continued operation based on crack growth analyses for a series of postulated flaws in the cold leg bounding nozzle boss weld in support of a Primary Water Stress Corrosion Cracking (PWSCC) susceptibility study at the Palisades Nuclear Plant (Palisades). The stresses due to the cold leg pipe interface loads which are determined in this calculation, and residual stresses extracted from a previous analysis [1], are used to calculate the stress intensity factors (K) which are used to perform crack growth analyses. The PWSCC crack growth analyses are performed using the **pc-CRACK** [2] program for both circumferential and axial flaws. The allowable detected flaw sizes are determined by back-calculating the predicted growth time to a maximum flaw size of 75% through wall thickness per ASME Code Section XI, IWB-3643.

2.0 DESIGN INPUTS

The finite element model shown in Figure 1 was developed in Reference [3] and is used for the determination of stress intensity factors.

2.1 Piping Interface Loads

Reference 4 [PDF file page 88] indicates that, for the cold leg, the bounding thermal transient stress is 7.307 ksi due to case Thermal 009, the deadweight (DW) stress is 0.459 ksi and the friction stress is 0.429 ksi. The cold leg loads are applied as an equivalent bending moment to the axial free end of the modeled cold leg. The equivalent bending moment is based on the combined stress which is assumed to occur at the outside surface of the cold leg. The maximum combined bending stress is:

$$DW + Friction + Thermal = 0.459 + 0.429 + 7.307 = 8.195 \text{ ksi}$$

The moment based on the bending stress is calculated as:

$$M = \frac{\sigma \cdot I}{OR} = \frac{\pi}{4} \cdot \frac{(17.84375^4 - 14.84375^4) \cdot 8.195}{17.84375} = 19056 \text{ in-kips}$$

where,

M = moment applied to the free end of the cold leg

σ = stress on the cold leg pipe

I = Moment of Inertia – $(\pi/4)(OR^4 - IR^4)$

IR = Inside radius of nozzle (in) = 14.84375" [3]

OR = Outside radius of nozzle (in) = 17.84375 [3]

Since half the cold leg pipe is modeled, the equivalent moment applied to the model is 9528 in-kips (= 19056 in-kips /2). The moment is applied to the axial free end of the cold leg run piping by means of a pilot node pair to transfer the loading. The pilot node pair is composed of a target node at the center of the pipe (ANSYS TARGE170 element) and a set of surface contact elements on the axial end of the pipe (ANSYS CONTA174 element). The surface elements are bonded to the pilot node in a slave/master coupling relationship, so that the moment load applied to the pilot node is transferred to the end of the pipe. The cold leg bounding nozzle piping loads are considered to have negligible effects on the resulting K's for the boss weld, and are therefore not considered.

2.2 Residual Stresses at Normal Operating Temperature and Pressure

Residual stresses at the fifth operating condition cycle (at time = 2106 minutes) are taken from Reference [1]. These stresses include the effects of normal operating temperature of 537°F and pressure of 2085 psig [1].

2.3 Mechanical Load Boundary Conditions

The mechanical load boundary conditions for the stress analyses are symmetric boundary conditions at the symmetry planes of the model, axial displacement restraint at the end of the nozzle, and axial displacement restraint on the pilot node, as shown in Figure 2. In the case where axial flaws are modeled on the symmetry planes, the boundary conditions are released at the nodes where the flaw exists.

2.4 Crack Growth Rate

The default PWSCC growth rate in **pc-CRACK** [2] is used. This relation is based on expressions in Reference [5, Section 4.3] and the resulting equation for the crack growth rate is as follows:

$$\frac{da}{dt} = C \exp \left[-Q \left(\frac{1}{T + 460} - \frac{1}{T_{ref} + 460} \right) \right] (K - K_{th})^{\beta} \quad \text{for } K > K_{th}$$

For times (t) in hours, temperatures (T and T_{ref}) in °F, crack length (a) in inches and K in ksi-√in, the following reference values are used:

$$T_{ref} = 617^{\circ}\text{F}$$

$$C = 2.47 \times 10^{-7} \text{ (constant)}$$

$$\beta = 1.6 \text{ (constant)}$$

$$Q = 28181.8^{\circ}\text{R (constant)}$$

$$K_{th} = 0 \text{ (threshold stress intensity factor below which there is no crack growth)}$$

$$T = \text{operating temperature at location of crack}$$

3.0 ASSUMPTIONS

The following assumptions are used in this analyses:

- The cold leg bounding nozzle piping loads are not considered in calculating stress intensity factors since loads on the nozzle do not produce Mode I crack opening stress intensity factors that contribute to crack growth in the boss weld.
- The maximum combined stress on the cold leg piping is assumed to occur at the outside surface of the cold leg.

4.0 DETERMINATION OF STRESS INTENSITY FACTOR

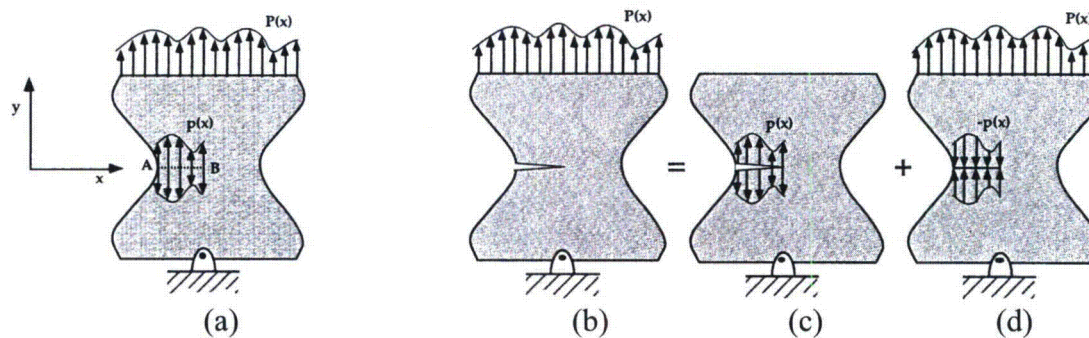
The stresses described in this section are used with a modified version of the finite element model (FEM) developed previously in Reference [3] to determine stress intensity factors. The modification of the FEM consists of adding crack tip elements as addressed in Section 4.2 and 4.3. The stress intensity factors (K_s) are calculated using the KCALC feature in ANSYS [6] which is based on the linear elastic fracture mechanics (LEFM) principles. For the LEFM evaluations, only the elastic properties are used in the FEA.

4.1 Crack Face Pressure Application

In order to determine the K_s for the circumferential and axial flaws due to residual stresses, the stresses on the boss weld-to-nozzle interface, at the fifth operating condition (at time = 2106 minutes in the residual stress analysis [1]), are extracted from the residual stress analysis and reapplied on the crack face as surface pressure loading.

This approach is based on the load superposition principle [7], which is utilized to transfer the stresses from the weld residual stress finite element model onto the fracture mechanics finite element model that contains crack tip elements. The superposition technique is based on the principle that, in the linear elastic regime, stress intensity factors of the same mode, which are due to different loads, are additive (similar to stress components in the same direction).

The superposition method can be summarized with the following sketches [7, page 66]:



A load $p(x)$ on an uncracked body, Sketch (a), produces a normal stress distribution $p(x)$ on Plane A-B. The superposition principle is illustrated by Sketches (b), (c), and (d) of the same body with a crack at Plane A-B. The stress intensity factors resulting from these loading cases are such that:

$$K_I(b) = K_I(c) + K_I(d)$$

Thus, $K_I(d) = 0$ because the crack is closed, and:

$$K_I(b) = K_I(c)$$

This means that the stress intensity factor obtained from subjecting the cracked body to a nominal load $p(x)$ is equal to the stress intensity factor resulting from loading the crack faces with the same stress distribution $p(x)$ at the same crack location in the uncracked body.

4.2 K Calculation for Circumferential Flaws

4.2.1 Finite Element Model with Circumferential Flaws

The stress intensity factors for full circumferential flaws in the nozzle boss weld are determined by finite element analysis using deterministic linear elastic fracture mechanics (LEFM) principles. As a result, five fracture mechanics finite element models are derived to include “collapsed” crack meshing that represent full (360°) circumferential flaws surrounding the nozzle at various depths within the boss weld.

The circumferential flaws align with the interface between the boss weld and the nozzle. The modeled flaw depths are: 0.13”, 0.88”, 1.45”, 2.32”, and 2.99” as measured at the 0° axial side of the cold leg pipe.

The modeling of the flaws, or cracks, involves splitting the crack plane and then inserting “collapsed” mesh around the crack tips followed by concentrated mesh refinements that surround the “collapsed” mesh, and are referred to as “crack tip elements”. This step is implemented on a source finite element model without the cracks (the FEM developed in Reference 3) where crack tip elements are inserted by an in-house developed ANSYS macro.

For the fracture mechanics models, 20-node quadratic solid elements (ANSYS SOLID95) are used in the crack tip region, while 8-node solid elements (ANSYS SOLID185) are used everywhere else in the model. The mid-side nodes for the SOLID95 elements around the crack tips are shifted to the “quarter point” locations to properly capture the singularities at the crack tips, consistent with ANSYS recommendations. The finite element model for the 2.99” deep circumferential flaw, with the crack tip mesh, is shown in Figure 3 as an example; the crack tip mesh for the other crack depths follows the same pattern.

The quarter point mid-side nodes combined with the extra layers of concentrated elements around the crack tips provide sufficient mesh refinement to determine the stress intensity factors for the fracture mechanics analyses.

4.2.2 *Stress Intensity Factor Results*

The radial stresses (radial to the nozzle axis) on the weld/nozzle interface are transferred to the circumferential flaws as crack face pressure per the superposition principle described in Section 4.1.

Figure 4 depicts, as an example, the transferred radial stresses as crack face pressure for the 2.99" circumferential crack depth. During the crack face pressure transfer, the operating pressure of 2085 psi is added to the crack face pressure to account for the internal pressure acting on the crack face due to cracking. A far field in-plane bending moment per Section 2.1 is also applied to the free end of the cold leg run piping to account for the pipe moment in the main loop piping.

Each crack model is analyzed as a steady state stress pass at the operating and reference temperature of 537°F [1] in order to use the material properties at the operating temperature, but without inducing additional thermal stresses.

At the completion of each analysis, the ANSYS KCALC post-processing is performed to extract the K's at each crack tip node around the nozzle. The maximum K results are summarized in Table 1 for various crack depth ratios "a/t". Since the crack tip location is same in the circumferential flaw, the maximum K from all locations at each crack size is conservatively used for the K vs. a profile. The "K vs. a/t" trends are then plotted in Figure 5.

4.3 K Calculation for Axial Flaws

4.3.1 *Finite Element Model with Axial Flaws*

The stress intensity factors for axial flaws are determined using the same methodology as the circumferential flaws. However, the mesh of weld nuggets was removed to insert thumbnail shape flaws in the model. Also, the orientation and shape of the flaws allow all crack depths at the 0° and 90° faces of the symmetric cold leg pipe model to be inserted simultaneously. Figure 6 shows the five modeled crack depths (0.25", 0.78", 1.37", 2.16", and 2.90") on the 0° face (cold leg axial face) and 90° face with crack tip elements inserted.

The modeling of the axial flaws uses the same crack tip elements as described in Section 4.2.1. The crack tip mesh is the same pattern used in the circumferential flaws and is shown in Figure 6 for the axial flaws at the 0° and 90° faces.

4.3.2 *Stress Intensity Factor Results*

Similar to the circumferential flaw analyses, the crack opening residual stresses and additional operating pressure are transferred to the axial flaws as crack face pressure. Figure 7 depicts, as an example, the

transferred hoop stresses as crack face pressure for the axial flaws. In addition, a far field in-plane bending moment per Section 2.1 is also applied to the free end of the cold leg run piping to account for the pipe moment in the main loop piping. The K results at the deepest point of the flaws are summarized in Table 2 for various crack depth ratios “a/t” and plotted in Figure 8. Since the deepest point of the postulated axial flaws has the smallest remaining wall thickness, the K at the deepest point is used for the K vs a profile.

5.0 CRACK GROWTH CALCULATION

Stress intensity factors (Ks) at four depths for 360° inside surface connected, part-through-wall circumferential flaws as well as two axial thumbnail flaws at the 0-and 90-degree azimuthal locations of the nozzle, are calculated using finite element analysis (FEA). For the circumferential flaw, the maximum K values around the nozzle circumference for each flaw depth are extracted and used as input into **pc-CRACK** to perform the PWSCC crack growth analyses. For the axial flaws, the K at the deep point of the thumbnail shape is used as input for performing the PWSCC crack growth analyses. Since the K vs. a profile is used as input, the shape of the component is not relevant.

For the crack growth analyses, two initial flaw sizes were chosen. These are based on expected engineering flaw sizes that could be present for a crack that would then grow by PWSCC. The final flaw size for these analyses is 75% of the wall thickness. This final depth is chosen as it is the maximum allowable flaw depth per Section XI of the ASME Code for pipe flaw evaluations. Additionally, a final flaw size of 95% of the wall thickness is also considered in this calculation.

The following are the additional parameters needed for the crack growth calculations:

Two initial crack depths = 0.025” and 0.1” (assumed)
Temperature = 537°F (operating temperature [1])
Wall thickness = 3” (Cold Leg thickness [3])

The resulting crack depths for the circumferential and axial flaws, as a function of time, as calculated by **pc-CRACK** are shown in Figure 9 for the 0.025” initial flaw size and Figure 10 for the 0.1” initial flaw size. The time for a flaw to grow from the initial flaw size to 75% and 95% through-wall is tabulated in Table 3 and Table 4 for both circumferential and axial flaw types, respectively. Table 5 shows the allowable detected flaw sizes for the postulated flaws if continued operation for 18 and 36 months is considered.

6.0 CONCLUSIONS

Stress intensity factors were calculated for the 360° circumferential flaws as well as the axial flaws at the 0° and 90° locations. The stress intensity factors were calculated using residual stress distributions for residual stress plus normal operating conditions. In addition, a far field in-plane bending moment is

applied to the free end of the cold leg run piping to account for piping moments in the main loop piping. This combined loading is used for the determination of the stress intensity factors for both the circumferential and axial flaws. Figure 5 and Figure 8 as well as Table 1 and Table 2, show the calculated stress intensity factors for the circumferential and axial flaws.

Crack growth evaluations were performed for circumferential and axial flaw configurations using two different initial flaw sizes. As shown in Figure 9 and Table 3, the shortest time for an initial 0.025" deep flaw to grow to 75% through-wall in all cases is 55.6 years for a circumferential flaw. Figure 10 and Table 3 show that the shortest time for an initial 0.1" deep flaw to grow to 75% through-wall in all cases is 53.5 years for a circumferential flaw. Table 5 shows the maximum allowable detected flaw sizes for 18 and 36 months of continued operation.

7.0 REFERENCES

1. SI Calculation No. 1400669.322, Rev. 0, "Cold Leg Bounding Nozzle Weld Residual Stress Analysis."
2. **pc-CRACK 4.1**, Version 4.1 CS, Structural Integrity Associates, December 2013.
3. SI Calculation No. 1400669.320, Rev. 0, "Finite Element Model Development for the Cold Leg Drain, Spray, and Charging Nozzles."
4. Palisades Document, Report No. CENC-1115, "Analytical Report for Consumers Power Piping," SI File No. 1300086.204.
5. *Materials Reliability Program: Crack Growth Rates for Evaluating Primary Water Stress Corrosion cracking (PWSCC) of Alloy 82, 182 and 132 Welds (MRP-115)*, EPRI, Palo Alto, CA: 2004, 1006696.
6. ANSYS Mechanical APDL and PrepPost, Release 14.5 (w/ Service Pack 1), ANSYS, Inc., September 2012.
7. Anderson, T. L., "Fracture Mechanics Fundamentals and Applications," Second Edition, CRC Press, 1995.

Table 1: Stress Intensity Factors for Circumferential Flaws

Depth (in)	a/t	Max K (ksi-in ^{0.5})
0.13	0.04	22.07
0.83	0.28	28.50
1.42	0.47	20.84
2.31	0.77	20.97
2.99	1.00	48.27

Table 2: Stress Intensity Factors for Axial Flaws

CL Axial Plane 0°			CL Circ. Plane 90°		
Crack Depth (in)	a/t	K at Deep Pt (ksi-in ^{0.5})	Crack Depth (in)	a/t	K at Deep Pt (ksi-in ^{0.5})
0.25	0.08	21.26	0.24	0.08	18.43
0.78	0.26	20.95	0.83	0.28	19.00
1.37	0.46	19.58	1.43	0.48	20.82
2.16	0.72	22.89	2.19	0.73	25.67
2.90	0.97	28.34	2.85	0.95	30.93

Table 3: Crack Growth Time to 75% Through-Wall

Initial Flaw Size (in)	Axial Crack (0° plane) (years)	Axial Crack (90° plane) (years)	Circ. Crack (years)
0.025	64.5	67.2	55.6
0.100	62.2	64.4	53.5

Table 4: Crack Growth Time to 95% Through-Wall

Initial Flaw Size (in)	Axial Crack (0° plane) (years)	Axial Crack (90° plane) (years)	Circ. Crack (years)
0.025	77.0	77.9	66.2
0.100	74.6	75.0	64.0

Table 5: Allowable Detected Flaw Size

Allowable Detected Flaw Size (a/t) Cold Leg Thickness, t = 3.00"						
Months of Continued Operation	Axial Flaw at 0° plane		Axial Flaw at 90° plane		Circumferential Flaw	
	a/t	a (in)	a/t	a (in)	a/t	a (in)
18	0.7238	2.1715	0.7202	2.1605	0.7269	2.1807
36	0.6871	2.0613	0.6788	2.0363	0.6273	1.8818

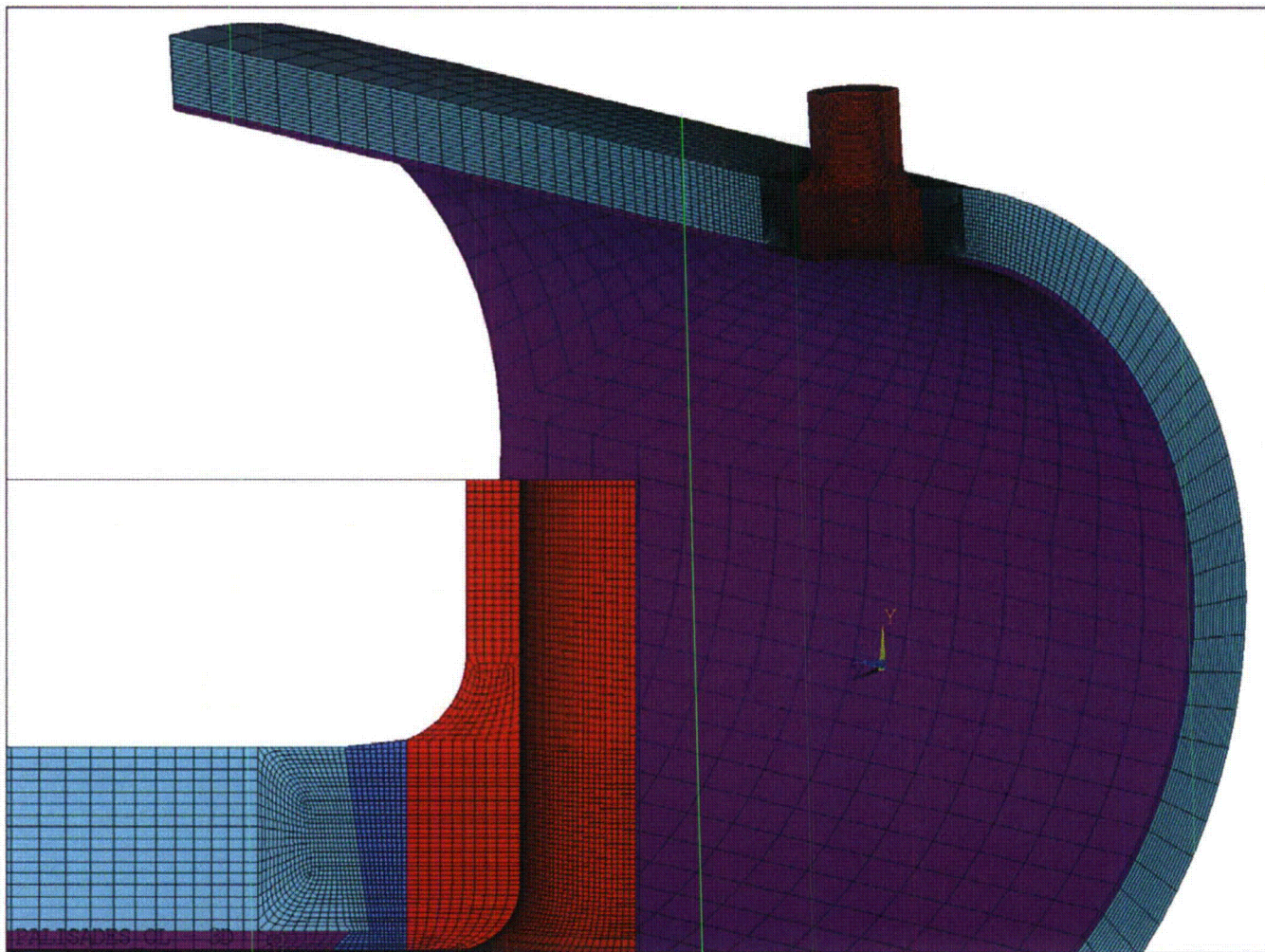


Figure 1. Base Finite Element Model Mesh

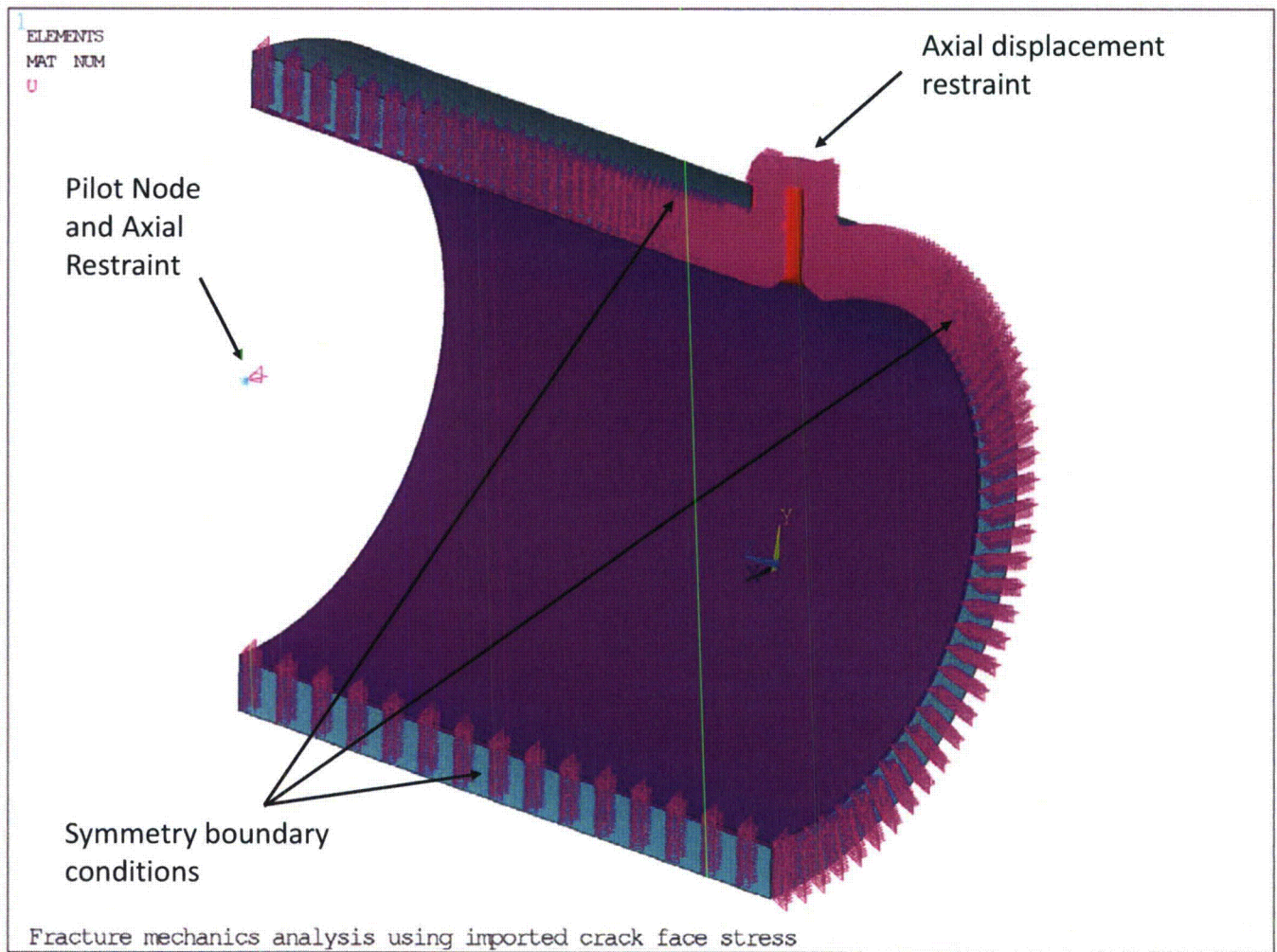


Figure 2. Applied Mechanical Load Boundary Conditions

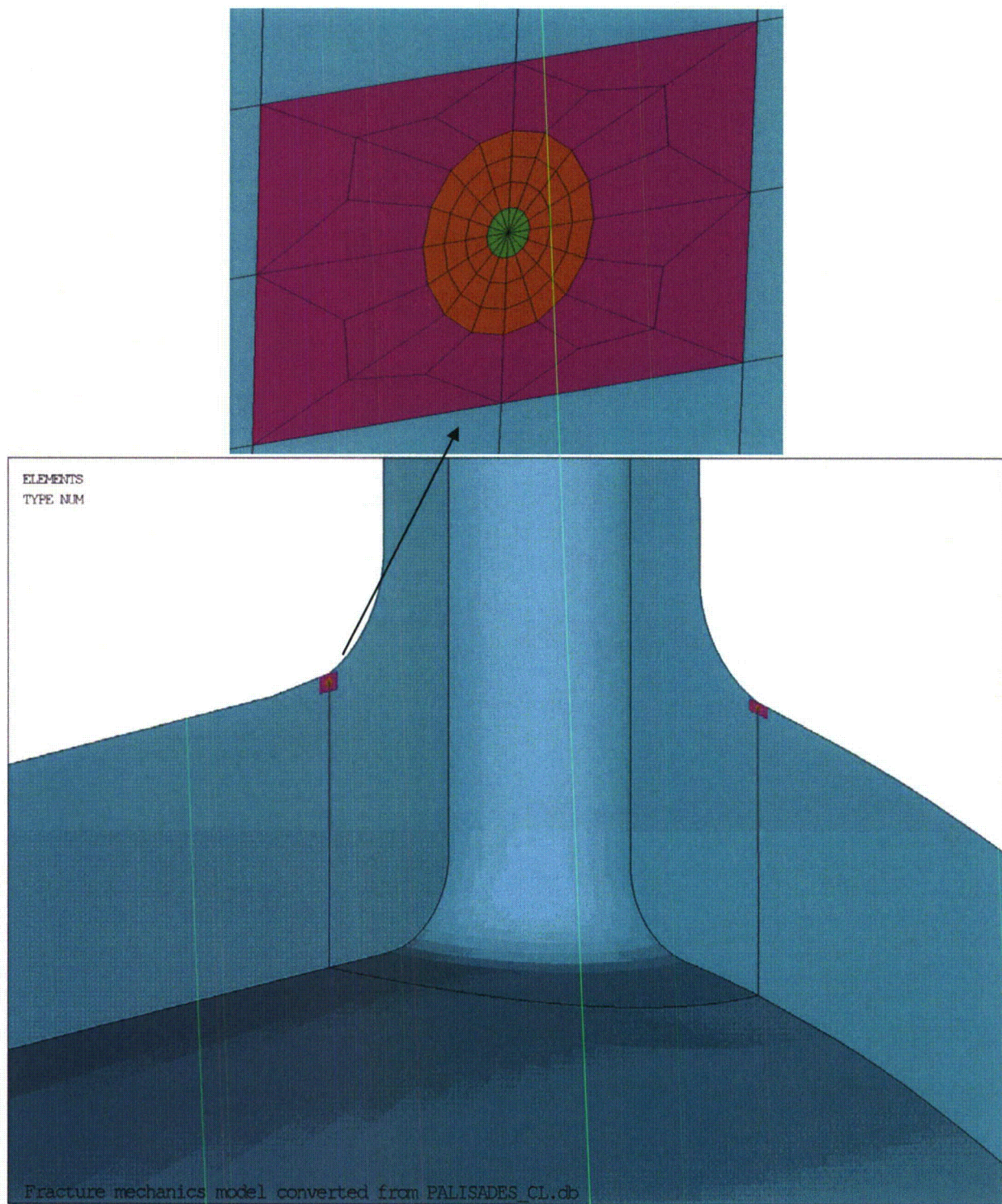


Figure 3. Circumferential Flaw with Crack Tip Elements Inserted

(Note: Deepest circumferential flaw shown for example)

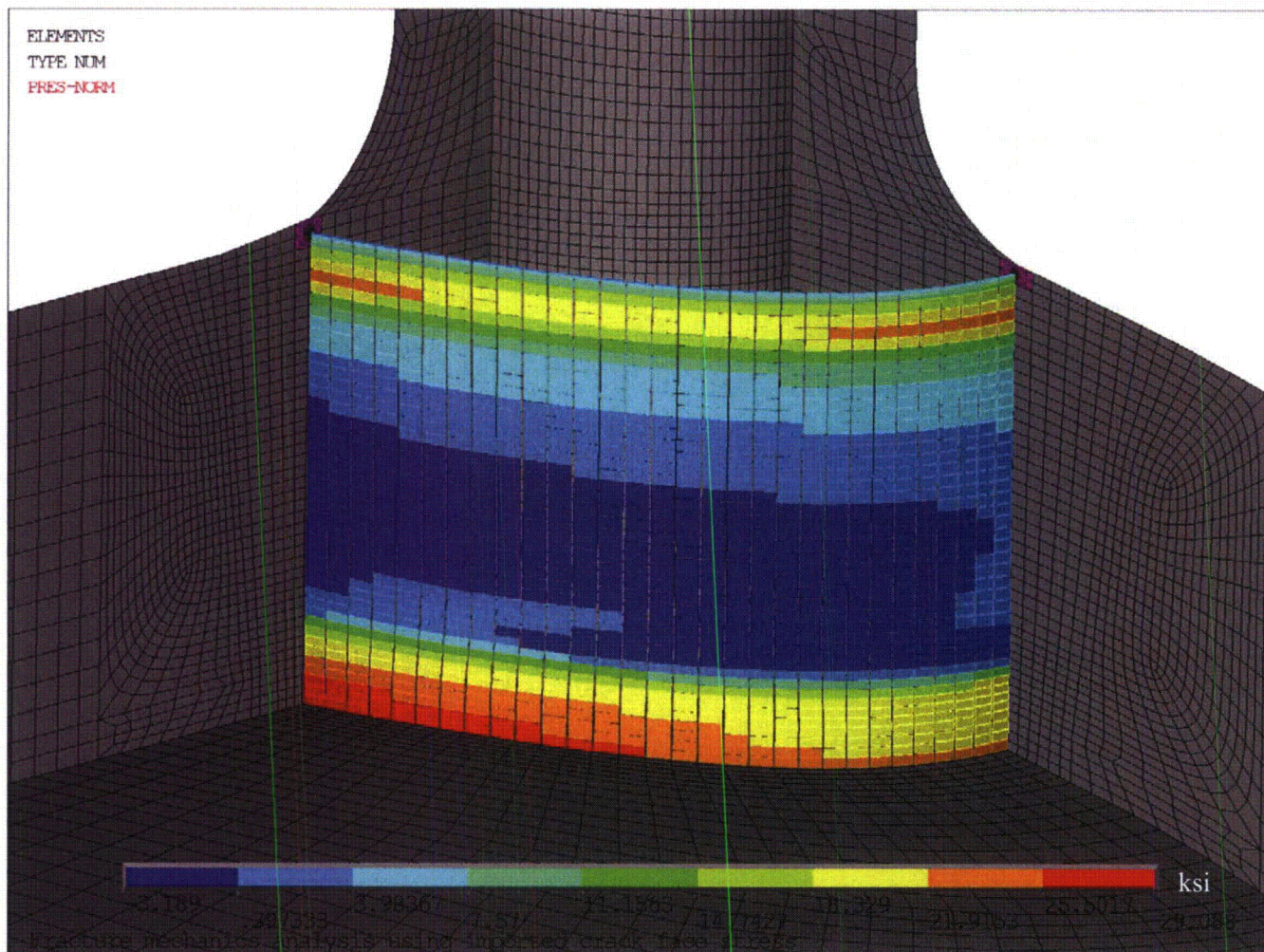


Figure 4. Transferred Residual Stress + NOC + Pressure Stress for Circumferential Flaws

(Note: Deepest circumferential flaw shown for example)

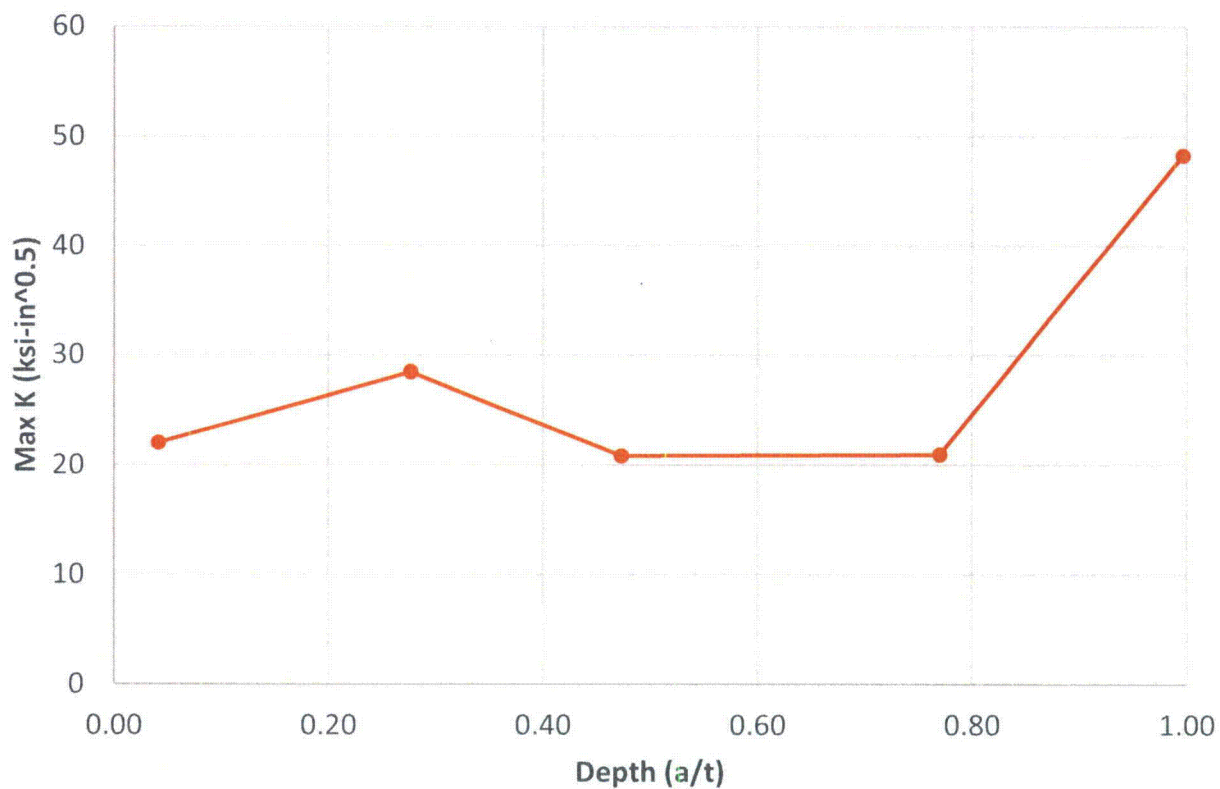
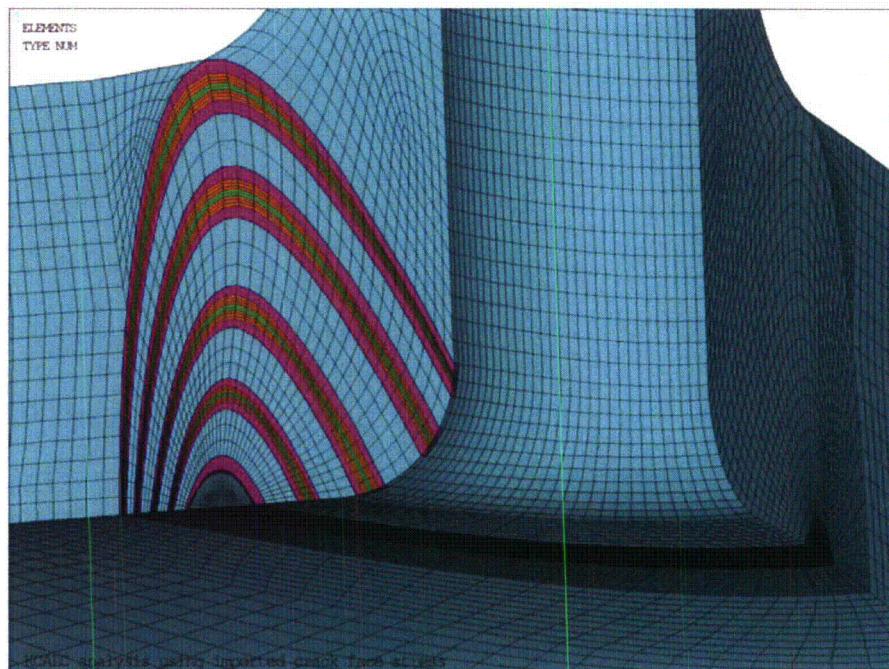
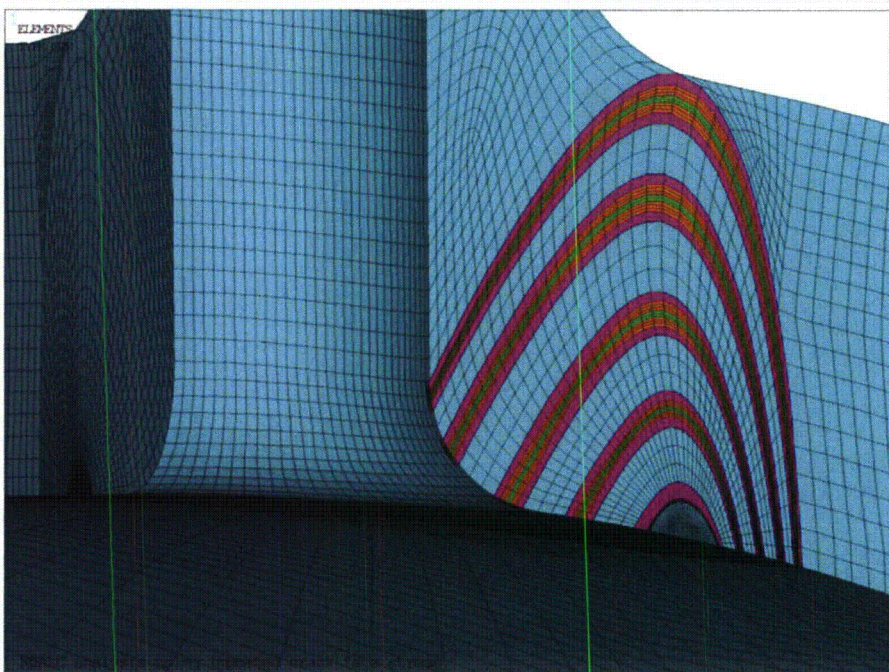


Figure 5. Stress Intensity Factors as a Function of Depth for Circumferential Flaws



0° plane



90° plane

Figure 6. Axial Flaws with Crack Tip Elements Inserted

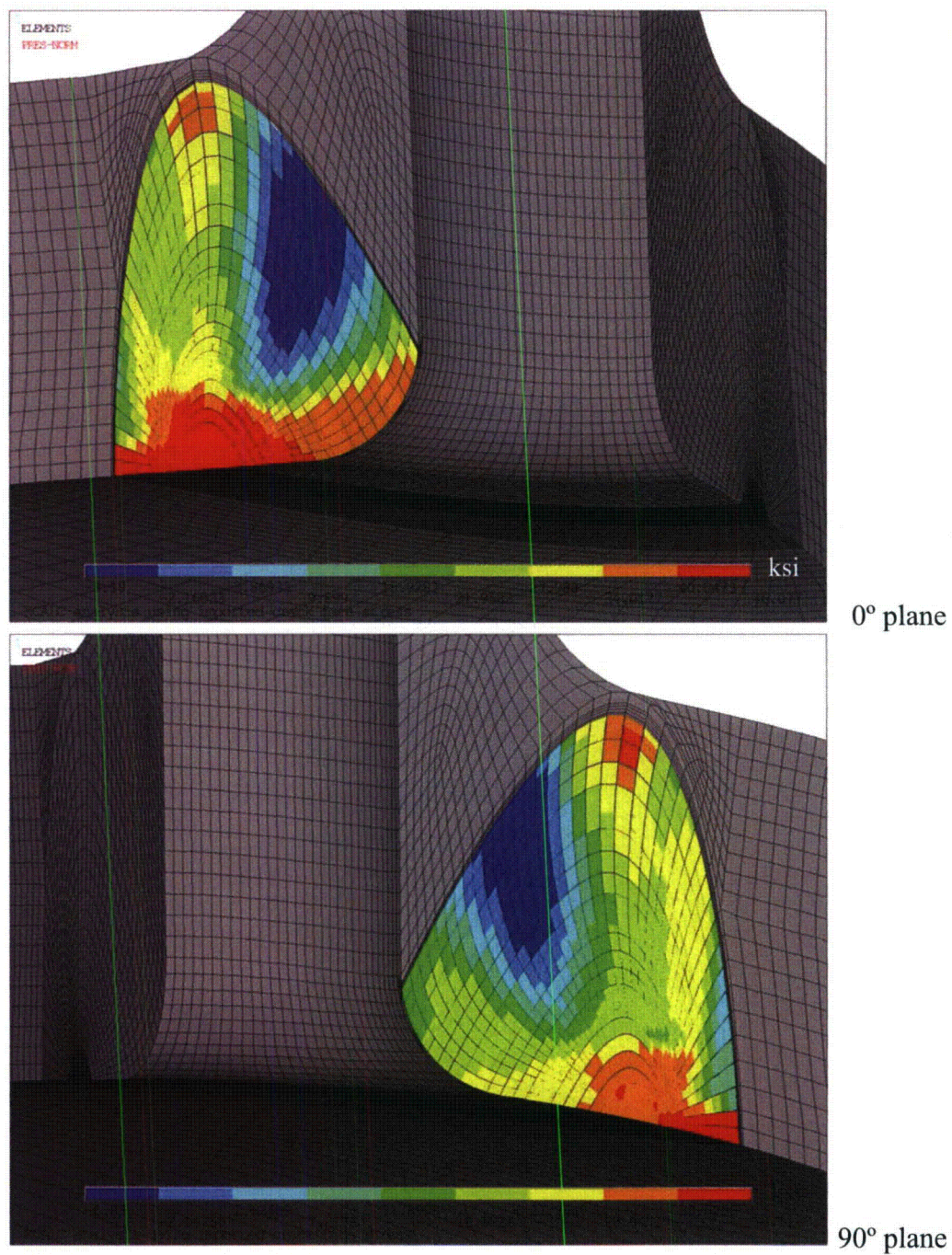


Figure 7. Transferred Residual Stress + NOC + Pressure Stress for Axial Flaws

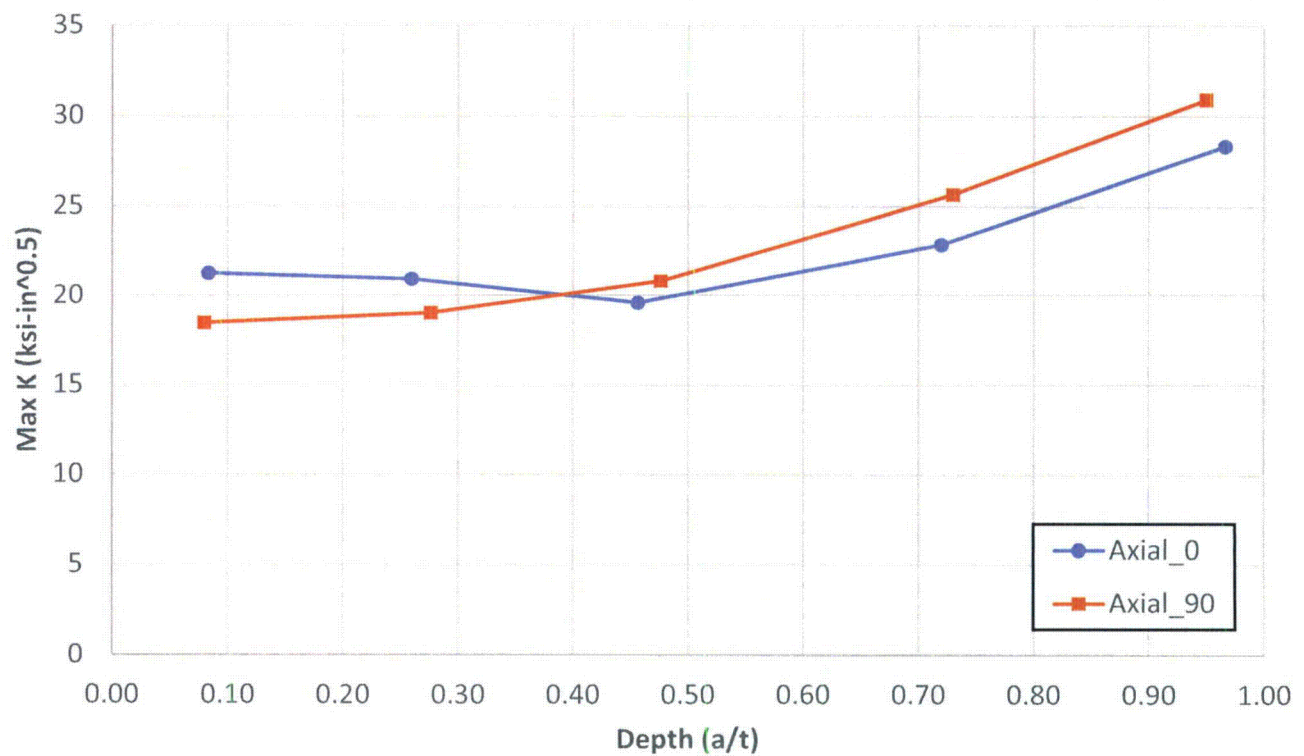


Figure 8. Stress Intensity Factors as a Function of Depth for Axial Flaws

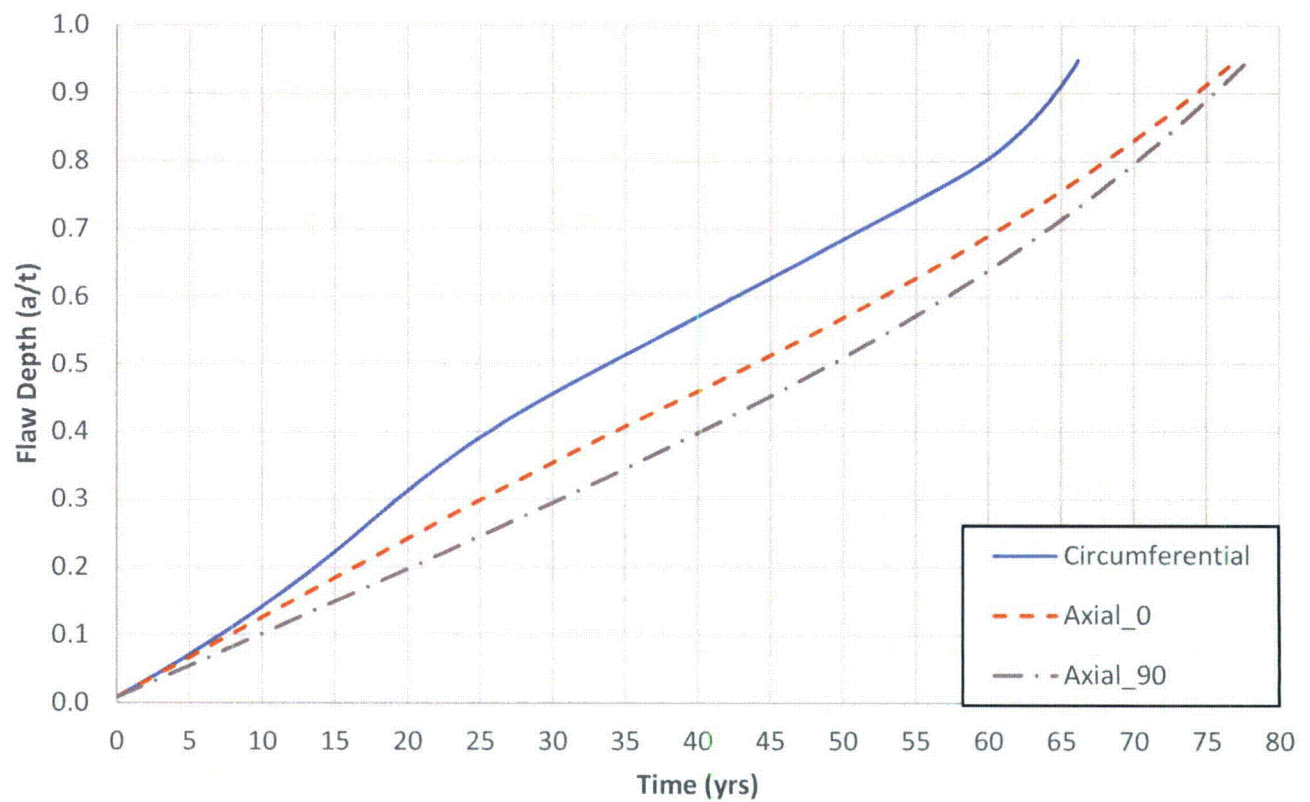


Figure 9. Crack Growth for All Flaw Types with 0.025" Initial Flaw Size

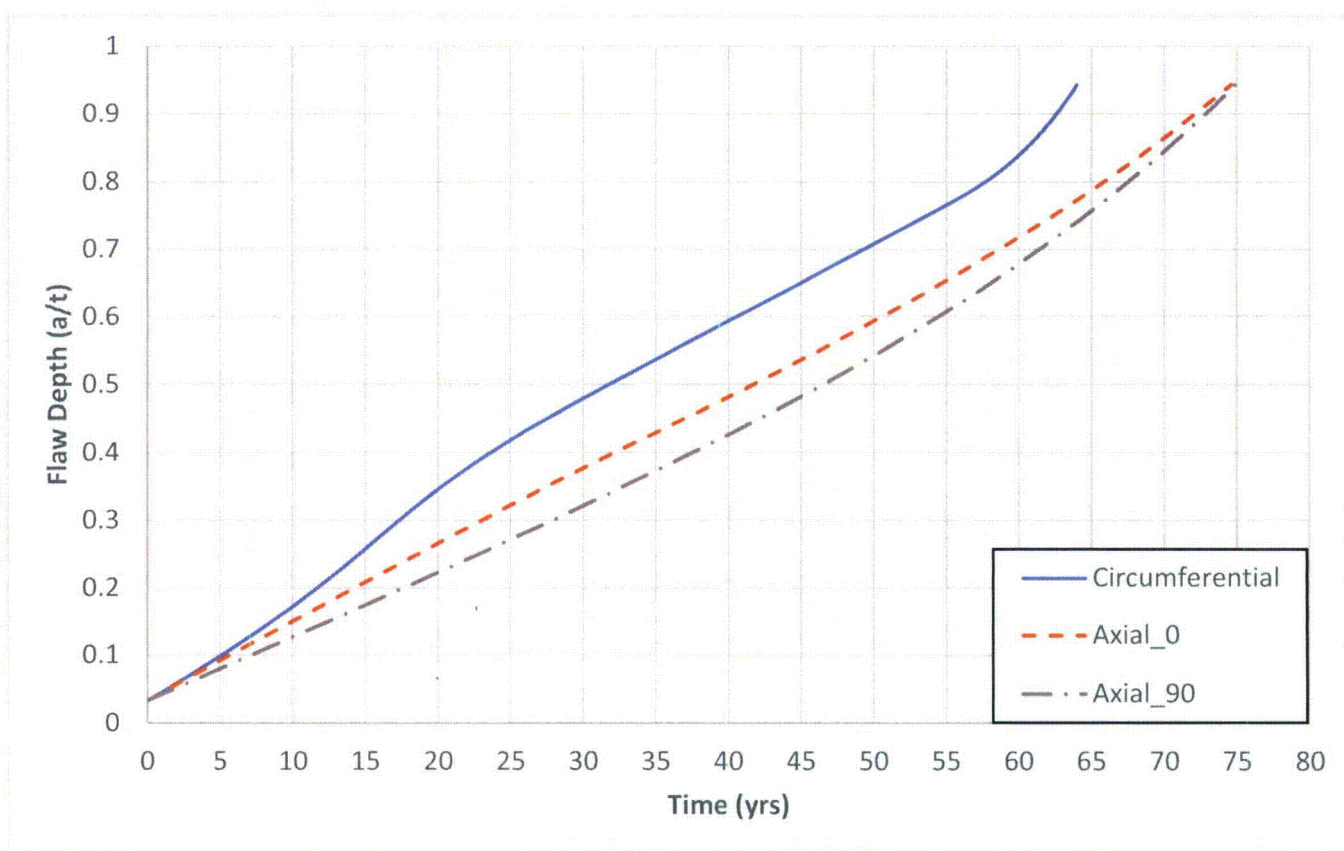


Figure 10. Crack Growth for All Flaw Types with 0.1" Initial Flaw Size